Antibacterial effectors of the type VI secretion system

Alistair Brian Russell

A dissertation

submitted in partial fulfillment of the

requirements for the degree of

Doctor of Philosophy

University of Washington

2014

Reading Committee:

Joseph D. Mougous, Chair

Caroline S. Harwood,

John A. Leigh

Program Authorized to Offer the Degree:

Microbiology

University of Washington

Abstract

Antibacterial effectors of the type VI secretion system

Alistair Brian Russell

Chair of the Supervisory Committee:
Professor Joseph D. Mougous
Microbiology

With the advent of high-throughput culture-independent sequencing it has become increasingly apparent that bacteria often live in complex communities, both in the environment and in association with the human body. Moreover, in polymicrobial settings there is often fierce competition for both space and resources, the results of which can have drastic effects on community composition. The evolutionary pressure exerted by competition is reflected by the significant portion of the coding capacity of many bacterial genomes dedicated to the production and regulation of antagonistic pathways. One such pathway, the type VI secretion system (T6SS), has emerged as a mechanism mediating the delivery of potent antibacterial effectors between contacting Gram-negative bacteria, granting the attacking organism a fitness benefit over sensitive neighbors. Initial studies of interbacterial T6S provided evidence that this system plays an important role in antagonism, however its mechanism of action on recipient cells remained elusive. This thesis describes the first biochemical characterization of antibacterial T6SS effector proteins, finding that they compromise basal features of bacterial physiology such as cell envelope integrity. By targeting highly conserved processes the T6SS has the capacity to mediate antagonism between highly disparate organisms. The cost of such versatility is that bacteria are susceptible to their own T6SS effectors. In order to overcome this hurdle

antibacterial effectors are invariably associated with cognate immunity proteins that prevent their toxicity, protecting the producing cell. Beyond initial biochemical characterization of antibacterial effector proteins, this work describes informatic efforts to identify substrates secreted by the interbacterial T6SS throughout sequenced bacterial genomes. This strategy uncovered highly divergent effector sequences comprising distinct families within superfamilies defined by a common enzymatic target. These divergent effectors not only exhibit distinct substrate specificities, but also vary in their capacity to be neutralized by different sets of immunity proteins. Lastly, our informatic efforts led to the discovery of antibacterial effector proteins in a phylum of Gram-negative bacteria not predicted to encode a T6SS, the Bacteroidetes. My work on this abundant environmental and human-associated phylum of bacteria has found that they possess a highly divergent T6S-like pathway, one that, like its Proteobacterial homolog, takes part in interbacterial antagonism. Together, these findings represent a significant advancement in the field of interbacterial T6S, and serve as a platform for further work defining the *in situ* benefit of this antagonistic pathway.

Table of Contents

ACKNOWLEDGEMENTS

I have been incredibly lucky to have the support of many amazing people in my graduate career. My successes have been in no small part due to their help and companionship, and graduate school would have been significantly tougher and much more lonely without their help and guidance.

First and foremost, I want to thank my advisor, Dr. Joseph D. Mougous. Joseph has been incredibly supportive throughout his time as my mentor, always pushing me to try new ideas, taking the time to teach me how to be a better communicator, and generally investing his time and energy into ensuring my success. He always made the time to chat with me about my project or science in general, and not only prevented me from going down blind alleys but also provided incredible insight into my projects. I cannot imagine having been in any other lab working on any other topic for my tenure in graduate school.

I would also like to thank all of the members of my thesis committee, Carrie Harwood, Nina Salama, John Leigh, and Colin Manoil. All of them were incredibly responsive to any questions I had, and were all willing to make time for me in their busy schedules. I would like to individually thank Carrie, who bolstered me when things weren't working and was always there as a friendly ear, even if it was just to share insignificant findings that I was nevertheless excited about, Nina, who took the time along with Joseph and Carrie to write me letters of recommendation, and John, who, with Joseph and Carrie, was willing to serve on my reading committee.

The other members of the Mougous laboratory were also absolutely integral to my success as a researcher. There were many faces during my tenure in Joseph's lab, all of whom were there for me when I needed it, even if it was just a small favor or a chat. Thank you so much to Justin DeLeon, Danielle Agnello, Laura Austin, Mike Carl, Rachel Hood, Rex Trinidad, Phil Tatman, Li Mo, Taylor Gardiner, Max Ferrin, Nick Andring, Brittany Harding, Robin Kirkpatrick, Rachel Kim, Elena Montauti, Sandra Schwarz, Michele LeRoux, Julie Silverman, Seemay Chou, John Whitney, Brook Peterson, and Aria Eshraghi. I would like to single out Michele LeRoux, Julie Silverman, and Brook Peterson, all of whom made time for me even when burdened with their own work, and provided invaluable insight and practical help on my projects. I can only hope I am so lucky as to work beside such giving folks in the future.

I was also blessed to take part in a number of collaborative projects. In every instance, our collaborators were absolutely essential to the study and worked with us as a true cohesive unit. I would therefore like to thank collaborators outside of Joseph's lab: Waldemar Vollmer at Newcastle and his postdoc Nhat Khai Bui, David R. Goodlett, currently at the University of Maryland, and his student Pragya Singh, Young Ah Goo and Bao Tran, also at the University of Maryland, Mitchell Brittnacher at the University of Washington, Paul Wiggins at the University of Washington, Sun Nyunt Wai and her postdoc Takahiko Ishikawa and student Kristina Hathazi, Tamir Gonen and his postdoc Hongjin Zheng, and, lastly, Andrew Goodman and his student Aaron Wexler and technician Natasha Barry.

The Department of Microbiology was also an incredibly collaborative environment. While there are many folks who provided small favors throughout my time in graduate school, I would like to thank Amy Schaefer and Boo Shan Tseng in particular. Both of these amazing scientists made time to talk shop with me on a consistent basis and served as an amazing resource to pull opinions from outside of Joseph's lab. While I do not feel I can repay their kindness, I certainly hope to emulate both Amy and Boo in the future and serve as a resource to other scientists.

Before I came to graduate school, I also was incredibly lucky to work in the lab of Alan Collmer at Cornell University. Alan trusted me with a degree of freedom that I doubt many people would give an undergraduate. By placing his trust in me Alan demanded more of me than anyone in my academic career to that point – success or failure was completely contingent on my willingness to work through problems, and this experience had a profound effect on my growth as a researcher. I am likewise indebted to Brian Kvitko, Alan's graduate student who trained me. Not only did he teach me bacterial genetics, a skill that has been the foundation of my research, but he also treated me as a researcher in my own right and forced me to rise to that expectation. It was in Alan's lab that I fell in love with research and felt truly at home and accepted by other researchers. In both Alan and Joseph's labs I have found collaborative environments, and will always try and shape the same as much as I can in my career.

Before I ever picked up a pipette, both of my parents were always supportive of my interests throughout childhood. Whether it was providing me with a microscope or taking me to herpetology conferences my father, David Russell, indulged my curiosity. My mother, Maureen Russell, has lifted me up when I have been ready to give up and has served as a constant

supporter of me in all that I do. I would also like to thank my siblings, Maeve, John, and Calum Russell for always being in my corner.

Last, and certainly not least, I would like to thank the love of my life, my fianceé Jacquelyn Braggin. I doubt another human being on this planet would have had the patience to deal with me when working long nights in order to finish manuscripts. She has been my strongest fan, always there to provide me with kind words when things get the best of me. I am looking forward to a lifetime with her and know all of my accomplishments will owe no small part of their success to her support.

CHAPTER I

Introduction to the Gram-negative type VI secretion system

Bacteria rarely grow in isolation, and are instead often found in dynamic communities; taking part in complex mutualistic, commensal, and antagonistic interactions with other microbes. These relationships in turn can affect community composition and thus have both ecological ramifications as well as implications for human health. It has therefore become paramount to understand interbacterial relationships in order to fully appreciate the impact of human intervention on intact microbial communities and to better manipulate community dynamics in order to promote environmental and human health.

One mechanism by which bacteria can influence their neighbors is through the delivery of toxic effector proteins by the Gram-negative type VI secretion system (T6SS) (1-5). Originally identified as a cluster of conserved genes containing distant orthologs to the T4S components DotU and IcmF, it was soon appreciated that the thirteen elements conserved between Proteobacterial T6SS-gene clusters define an evolutionarily distinct secretion system (6, 7). While a few early studies on the T6SS demonstrated that in a few organisms it, like the T3SS or T4SS, could target proteins to eukaryotic cells and thus play a direct role in virulence, for the most part research on this system identified cryptic phenotypes in processes such as biofilm formation that were unexplainable by host-cell targeting (8-13).

A significant breakthrough was made with the observation that a T6SS encoded by the organism *Pseudomonas aeruginosa* could be utilized to deliver a cytotoxic protein, type VI secretion exported 2 (Tse2), to neighboring cells (14). As Tse2 is an antibacterial protein, *P. aeruginosa* prevents its own intoxication by a cognate immunity protein, type VI secretion immunity 2 (Tsi2). The paradigm defined by these two proteins has revolutionized the study of the T6SS as

mediating interbacterial interactions, allowing for a more complete understanding of its adaptive benefit to the vast majority of organisms that possess this pathway.

Gram-negative cell envelope

In order to discuss the form and function of Gram-negative secretion systems it is important to elaborate upon the architecture of the Gram-negative cell envelope (Figure 1.1). Understanding the physiology of this structure is also integral to the study of interbacterial antagonism, as it is often a target of antibacterial strategies. Unlike most other organisms, Gram-negative bacteria possess a membrane external to the cytoplasmic membrane – granting them an additional compartment, the periplasm, as well as contributing to the envelope barrier against environmental stress. Significantly, the outer membrane protects the Gram-negative cell wall, located between the inner and outer membranes. This defense is lacking in Gram-positive organisms, explaining the greatly increased thickness and more extensive modification of cell wall architecture present in those lineages as compared to Gram-negative phyla (15).

The cytoplasmic (inner) membrane consists of a phospholipid bilayer, and provides similar function to the sole cytoplasmic membrane found in other organisms. It is across this membrane that a proton-motive force is generated and transport systems such as the universally conserved Sec operate. The phospholipid composition of this membrane varies between bacteria and environmental conditions, however common phospholipids include phosphatidylserine, phosphatidylyglycerol, phosphatidylethanolamine, and cardiolipin (16, 17). These different headgroups affect the charge characteristics as well as the curvature of the bacterial membrane,

although unlike in eukaryotes there is no evidence to suggest that they function as specific signaling molecules.

Beyond the inner membrane lies the periplasmic compartment. The periplasm contains many hydrolytic enzymes, processing larger substrates prior to their import across the inner membrane. Importantly, within the periplasm is the Gram-negative cell wall, comprised of the polymer peptidoglycan. Peptidoglycan consists of glycan strands with a disaccharide repeat unit of *N*-acetylglucosamine and *N*-acetylmuramic acid connected by a β1,4 linkage. Connected to the C3 carbon of *N*-acetylmuramic acid is a pentapeptide consisting of both L and D amino acids as well as an unusual amide linkage between the γ-carbon of D-glutamate and the L-stereocenter of *meso*-diaminopimelic acid (18). This pentapeptide can participate in cross-links with neighboring gylcan strands, with energy provided for transpeptidation by the loss of the terminal amino acid of the pentapeptide. For strands not participating in crosslinks, specialized D,D endopeptidases cleave the terminal peptide of the pentapeptide, leaving the resulting tetrapeptide without a leaving group and thus unable to participate in transpeptidation. The resulting polymer forms a resilient meshwork that provides hydrostatic support and gives the cell shape. Additionally, due to the unusual linkages found in peptidoglycan this molecule is recalcitrant to hydrolysis by standard proteases and glycosylases, and specialized enzymes are involved in its remodeling (19).

The last layer of the Gram-negative cell envelope is the outer membrane. Unlike the inner membrane, the outer membrane consists of an inner-leaflet phospholipid monolayer, and an outer-leaflet lipopolysaccharide (LPS) monolayer. The outer membrane is anchored to the

peptidoglycan cell wall covalently through Braun's lipoprotein and non-covalently through the outer membrane protein OmpA and the Tol-Pal system (15, 20). The externally-facing LPS forms a permeability barrier, protecting the cell wall from the activity of various bacteriolytic enzymes as well as preventing the uptake of a number of antibiotics. Modification of LPS also allows bacteria to escape immune detection, explaining the prevalence of Gram-negative organisms in close association with vertebrate hosts (21). This permeability barrier is a double-edged sword, as while it protects Gram-negative bacteria it also prevents nutrient uptake and export of exoproteins. To solve the first problem, Gram-negative bacteria possess substrate-specific channels allowing free diffusion into the periplasm as well as energy-dependent uptake across the outer membrane through interaction with the periplasm-spanning TonB protein – which transduces energy generated from proton-motive force across the inner membrane to the outer membrane (22). To address the second challenge, Gram-negative bacteria possess a number of specialized secretion systems.

Gram-negative secretion systems

The unique physiology of Gram-negative bacteria necessitates complex mechanisms of protein export. Unlike Gram-positive cells, Gram-negative bacteria cannot utilize the Sec pathway for secretion. Instead the Gram-negative Sec pathway serves to export proteins to the periplasm. However, to address this problem there are a number of evolutionarily and mechanistically distinct pathways for export from the Gram-negative cytoplasm to the extracellular space. By convention each newly identified system is ascribed an ascending numerical designation, with current nomenclature describing nine secretion pathways, the type I-IX secretion systems (T1-9SS, although there are nomenclature disagreements with the T7SS and T8SS with one proposed

T7SS describing a system absent from Gram-negative bacteria) (23-30). Of these, the mechanisms of type I-VI are perhaps best understood. Interestingly, not only do these divergent secretion systems cross the Gram-negative envelope using unique assemblages of proteins, but some only traverse the outer membrane, relying on the general Sec pathway for passage across the inner membrane, whereas others comprise a channel for egress of substrates from the cytoplasm in a one-step process. In addition to providing a protected channel for export across one or both Gram-negative membranes, each of these export systems must also solve the problems of selecting distinct substrates from among the total pool of proteins present in the cytoplasm (or periplasm) and energizing the secretion process in order to efficiently export substrates with rates and selection above those permitted by simple diffusion. Different systems solve these problems through distinct mechanisms, such as chaperone proteins for recognition and ATPases to provide chemical energy for secretion.

Lastly, while some secretion systems export proteins only across the Gram-negative cell envelope (types I, II, and V, VII, VIII, and IX secretion), others translocate substrates into a recipient cell (types III, IV, and VI secretion). These substrates are often potent toxins, and have been collectively referred to as effector proteins. The difference between a toxin and an effector has at times been contested, however the most common usage is that a toxin is secreted to the extracellular milleux and affects its target when delivered exogenously, whereas an effector lacks the capacity to act externally and must instead be delivered by a secretion apparatus (31). Effector proteins are often both highly potent and incredibly specific, giving significant insight into the biological processes which they impact.

Components and mechanism of the T6SS

An early informatic analysis by Boyer et al. of T6SS gene clusters found a core set of thirteen genes invariantly associated with this secretion system (6). Subsequent studies of these core elements has indicated that each is essential to function, with inactivation of any of the thirteen leading to significant defects in secretion (28). Subcellular localization and two-hybrid and co-immunoprecipitation interaction experiments performed on these thirteen proteins have revealed that the T6SS consists of two distinct subassemblies, one which spans the Gram-negative cell envelope and another with extensive homology to bacteriophage. Contacts between proteins within a given assembly are extensive, and, unsurprisingly, subcellular localization data correlates well with two-hybrid and co-immunoprecipitation interaction data indicating co-occurrence of interacting proteins within the same cellular compartment.

The envelope-spanning subassembly consists of three proteins (type VI secretion J, L, and M – TssJ, L, and M) including those bearing distant homology to the T4SS components DotU and IcmF (TssL and TssM). Both TssL and TssM are integral inner membrane proteins, while TssJ, is an outer membrane lipoprotein. Contacts have been defined between TssL and TssM, and TssM and TssJ, leading to an assembly that spans the inner membrane and periplasmic space (28). While little functional data concerning this complex have been obtained save for the essentiality of these components to an active secretion system, studies have revealed a few interesting facets of the function of TssL and TssM. The TssL protein is often found with an additional peptidoglycan (PG)-binding domain at its C-terminus (32). This has been taken to indicate that the function of the envelope-spanning subassembly is to anchor the T6SS to the relatively static cell wall. Moreover, some T6SSs wherein TssL lacks a PG-binding domain

encode an additional membrane protein, TagJ (type VI associated gene J), with a PG-binding domain. This protein might serve as an anchor when PG-binding function is absent from TssL. While TssM does not possess clear anchoring domains, many, but not all, homologs of this protein possess a Walker ATP-binding and hydrolysis motif. Common in ATPases, this motif is often associated with conformational changes upon both ATP-binding and hydrolysis. Such motifs are observed in energy-dependent processes wherein the ATP-driven conformational change provides the appropriate energetic input. The function of this domain in TssM is still unclear, as in some organisms it appears essential for function, whereas in others it is absent, or, if present, dispensable (28). Still, in *Agrobacterium tumefaciens*, TssM hydrolysis of ATP has been correlated with the capacity of TssL to bind a component of the bacteriophage-related subassembly, Hcp (33, 34). Thus, at least in some organisms, the walker motif in TssM might modulate assembly of an active T6SS apparatus once appropriate contacts in the envelope-spanning complex have been established.

The bacteriophage-like subassembly contains five proteins (TssB, TssC, Hcp, ClpV and VgrG), three of which have structural homology to phage infection machinery (TssC, Hcp, and VgrG) (28, 35, 36). While research on the envelope-spanning sub-complex has thus far failed to yield meaningful explanations of T6S function, study of the bacteriophage-like assembly has provided significant advancements in our understanding of the mechanism of T6S. This is due to the ability of researchers to leverage the extensive knowledge of the mechanism of bacteriophage infection – wherein a sheathe complex undergoes a contractile event, forcing a penetrating spike and associated tail tube through the outer membrane of a Gram-negative bacterium. The phage genome is subsequently delivered to the periplasmic space and then accesses the cytoplasm via

an as-yet uncharacterized mechanism (37). By analogizing T6SS substrate delivery to this process, a number of significant insights have been obtained.

The proteins TssB and TssC provide one of the most direct comparisons between bacteriophage infection and the T6SS. These two proteins comprise a bacteriophage sheathe-like complex that can be observed in both extended and contracted states *in vivo* by transmission electron microscopy (TEM) (38). Further study utilizing fluorescently tagged TssC revealed that the TssB–TssC complex shifts between contracted and extended states, indicating that the two forms statically observed by TEM represent different steps in active T6S rather than discrete stable subpopulations. It is the contraction of the TssB–TssC sheathe that is thought to provide the energy to penetrate a recipient cell, similar to how phage contraction is thought to help drive the tail spike through the outer membrane of a Gram-negative bacterium.

If the contraction of TssB–TssC does indeed provide energy input into substrate translocation, one would have to posit a mechanism for recycling the complex once it has fired.
This function appears to be performed by the ClpV AAA^+ ATPase, known to remodel the TssB–TssC complex *in vitro*, and which possesses Walker ATP-binding and hydrolysis motifs (39, 40). Using an empirically-derived modeling approach based on a low-resolution cryo-EM structure of a contracted TssB–TssC filament and fitting partial TssB and TssC structures (and where data was lacking the crystal structure of the analogous gp18 viral protein) to the solved extended T4 bacteriophage sheathe, Wendler and colleagues have developed a mechanistic hypothesis of ClpV function. Their model states that contraction of a TssB–TssC sheathe reveals a Clp-binding motif that is recognized by ClpV, leading to dissolution of the contracted sheathe and subsequent

recycling of TssB and TssC into the extended state (41). Thus the energy for T6S as a whole is derived from ATP hydrolysis. Consistent with this model, ClpV–GFP fusions have been observed to form punctate foci for brief periods of time before returning to diffuse localization throughout the cell; implying that this protein only localizes to the T6SS during a discrete step of secretion rather than remaining associated with the apparatus (42).

Significant conjecture surrounds the events that follow the contraction of the TssB–TssC sheathe, particularly surrounding the fate of the proteins VgrG and Hcp – homologous to the bacteriophage tail spike and tail tube, respectively. Both of these proteins are unusual in that they are not only structural components, but are also exported substrates of the T6SS. The secretion of Hcp in particular has been considered a marker for T6S as unlike other T6SS substrates it can be readily identified informatically and it is often one of the most abundant proteins secreted by the apparatus. It is presumed that the TssB–TssC contractile event coincides with the puncturing of a recipient and delivery of both VgrG and Hcp. VgrG is hypothesized to lead the penetration of the membrane of the recipient, capping the apparatus, and Hcp, known to form homomeric tubes *in vivo*, is thought to reside within the TssB–TssC sheathe and become ejected upon contraction (43). While both hypotheses currently lack validation, there is a known role for both proteins in effector recognition by the T6S apparatus – indicating that their translocation into a recipient cell is likely required for concomitant delivery of their effector cargo.

Substrate recognition by Hcp appears to occur via an interaction between effector proteins and the internal pore of the Hcp tube (44). The Hcp polymer consists of stacked hexameric rings, with an internal pore diameter consistent with the known size and shape of at least one Hcp-

dependent T6SS effector (42, 45). Moreover, both cryo-EM of an effector–Hcp complex and mutational analyses probing the effector–Hcp interface are consistent with effector recognition proceeding via encapsulation by an Hcp hexamer (44). In a few instances effector proteins can be found directly fused to Hcp, however none of these fusions have been experimentally validated to retain activity and thus the placement of such effectors within or outside of the Hcp pore cannot currently be speculated upon (46).

In addition to Hcp-recognition of effector proteins, some require an associated VgrG-protein for their recruitment and translocation. The first VgrG-associated effectors identified were domains directly fused to the C-terminus of VgrG (9, 13, 47). Unlike Hcp fusions, these effectors have been experimentally validated. Additionally, VgrG, like Hcp, appears to be able to recruit effector proteins by direct interaction. This was first uncovered when the structure of a co-crystal consisting of a hybrid bacteriophage-VgrG chimera and a protein containing the domain PAAR was solved (48). The PAAR domain is found at the N-terminus of many, but not all, VgrG-dependent T6SS substrates, suggesting it acts as a common feature allowing these proteins to interact with VgrG and subsequently become recruited to the secretion apparatus. Informatic data demonstrating genetic linkage of PAAR proteins with downstream effectors also suggests that PAAR domains that are not fused to effectors might still act as a bridging element, interacting both with VgrG and independent effector proteins. Lastly, with strikingly similar organization to PAAR proteins, genes encoding products containing a domain of unknown function (DUF4123) are often found adjacent to VgrG-dependent effectors. One of these proteins, VasW in *V. cholerae*, has been demonstrated to be necessary for secretion of the adjacent VgrG-dependent effector, VasX, indicating that it, like PAAR, might recruit effectors to VgrG (49).

As critical determinants of substrate recognition, it is also of note that a single T6SS locus is often associated with multiple Hcp or VgrG proteins (50). This is in contrast to the other eleven conserved T6SS elements, which are usually found in single copy within a given T6SS gene cluster. Additionally, *vgrG* and *hcp* substrate islands are often found throughout bacterial genomes, unlinked to the T6SS through which they transit. Lastly, both *vgrG* and *hcp* are often, but not always, found encoded adjacently to their associated effector proteins (51). By possessing a multiplicity of VgrG and Hcp proteins a single T6SS apparatus gains a greater plasticity in its potential cargo. The genetic association of *vgrG* and *hcp* with their associated effectors also provides a partial mechanism for what appears to be the frequent horizontal transmission of effector genes between organisms. While not providing an explanation for the actual horizontal gene transfer event, by the very act of being in proximity a transferred effector is more likely to be co-inherited with the *vgrG* or *hcp* responsible for its recognition. Moreover, in the case of VgrG, effector recognition appears to localize to the C-terminus, a region with an often-divergent evolutionary history to the rest of the protein. Thus in a single recombination event replacing the C-terminus of an endogenous VgrG protein with a transferred element and downstream effector, a T6SS could, in theory, acquire a novel effector protein.

The function of the remaining five proteins (TssA, TssE, TssF, TssG, and TssK) in either subcomplex is unclear. While TssE, like VgrG, Hcp, and TssC, has homology to a phage element (the gp25 baseplate), it is not known whether it strictly participates in the phage-like subassembly (28). Additionally, while one report places TssK as bridging the two subassemblies through interactions with TssL, TssC, and Hcp, a more recent study of TssK did not identify

these interactions and instead found that this protein participates in a complex with TssF and TssG (52, 53).

In summary, the current state of the T6SS field defines the T6S as complex consisting of thirteen different proteins comprising distinct envelope-spanning and bacterophage-like subcomplexes. The envelope-spanning complex is presumed to act as a scaffold and anchor for the bacteriophage-like assembly, which in turn undergoes a dynamic contractile event, providing energy for the translocation of the substrate-associated proteins VgrG and Hcp into a recipient cell (Figure 1.2).

Interbacterial T6S

Initial studies of the T6SS focused on its potential role in targeting Eukaryotic cells, particularly in the context of virulence. This was bolstered by the early identification of host-targeting T6SSs in the organisms *Vibrio cholerae* and *Aeromonas hydrophila*, and the known impact of the T3SS and T4SS on virulence. In *V. cholerae* it was found that the T6SS could contribute to protection from predation by amoebae and killing by macrophage (54). Further investigation found that a VgrG protein secreted by the T6SS in this organism possesses a C-terminal actin crosslinking domain (9). Upon phagocytosis by amoeba or macrophage, *V. cholerae* is able to translocate this domain into the eukaryotic cell whereupon it compromises the integrity of the actin cytoskeleton (55). A VgrG protein in *A. hydrophila* also possesses an effector domain that targets actin, although it ADP-ribosylates, rather than crosslinks, the eukaryotic protein (13). The T6SS in this organism was found to contribute to cell rounding in *in vitro* infections, and, more importantly, is a significant contributor to mortality in a mouse model of infection (8).

The activities ascribed to both the VgrG-fused effectors of *V. cholerae* and *A. hydrophila* fit a general model of virulence factors. By targeting a eukaryotic-restricted molecule, actin, the effects of these toxins are fundamentally restricted to host cells. In this manner *V. cholerae* and *A. hydrophila* can utilize potent toxins indiscriminately without concern of compromising their own physiology. Indeed, even when targeting a molecule conserved between bacteria and eukaryotes virulence factors often still retain limited activity against the producing organism by requiring co-activators that are lineage restricted, such as calmodulin (56).

Nevertheless, despite these findings in *V. cholerae* and *A. hydrophila*, many T6SSs are resident in bacteria that are avirulent (57). While it is certainly possibly that some of these organisms could use the T6SS as a means of escaping amoebal predation, there were many instances in which no clear eukaryotic-targeting domains could be found associated with the T6SS gene clusters. In addition, early phenotypic studies of organisms bearing mutations inactivating T6SSs often found no effect on virulence but did find effects on processes such as biofilm formation, suggesting a role for the T6SS in interbacterial interactions (8-13). Informatic arguments also suggested roles for the T6SS beyond host-targeting. For example, the host-adapted *Burkholderia mallei* possesses only a single T6SS relative to the between five and six distinct systems found in its free-living relatives *B. thailandensis* and *B. pseudomallei* – indicating that there was no longer an adaptive benefit to maintaining these systems in an obligate pathogen, and that they likely do serve a function in the environment (58).

A breakthrough in the study of T6S was achieved with the finding that the hemolysin co-regulated secretion island I T6SS (H1-T6SS) of *P. aeruginosa* could deliver an antibacterial effector to neighboring *P. aeruginosa* cells (14). Three substrates of the H1-T6SS were identified by comparing culture supernatants of a *P. aeruginosa* strain bearing mutations hyperactivating the H1-T6SS with a strain possessing a mutationally-inactivated H1-T6SS by mass spectrometry. These substrates were named Tse1-3 for type VI secretion exported 1-3. One, Tse2, was found encoded in a bicistron with a gene that contained no transposon insertions in defined *P. aeruginosa* mutant libraries. It was subsequently discovered that this gene, named *tsi2* for type VI immunity 2, directly interacts with, and prevents the toxicity of, Tse2. Therefore Tse2–Tsi2 appeared to constitute a canonical toxin-antitoxin pair.

While there has been a robust study of toxin–antitoxin pairs, secretion of the toxin was unprecedented (59). Expression of Tse2 in yeast demonstrated that it was toxic to eukaryotic cells, suggesting that perhaps Tse2 was an anti-eukaryotic effector, but one that targets a process shared between bacteria and eukaryotes – thus necessitating the presence of an antitoxin protein. Nevertheless, experiments with *P. aeruginosa* failed to demonstrate that Tse2 could be delivered to eukaryotic cells via the T6SS. As Tse2 is universally toxic, it was instead hypothesized that it could serve as an antibacterial effector. When *P. aeruginosa* cells lacking *tse2* and *tsi2* were placed in competition with a parental strain hyperactive for the H1-T6SS they were outcompeted in a fashion dependent upon Tse2 and the H1-T6SS in the attacking strain. This was the first demonstration that the T6SS could deliver antibacterial effectors between neighboring bacteria, and the generation of a significant paradigm in T6S – an antibacterial effector protein paired with a cognate immunity determinant.

This finding completely changed the approach of many labs in studying the T6SS, and it is now recognized that the majority of organisms utilize this system in order to mediate interbacterial interactions. After the initial finding in *P. aeruginosa*, reports closely followed of T6SSs providing adaptive benefits to *B. thailandensis* and *V. cholerae* in co-culture with the competitor organisms *P. putida* and *E. coli*, respectively – extending not only the original observation to additional bacteria, but also demonstrating that interbacterial T6S can function between relatively unrelated bacteria (58, 60). This is in contrast to most other proteinaceous antibacterial toxins, such as bacteriocins, which generally only target organisms that are closely related to the producer (61). Intriguingly, *V. cholerae* possesses only a single T6SS, which it utilizes to target both eukaryotic and bacterial cells. This indicates that evidence of one activity should not be taken to preclude the other. Overall, more T6SSs have been identified that possess the capability to target bacterial cells than eukaryotes, suggesting that the basal function of the system is to mediate interbacterial interactions with a few derived systems additionally capable of participating directly in host cell or amoebal interactions.

Objectives of this thesis

Interbacterial interactions have the capacity to influence a myriad of processes of interest, including both human and environmental health. It is therefore important to understand the newly discovered T6SS as a potent mechanism mediating interbacterial antagonism. While studies have identified this pathway as granting bacteria the capacity to restrict the growth or kill neighboring cells, only a single antibacterial effector, Tse2, has been identified. Moreover, the activity of Tse2 has remained undefined, severely hampering attempts to understand the general

nature of interbacterial T6S. The aim of this thesis is to better understand bacterial-targeting T6S through the identification and characterization of its effector proteins, attempting to define broadly-applicable paradigms using model organisms and laboratory experiments that can be extrapolated to a large number of organisms by further *in silico* analysis.

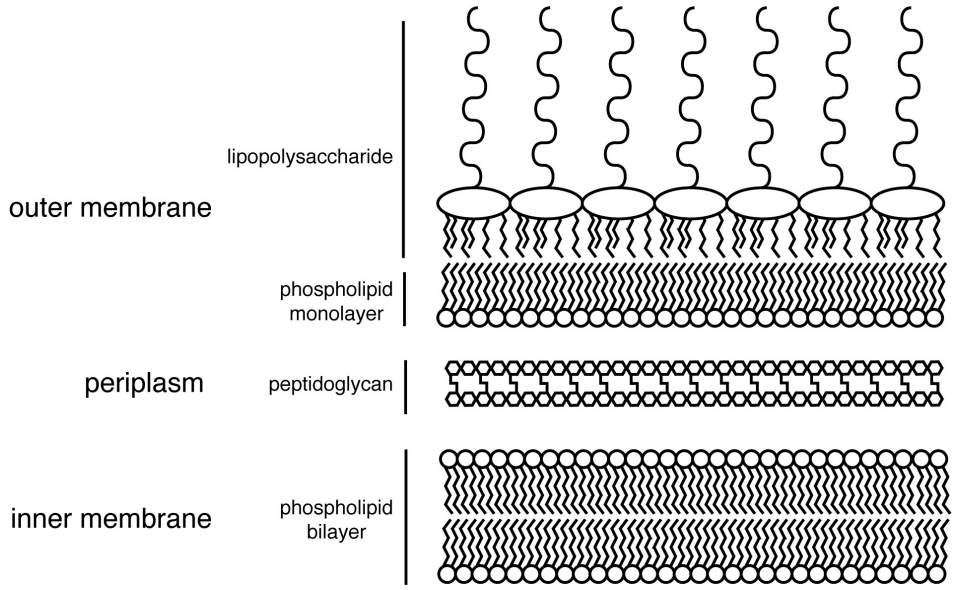

Figure 1.1: Structure of the Gram-negative cell envelope. Schematic depicting the composition of a prototypical Gram-negative cell envelope.

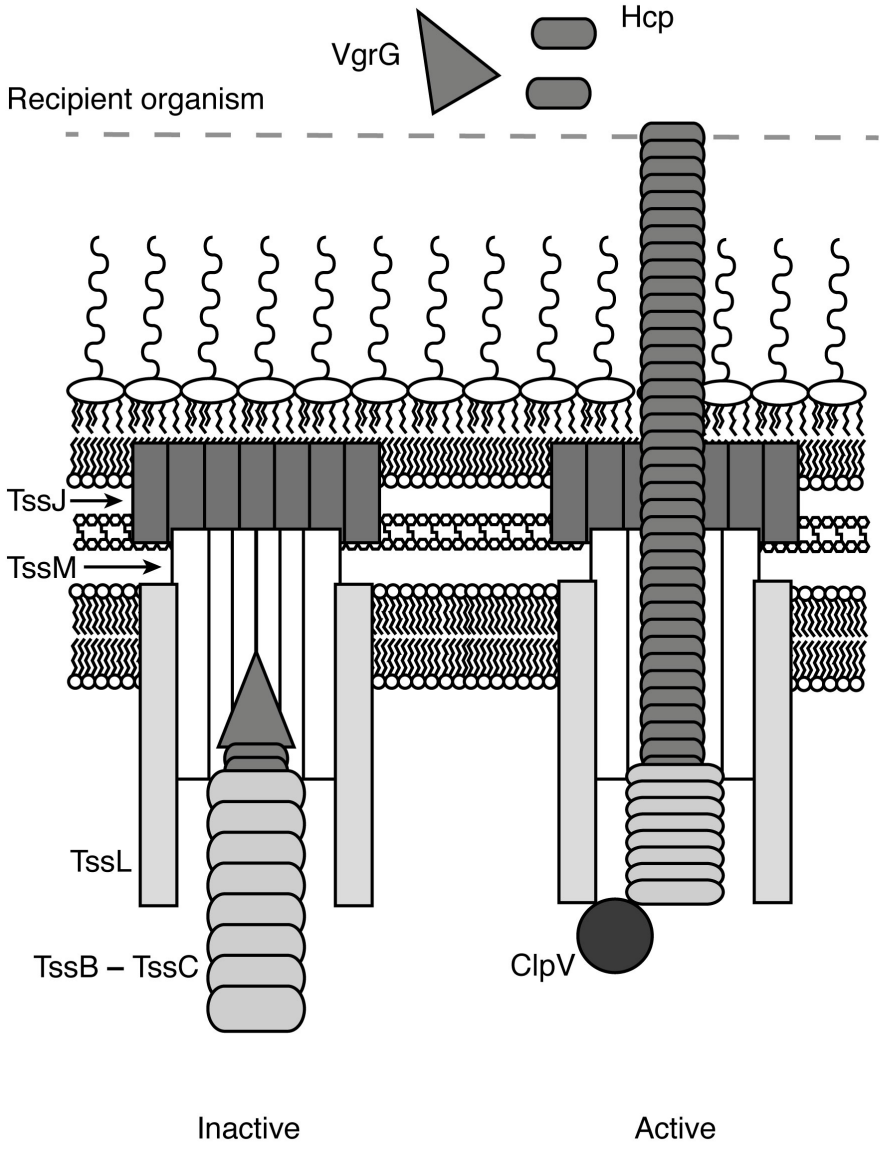

Figure 1.2: Hypothetical model of T6SS function. Schematic depicting the current model of T6SS function. Gram-negative cell envelope presented as in Figure 1.1.

CHAPTER II

Type VI secretion delivers bacteriolytic effectors to target cells

Published as: Russell, A.B., Hood, R.D., Bui, N.K., LeRoux, M., Vollmer, W., and Mougous, J.D. 2011. *Nature* 475, 343–347

A.B.R. contribution: Working with J.D.M. conceived of study and wrote paper. Carried out informatic analyses of Tse1 and Tse3, *E. coli* growth experiments of strains bearing Tse1 and Tse3 expression vectors, subcellular fractionation of *P. aeruginosa* cells expressing epitope-tagged Tsi1 and Tsi3, Tse2 secretion analyses, intraspecific bacterial competitions, analyses of isogenic intercellular intoxication of *P. aeruginosa*, analysis of expression in *E. coli* cells, measurements of the activity of purified Tse1 on permeabilized *P. aeruginosa*, and generation of a significant portion of the vector constructs and mutants used in this study.

ABSTRACT

Peptidoglycan is the major structural constituent of the bacterial cell wall, forming a meshwork outside the cytoplasmic membrane that maintains cell shape and prevents lysis. In Gram-negative bacteria, peptidoglycan is located in the periplasm, where it is protected from exogenous lytic enyzmes by the outer membrane. Here we show that the type VI secretion system (T6SS) of *Pseudomonas aeruginosa* breaches this barrier to deliver two effector proteins, Tse1 and Tse3, to the periplasm of recipient cells. In this compartment, the effectors hydrolyze peptidoglycan, thereby providing a fitness advantage for *P. aeruginosa* cells in competition with other bacteria. To protect itself from lysis by Tse1 and Tse3, *P. aeruginosa* utilizes specific periplasmically-localized immunity proteins. The requirement for these immunity proteins depends on intercellular self-intoxication through an active T6SS, indicating a mechanism for export whereby effectors do not access donor cell periplasm in transit.

INTRODUCTION

Competition among bacteria for niches is widespread, fierce and deliberate. These organisms elaborate factors ranging in complexity from small diffusible molecules, to exported proteins, to multicomponent machines, in order to inhibit the proliferation of rival cells (62, 63). A common target of such factors is the peptidoglycan cell wall (61, 64-66). The conserved, essential, and accessible nature of this molecule makes it an Achilles heel of bacteria.

The T6SS is a complex and widely distributed protein export machine capable of cell contact-dependent targeting of effector proteins between Gram-negative bacterial cells (6, 14, 57, 67). However, the mechanism by which effectors are delivered via the secretory apparatus, and the

function(s) of the effectors within recipient cells, have remained elusive. Current models of the T6SS derive from the observation that several of its components share structural homology to bacteriophage proteins (36, 42, 68); it has been proposed that target cell recognition and effector delivery occur in a process analogous to bacteriophage entry (35).

The observation that T6S can target bacteria was originally made through studies of the hemolysin co-regulated protein secretion island I (HSI-I)-encoded T6SS (H1-T6SS) of *P. aeruginosa*, which exports at least three proteins, Tse1-3 (14, 42). These proteins are unrelated to each other and lack significant primary sequence homology to characterized proteins. One substrate, Tse2, is toxic by an unknown mechanism in the cytoplasm of recipient cells lacking Tsi2, a Tse2-specific immunity protein. Here we show that Tse1 and Tse3 are lytic enzymes that degrade peptidoglycan via amidase and muramidase activity, respectively. Unlike related enzymes associated with other secretion systems (69), these proteins are not required for the assembly of a functional secretory apparatus. Instead, Tse1 and Tse3 function as lytic antibacterial effectors that depend upon T6S to breach the barrier imposed by the Gram-negative outer membrane.

Contacting *P. aeruginosa* cells actively intoxicate each other with Tse1 and Tse3. However, the peptidoglycan of *P. aeruginosa* is not inherently resistant to the activities of these enzymes. To protect itself, the bacterium synthesizes immunity proteins – type VI secretion immunity 1 and 3 (Tsi1 and Tsi3) – that specifically interact with and inactivate cognate toxins in the periplasm. Orthologs of *tsi1* and *tsi3* appear restricted to *P. aeruginosa*, therefore the species is able to

exploit the H1-T6SS to target closely related organisms that are likely to compete for overlapping niches, while minimizing the fitness cost associated with self-targeting.

RESULTS

Tse1 and Tse3 are lytic enzymes

To identify potential functions of Tse1 and Tse3, we searched their sequences for catalytic motifs using structure prediction algorithms (70). Interestingly, motifs present in peptidoglycan degrading enzymes were apparent in both proteins (Figure 2.1A). Tse1 contains invariant catalytic amino acids present in cell wall amidases (DL-endopeptidases) (71), whereas Tse3 possesses a motif that includes a catalytic glutamic acid found in muramidases (19, 72).

To test our predictions, we incubated purified Tse1 and Tse3 with isolated *E. coli* peptidoglycan sacculi. Soluble products released by the enzymes were separated by high performance liquid chromatography (HPLC) and analyzed by mass spectrometry (MS). To generate separable fragments, Tse1-treated samples were digested with cellosyl, a muramidase, prior to HPLC. The observed absence of the major crosslinked fragment, and the formation of two Tse1-specific products, is consistent with enzymatic cleavage of an amide bond in the peptidoglycan peptide crosslink (Figure 2.1A). Moreover, our MS data suggest that the enzyme possesses specificity for the γ-D-glutamyl-L-*meso*-diaminopimelic acid bond in the donor peptide stem (Figure 2.1C). A variant of Tse1 containing an alanine substitution in its predicted catalytic cysteine ((C30A), Tse1*) did not degrade peptidoglycan (Figure 2.1B).

Soluble peptidoglycan fragments released by Tse3 confirmed our prediction that the enzyme cleaves the glycan backbone between *N*-acetylmuramic acid (Mur*N*Ac) and *N*-acetylglucosamine (Glc*N*Ac) residues (Figure 2.1D). Enzymes that cleave this bond can do so hydrolytically (lysozymes) or non-hydrolytically (lytic transglycosylases); the latter results in the formation of 1,6-anhydroMur*N*Ac. Our analyses showed that Tse3 possesses lysozyme-like activity and furthermore suggest that its activity is limited to a fraction of the Mur*N*Ac-Glc*N*Ac bonds. The enzyme solubilized a significant proportion of the sacculi to release non-crosslinked peptidoglycan fragments and high molecular weight, soluble peptidoglycan fragments (Figure 2.1C). A Tse3 protein with glutamine substituted at the site of the predicted catalytic glutamic acid ((E250Q), Tse3*) displayed significantly diminished activity.

If Tse1 and Tse3 degrade peptidoglycan, we reasoned the enzymes might have the capacity to lyse bacterial cells. Ectopic expression of Tse1 and Tse3 in the cytoplasm of *Escherichia coli* resulted in no significant lysis (Figure 2.2A). However, periplasmically-localized forms of both proteins (peri-Tse1, peri-Tse3) abruptly lysed cells following induction (Figures 2.2B and C). In accordance with our *in vitro* studies, peri-Tse1* and peri-Tse3* did not induce lysis at expression levels equivalent to those of the native enzymes (Figures 2.2B and D). We also examined cells producing the periplasmically localized enzymes using fluorescence microscopy. Consistent with our biochemical data, cells producing peri-Tse1 were amorphous or spherical, while those producing peri-Tse3 were swollen and filamentous (Figure 2.2E). In total, these data demonstrate that Tse1 and Tse3 are enzymes that degrade peptidoglycan *in vivo*, and that, unlike related enzymes involved in cell wall metabolism, they possess no inherent means of accessing their substrate in the periplasmic space.

T6S function does not require Tse1&3

Since the Tse enzymes alone are unable to reach their target cellular compartment, we hypothesized that their function must be linked to export by the T6SS. In this regard, they could: 1) remodel donor peptidoglycan to allow for the assembly of the mature T6S apparatus, 2) remodel recipient cell peptidoglycan to facilitate the passage of the T6S apparatus through the recipient cell wall, or 3) act as antibacterial effectors that compromise recipient cell wall integrity. To determine if Tse1 and Tse3 are essential for T6S apparatus assembly, we examined whether the enzymes are required for export of the third effector, Tse2. The secretion of Tse2 was not diminished in a strain lacking *tse1* and *tse3*, suggesting that assembly of the T6S apparatus is unhindered by their absence (Figure 2.3A). If Tse1 and Tse3 act as enzymes that remodel recipient cell peptidoglycan to facilitate effector translocation, Tse2 action on recipient cells should be severely impaired or nullified in the Δ*tse1* Δ*tse3* background. Instead, we found that this strain retained the ability to functionally target Tse2 to recipient cells (Figure 2.3B). These findings led us to further examine the hypothesis that Tse1 and Tse3 are effector proteins rather than accessory enzymes of the T6S apparatus.

Immunity proteins inhibit Tse1&3

Previous data indicate that *P. aeruginosa* can target itself via the T6SS (14). If Tse1 and Tse3 act as antibacterial effectors, it follows that *P. aeruginosa* must be immune to their toxic effects. The *tse1* and *tse3* genes are each found in predicted bicistronic operons with a hypothetical gene, henceforth referred to as *tsi1* and *tsi3*, respectively. Immunity proteins often inactivate their cognate toxin by direct interaction (73); therefore, as a first step toward defining a functional link

between cognate Tsi and Tse proteins, we asked whether they physically associate. A solution containing a mixture of purified Tse1 and Tse3 was mixed with *E. coli* lysates containing either Tsi1 or Tsi3. Co-immunoprecipitation studies indicated that Tsi1 and Tsi3 interact specifically with Tse1 and Tse3, respectively, and interactions between non-cognate pairs were not detected (Figure 2.4A). To investigate the immunity properties of the Tsi proteins, we measured their ability to inhibit toxicity of peri-Tse1 and peri-Tse3 in *E. coli*. Both Tsi1 and Tsi3 significantly decreased the toxicity of cognate, but not non-cognate Tse proteins (Figure 2.4B). These results show that the activity of periplasmic Tse1 and Tse3 is specifically inhibited by cognate Tsi proteins.

T6S delivers Tse1&3 to the periplasm

Most genes encoding immunity functions are essential in the presence of their cognate toxins. However, mutations that inactivate *tsi1* and *tsi3* are readily generated in *P. aeruginosa* strains that constitutively express and export Tse1 and Tse3. Based on this observation, we hypothesized that under standard laboratory conditions, the Tse proteins do not efficiently access their substrate in the periplasm. This suggests that T6S occurs by a mechanism wherein effectors are denied access to donor cell periplasm and are instead released directly to the periplasm of the recipient cell. According to this mechanism, the *tsi* genes would only be essential when a strain is grown under conditions that permit intercellular transfer of effectors between neighboring cells by the T6SS. As predicted, deletions in *tsi1* and *tsi3* severely impaired the growth of *P. aeruginosa* on a solid substrate, a condition conducive to T6S-based effector delivery (Figure 2.4C) (58, 74). In contrast, this growth inhibition did not occur in liquid media, which is not conducive to effector delivery by the T6SS (Figure 2.4D). The growth inhibition phenotype

required a functional T6SS and intact cognate effector genes, and consistent with the proposed functions of Tse1 and Tse3 in compromising cell wall integrity, growth of immunity deficient strains was fully rescued by increasing the osmolarity of the medium (Figure 2.4C).

Bioinformatic analyses suggested that the Tsi proteins reside in the periplasm – Tsi1 as a soluble periplasmic protein and Tsi3 as an outer membrane lipoprotein. These predictions were confirmed by subcellular fractionation experiments, which indicated enrichment of the proteins in the periplasmic compartment (Figure 2.5A). This result, taken together with the observation that the Tsi proteins interact directly with their cognate Tse proteins (Figure 2.4A), provided us with a means of addressing whether the T6SS delivers Tse proteins intercellularly to the periplasm. We reasoned that if the Tse proteins are indeed delivered to the periplasm of another bacterial cell, not only should we be able to observe intoxication between distinct donor and recipient strains of *P. aeruginosa*, but the production of an otherwise competent immunity protein that is mislocalized to the cytoplasm should not be able to prevent such intoxication.

In growth competition assays between distinct donor and recipient strains of *P. aeruginosa*, we found that recipient cells that lack Tse3 immunity and are incapable of self-intoxication (Δ*tse3* Δ*tsi3*), display a growth disadvantage against donor bacteria. This phenotype depends on H1-T6SS function and Tse3 in the donor strain. In the recipient strain, ectopic expression of wild-type *tsi3*, but not an allele encoding a signal sequence-deficient protein (Tsi3–SS), rescues the fitness defect (Figure 2.5B). Importantly, the Tsi3–SS protein used in this experiment does not reach the periplasm, and retains activity *in vitro* as judged by interaction with Tse3 (Figure

2.5A,C). Analogous experiments with Tsi1 were not feasible, as the protein was unstable in the cytoplasm.

The most parsimonious explanation for T6S-mediated intercellular toxicity by Tse1 and Tse3 is that the apparatus provides a conduit for the effectors through the outer membrane of recipient cells. This led us to predict that exogenous Tse1 and Tse3 would not lyse intact *P. aeruginosa*. Furthermore, we posited that if the outer membrane was the relevant barrier to Tse1 and Tse3 toxicity, compromising its integrity should render *P. aeruginosa* susceptible to exogenous administration of the enzymes.

To test these predictions, we measured lysis of permeabilized and intact *P. aeruginosa* following addition of exogenous Tse1. We did not test Tse3, as the filamentous phenotype induced by this enzyme would not affect non-growing, permeabilized cells. Intact *P. aeruginosa* cells were not affected by the addition of exogenous Tse1; conversely, permeabilized *P. aeruginosa* was highly susceptible to lysis by the enzyme (Figure 2.5D). Lysis induced by Tse1 is linked to its enzymatic function, as Tse1* failed to significantly lyse cells. In total, our data show that the T6SS breaches the outer membrane to deliver lytic effector proteins directly to recipient cell periplasm.

To determine whether the T6SS can target the Tse proteins to cells of another Gram-negative organism, we conducted growth competition assays between *P. aeruginosa* and *P. putida*. These bacteria can be co-isolated from the environment (75) and are likely to compete for niches (76). While inactivation of either *tse1* or *tse3* only modestly affected the outcome of *P. aeruginosa*-*P.*

putida competition assays, the fitness of *P. aeruginosa* lacking both genes or a functional T6SS was dramatically impaired (Figure 2.6). This partial redundancy is congruent with the enzymes exerting their effects through a single target–peptidoglycan–in the recipient cell. The fitness advantage provided by Tse1 and Tse3 was lost in liquid medium, consistent with cell contact-dependent delivery of the proteins to competitor cells (Figure 2.6). These data indicate that the T6SS targets its effectors to other species of bacteria and that these proteins can be key determinants in the outcome of interspecies bacterial interactions. In contrast with intraspecies intoxication, interspecies intoxication via the T6SS does not require the inactivation of a negative regulator of the system (eg. Δ*retS*), suggesting that T6S function is stimulated in response to rival bacteria.

DISCUSSION

Our data lead us to propose a model for T6S-catalyzed translocation of effectors to the periplasm of recipient bacteria (Figure 2.7). This model provides a mechanistic framework for understanding the form and function of this complex secretion system. Our findings strengthen the existing hypothesis that the T6SS is evolutionarily and functionally related to bacteriophage (9, 35, 57). Neither the T4 bacteriophage tail spike nor other components of the puncturing device are thought to cross the inner membrane; instead, bacteriophage DNA is released to the periplasm and subsequently enters the cytoplasmic compartment using another pathway (37). By analogy, the Tse proteins would utilize T6S components as a puncturing device to gain access to the periplasm, whereupon Tse2 may then utilize an independent route to access the cytoplasm (Figure 2.7).

Niche competition in natural environments has clearly selected for potent antibacterial processes; however, the human body is also home to a complex and competitive microbiota (77, 78). Commensal bacteria form a protective barrier, and the ability of pathogens to colonize the host is not only dependent upon suppression or subversion of host immunity, but also can depend on their ability to displace these more innocuous organisms (79-81). In polymicrobial infections, Gram-negative bacteria, including *P. aeruginosa*, often vie with other Gram-negative bacteria for access to nutrient-rich host tissue (82). Factors such as the T6SS, that influence the relative fitness of these organisms, are thus likely to impact disease outcome.

MATERIALS AND METHODS

Bacterial strains, plasmids, and growth conditions

P. aeruginosa strains used in this study were derived from the sequenced strain PAO1(83). *P. aeruginosa* strains were grown on either Luria-Bertani media (LB), or the equivalent lacking additional NaCl (LB low salt (LB-LS): 10 g bactopeptone and 5 g yeast extract per liter) at 37 °C supplemented with 30 μg ml^{-1} gentamycin, 25 μg ml^{-1} irgasan, 5% w/v sucrose, 40μg/ml X-gal, and stated concentrations of IPTG as required. *E. coli* strains included in this study included DH5α for plasmid maintenance, SM10 for conjugal transfer of plasmids into *P. aeruginosa*, BL21 pLysS for expression of Tse1 and Tse3 for toxicity and lysis, and Shuffle® T7 pLysS Express (New England Biolabs), for purification of Tse1 and Tse3. All *E. coli* strains were grown on either LB or LB-LS at 37 °C supplemented with 15 μg ml^{-1} gentamycin, 150 μg ml^{-1} carbenicillin, 50 μg ml^{-1} kanamycin, 30 μg ml^{-1} chloramphenicol, 200 μg ml^{-1} trimethoprim, 0.1% rhamnose, and stated concentrations of IPTG as required. *P. putida* used in this study was

the sequenced strain, KT2440 (76). *P. putida* was grown on LB or LB-LS at 30°C. In all experiments where expression from a plasmid was required, strains were grown on media supplemented with required antibiotics to select for plasmid maintenance.

Plasmids used for inducible expression were pPSV35CV for *P. aeruginosa* and pET29b+ (Novagen), pET22b+ (Novagen), pSCrhaB2 (84) and pPSV35CV for *E. coli* (85) . Chromosomal deletions were made as described previously (86).

DNA manipulations

The creation, maintenance, and transformation of plasmid constructs followed standard molecular cloning procedures. All primers used in this study were obtained from Integrated DNA Technologies. DNA amplification was carried out using either Phusion® (New England Biolabs) or Mangomix™ (Bioline). DNA sequencing was performed by Genewiz® Incorporated. Restriction enzymes were obtained from New England Biolabs. SOE PCR was performed as previously described (87).

Plasmid construction

pPSV35CV, pEXG2, and pSCrhaB2 have been described previously (84-86). *E. coli* pET29+ expression vectors for Tse1 and Tse3 were constructed by standard cloning techniques following amplification from PAO1 chromosomal DNA . Point mutations were introduced using Quikchange (Stratagene).

pPSV35CV and pSCrhaB2 expression vectors were generated by amplifying the genes from genomic DNA. A VSV-epitope tag was additionally cloned downstream of genes in pSCrhaB2 for the purpose of tagged-expression. All deletions were in-frame and were generated by exchange with deletion alleles constructed by SOE PCR.

Growth curves

For *E. coli* growth curves BL21 pLysS cells harboring expression plasmids were grown overnight in liquid LB shaking at 37°C and subinoculated to a starting optical density at 600 nm (OD_{600}) of between 0.01 and 0.02 in LB-LS. Cultures were grown to OD_{600} 0.1-0.2 and induced with 0.1mM IPTG. The vector pET29b+ was used for expression of native Tse1 and Tse3, and the pET22b+ vector was used for expression of periplasmic Tse1 and Tse3, and catalytic amino acid substitutions thereof. Both vectors added a C-terminal hexahistidine tag to expressed proteins, allowing for western blot analysis of expression. Samples for western blot analysis were taken 30 minutes after induction for Tse1, peri-Tse1, and peri-Tse1* and 45 minutes after induction for Tse3, peri-Tse3, and peri-Tse3*.

For *P. aeruginosa* growth curves, cells were grown overnight at 37 °C in liquid LB with shaking and sub-inoculated 1:1000 into LB-LS. Growth was measured by enumerating c.f.u. from plate counts of samples taken at the indicated time points.

***E. coli* toxicity measurements**

Overnight LB cultures of *E. coli* harboring pET22b+ expression vectors and *E. coli* harboring both pET22b+ and pSCrhaB2 expression vectors were serially diluted in LB to 10^6 as 10-fold

dilutions. These dilutions were spotted onto LB-LS agar with the following concentrations of inducer molecules: 0.075mM IPTG for pET22b+::*tse1*, pET22b+::*tse3* and the associated vector control, 0.02 mM IPTG and 0.1% rhamnose for pET22b+::*tse1* pSCrhaB2::*tsi1* and all associated controls, and 0.05mM IPTG and 0.1% rhamnose for pET22b+::*tse3* pSCRhaB2::*tsi3* and all associated controls. Pictures were taken between 20 and 26 hours after plating.

Subcellular fractionation

P. aeruginosa Δ*retS* cells harboring expression vectors for Tsi1-V, Tsi3-V, or Tsi3–SS-V and an additional vector expressing TEM-1 (pPSV18) were grown overnight. This overnight culture was sub-inoculated into LB supplemented with 0.1mM IPTG and grown to late logarithmic phase. Periplasmic and cytoplasmic fractions were prepared as described (88, 89).

E. coli BL21 cells harboring expression vectors for Tse1*, Tse3*, peri-Tse1*, and peri-Tse3* were grown overnight and sub-inoculated into LB. For Tse1* and Tse3* fractionation cells also carried an empty pET22b vector to provide expression of TEM-1. Cells were grown to an OD_{600} of 0.1 and induced with either 0.1 mM IPTG (Tse1* and peri-Tse1*) or 0.5 mM IPTG (Tse3* and peri-Tse3*). Cells were then harvested and fractionated as described (90).

Preparation of proteins and Western blotting

Cell-associated and supernatant samples were prepared as described previously (85). Western blotting was performed as described previously for α-VSV–G and α-RNA polymerase (42) with the modification that α-VSV–G antibody probing was performed in 5% BSA in Tris-buffered saline containing 0.05% v/v Tween 20. The α-Tse2 polyclonal rabbit antibody was raised against

the peptide YDGDVGRYLHPDKEC (GenScript). Western blots using both this antibody and the α-β-lactamase antibody(QED Biosciences Inc.) were performed identically to those using α-VSV–G. The α-His_5 Western blots were performed using the Penta-His HRP Conjugate Kit according to manufacturer's instructions (Qiagen).

Immunoprecipitation

BL21 pLysS cells expressing VSV–G-tagged Tsi1, Tsi3, or Tsi3–SS were pelleted and resuspended in lysis buffer (20mM Tris-Cl pH 7.5, 50 mM KCl, 8.0% v/v glycerol, 0.1% v/v NP 40, 1.0% v/v triton, supplemented with Dnase I (Roche), lysozyme (Roche), and Sigmafast^{tm} protease inhibitor (Sigma) according to manufacturer instructions). Cells were disrupted by sonication to release VSV–G-tagged Tsi proteins into solution. To this suspension, Tse1 and Tse3 were added to concentrations of 30 μg ml^{-1} and 25 μg ml^{-1}, respectively. This mixture was clarified by centrifugation, and a sample of the supernatant was taken as a pre-immunoprecipitation sample. The remainder of the supernatant was incubated with 100 μL α-VSV–G agarose beads (Sigma) for 2 hr at 4°C. Beads were washed three times with IP-wash buffer (100mM NaCl, 25mM KCl, 0.1% v/v triton, 0.1% v/v NP-40, 20mM Tris-Cl pH 7.5, and 2% v/v glycerol). Proteins were removed from beads with SDS loading buffer (125 mM Tris, pH 6.8, 2% (w/v) 2-Mercaptoethanol, 20% (v/v) Glycerol, 0.001% (w/v) Bromophenol Blue and 4% (w/v) SDS) and analyzed by Western blot.

Interbacterial competition assays

The inter-*P. aeruginosa* competitions were performed as described previously with minor modifications(14). For experiments described in both Figure 2.2B and Figure 2.5B, competition

assays were performed on nitrocellulose on LB or LB-LS 3% agar, respectively. Plate counts were taken of the initial inoculum to ensure a starting c.f.u. ratio of 1:1, and again after either 24 hours (Figure 2.2B) or 12 hours (Figure 2.5B) to obtain a final c.f.u. ratio. Donor and recipient colonies were disambiguated through fluorescence imaging (Figure 2.2B) or through the activity of a β−galactosidase reporter as visualized on plates containing 40μg/ml X-gal (Figure 2.5B). Data were analyzed using a two-tailed Student's T-Test.

For interspecies competition assays, overnight cultures of *P. aeruginosa* and *P. putida* were grown overnight in LB broth at 37°C and 30°C, respectively. Cultures were then washed in LB and resuspended to an OD_{600} of 4.0 for *P. aeruginosa* and 4.5 for *P. putida*. *P. putida* and *P. aeruginosa* were mixed in a one-to-one ratio by volume, this mixture was spotted on a nitrocellulose membrane placed on LB-LS 3% agar, and the c.f.u. ratio of the organisms was measured by plate counts. The assays were incubated for 24 hours at 30°C, after which the cells were resuspended in LB broth and the final c.f.u. ratio determined through plate counts. Data were analyzed using a one-tailed Student's T-Test.

Purification of Tse1 and Tse3

For purification, Tse1, Tse3, Tse1*, and Tse3* were expressed in pET29b+ vectors in Shuffle® Express T7 lysY cells (New England Biolabs). The proteins were purified to homogeneity using previously reported methods (91), except that in all steps no reducing agents or lysozyme were used.

Bioinformatic analyses

Predicted structural homology was queried using PHYRE (70). Alignments were performed using T-Espresso (92). Sequences of cell wall amidases and muramidases for alignments were obtained from seed sequences from PFAM (93). Critical motifs were defined by previous work in the study of NlpC/P60 and lytic transglycosylase/GEWL enzymes (71, 72).

Enzymatic assays

Tse1 and Tse1:* Purified peptidoglycan sacculi (300 μg) from *E. coli* MC1061(94) were incubated with Tse1 or Tse1* (100 μg/ml) in 300 μl of 20 mM Tris/HCl, pH 8.0 for 4 h at 37°C. A sample with enzyme buffer instead of Tse1 served as a control. The pH was adjusted to 4.8 and the sample was incubated with 40 μg/ml of the muramidase cellosyl (kindly provided by Höchst AG, Frankfurt, Germany) for 16 h at 37°C to convert the residual peptidoglycan or solubilized fragments into muropeptides. The sample was boiled for 10 min and insoluble material was removed by brief centrifugation. The reduced muropeptides were reduced with sodium borohydride and analysed by HPLC as described (94). Fractions 1 and 2 were collected, concentrated in a SpeedVac, acidified by 1% trifluoroacetic acid and analysed by offline electrospray mass spectrometry on a Finnigan LTQ-FT mass spectrometer (ThermoElectron, Bremen, Germany) as described (95).

Tse3 and Tse3.* Purified peptidoglycan sacculi (300 μg) from *E. coli* MC1061 were incubated with Tse3 or Tse3* (100 μg/ml) in 300 μl of 20 mM sodium phosphate, pH 4.8 for 20 h at 37°C. A sample with enzyme buffer instead of Tse3 served as a control. The samples were boiled for 10 min and centrifuged for 15 min (16,000×g). The supernatant was reduced with sodium

borohydride and analysed by HPLC as described above (supernatant samples). The pellet was resuspended in 20 mM sodium phosphate, pH 4.8 and incubated with 40 μg/ml cellosyl for 14 h at at 37°C. The samples were boiled for 10 min, cleared by brief centrifugation and analysed by HPLC as described above (pellet samples). Fractions 3, 4 and 5 were collected and analysed by mass spectrometry as described above.

Self-intoxication assays

PAO1 Δ*retS* attTn7::*gfp* cells bearing the indicated gene deletions were grown overnight in LB broth at 37°C. Cells were then diluted to 10^3 c.f.u./mL and 20 μL of this solution was placed on a nitrocellulose membrane placed on LB-LS 3% agar or LB 3% agar (contains 1.0% w/v NaCl). Fluorescence images were acquired following 23 hours of incubation at 37°C. For quantification and complementation, non-fluorescent strains were used and 1 mM IPTG was included for induction of all strains – except for the *tsi3*-complemented strain, for which no IPTG was required to achieve comparable levels of expression to the *tsi3*–SS-complemented strain. At 23 hours cells were resuspended in LB. Plate counts of the initial inoculum and the final suspension were used to determine growth. Data were analyzed using a one-tailed Student's T-test.

Fluorescence microscopy

BL21 pLysS cells harboring periplasmic-expression vectors for Tse1, Tse3, and catalytic substitution mutants were grown in conditions identical to those in the *E. coli* growth curve experiments. Cells were harvested 30 minutes post-induction for Tse1 experiments and one-hour post-induction for Tse3 experiments. These cells were resuspended in PBS and incubated with 0.3 μM TMA-DPH (1-(4-trimethylammoniumphenyl)-6-phenyl-1,3,5-hexatriene *p*-

toluenesulfonate) for 10 minutes. The stained cells were placed on 1% agarose pads containing PBS for microscopic analysis. Microscopy was performed as described previously (85).

EDTA-permeabilization lysis assay

Assays were performed as previously described with minor modifications (96). Cells were sub-inoculated into LB broth from overnight liquid cultures and grown to late logarithmic phase. Cells were washed in 20 mM Tris-Cl pH 7.5 and Tse1, Tse1*, or lysozyme were added to a final concentration of 0.01 mg/mL. An initial OD_{600} measurement was taken before EDTA pH 8.0 was added to a final concentration of 1.5 mM. Cells were incubated with shaking at 37°C for 5 minutes and a final OD_{600} reading was taken. *P. aeruginosa* undergoes rapid autolysis under these assay conditions, thus lysis was expressed as a percentage of lysis above a buffer-only control.

Acknowledgements

We thank P. Singh, E. Nester, H. Kulasekara, N. Salama, E.P. Greenberg, L. Ramakrishnan and members of the Mougous laboratory for insightful discussions and critical reading of the manuscript, the Harwood laboratory for use of their microscope, and Joe Gray of the Pinnacle Laboratory of Newcastle University for MS analysis. This work was supported by the National Institutes of Health (J.D.M.; RO1 AI080609) and the European Commission within the DIVINOCELL programme (W.V.). A.B.R was supported by a Graduate Research Fellowship from the National Science Foundation.

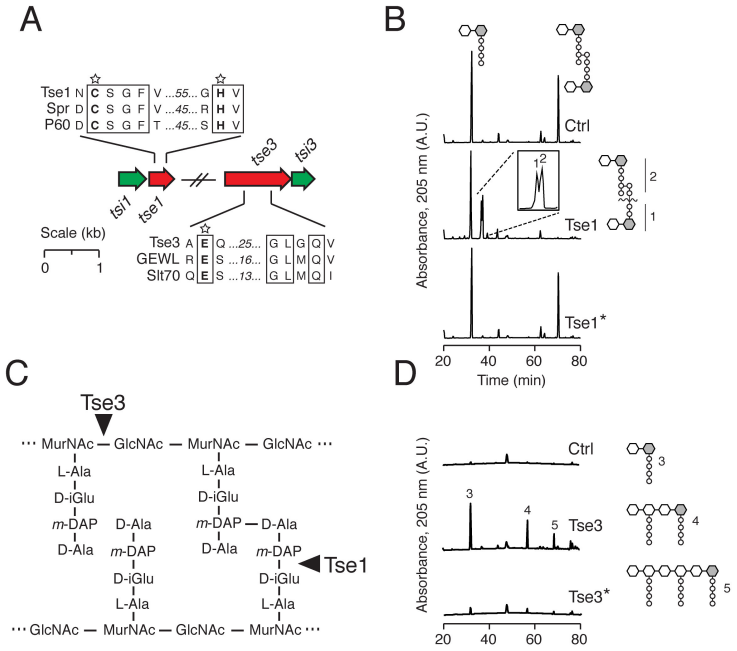

Figure 2.1: Tse1 and Tse3 are members of the amidase and muramidase enzyme families. (A) Genomic organization of *tse1* and *tse3* and homology with characterized amidase and muramidase enzymes, respectively. Highly conserved (boxed) and catalytic (starred) residues indicated. **(**B,D) Partial HPLC chromatograms of soluble *E. coli* peptidoglycan products resulting from (B) digestion with Tse1 and subsequent cleavage with cellosyl or (D) digestion with Tse3 alone. Peak assignments were made based on MS; predicted structures are shown schematically with hexagons and circles corresponding to sugars and amino acid residues, respectively. Reduced sugar moieties are shown with grey fill. **c.** Simplified representation of Gram-negative peptidoglycan showing cleavage sites of Tse1 and Tse3 based on data summarized in (B) and (D).

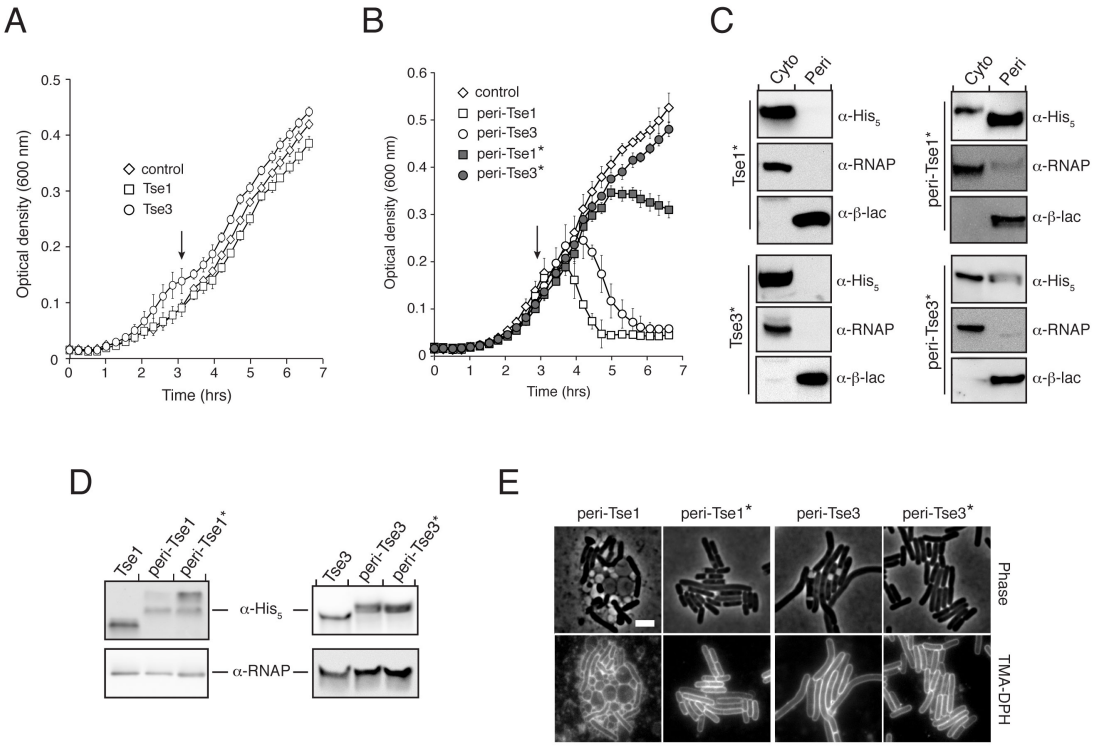

Figure 2.2: Tse1 and Tse3 are lytic when directed to the periplasm. (A,B) Growth in liquid media of *E. coli* producing the indicated Tse proteins. Periplasmic localization was achieved by fusion to the PelB leader sequence (97). Cultures were induced at the indicated time (arrow). Error bars ± s.d. (n=3). (C) . Western blot analysis of subcellular distributions of the indicated Tse* proteins in E. coli. To avoid cellular lysis during sample preparation, the catalytically inactive Tse variants (Tse*) were used in this experiment. Native proteins (B) and those containing an N-terminal PelB leader sequence (V) were analyzed. Equivalent fractions of the cytoplasmic (Cyto) and periplasmic (Peri) samples were loaded in each panel. The oligohistidine-tagged Tse proteins were detected with an α-His5 antibody. RNA polymerase (RNAP) and β-lactamase (β-lac) enzymes were used as cytoplasmic and periplasmic fractionation controls, respectively. (D) Western blot analysis of total Tse protein levels for strains used in experiments presented in (A) and (B). RNA polymerase was used as a loading control. Error bars ± s.d. (n=3). (E) Representative micrographs of strains shown in (B) acquired prior to complete lysis. The lipophilic dye TMA-DPH is used to highlight the cellular membranes All images were acquired at the same magnification. Scale bar = 2 μm.

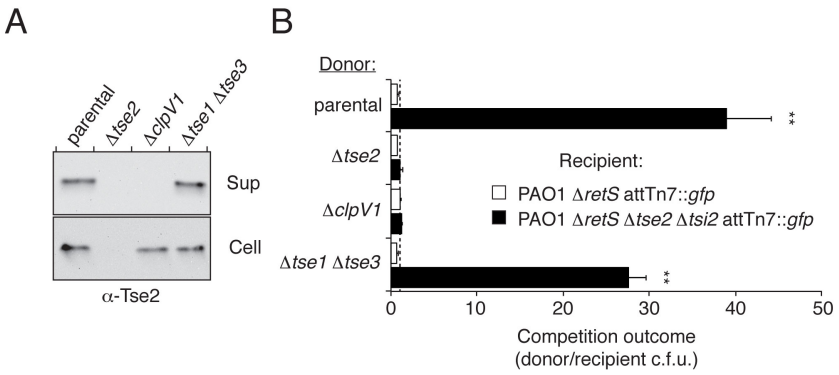

Figure 2.3: Tse1 and Tse3 are not required for Tse2 export or transfer to recipient cells via the T6S apparatus. (A) Western blot analysis of supernatant (Sup) and cell-associated (Cell) fractions of the indicated *P. aeruginosa* strains. The parental background for all experiments represented in this figure is PAO1 Δ*retS*, a strain in which the H1-T6SS is activated constitutively (42, 98). (B) Growth competition assays between the indicated donor and recipient strains under T6S-conducive conditions. Experiments were initiated with equal colony forming units (c.f.u.) of donor and recipient bacteria as denoted by the dashed line. The Δ*clpV1* strain is a T6S-deficient control. Asterisks indicate significant differences in competition outcome between recipient strains against the same donor strain. $^{**}P < 0.01$. Error bars ± s.d. (n=3).

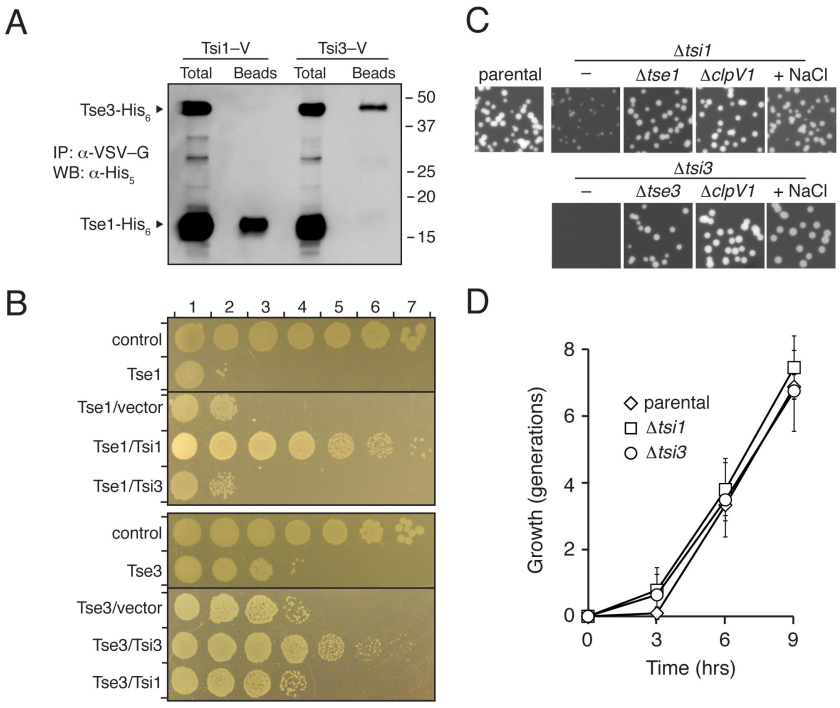

Figure 2.4: Tsi1 and Tsi3 provide immunity to cognate toxins. (A) Western blot analysis of hexahistidine-tagged Tse proteins (–His_6) in total and bead-associated fractions of an α-VSV–G (vesicular stomatitis virus glycoprotein) immunoprecipitation of VSV–G epitope fused Tsi proteins (–V) from *E. coli*. (B) Growth of *E. coli* harboring a vector expressing the indicated *tse* gene (top panels) or vectors expressing the indicated *tse* and *tsi* genes (bottom panels). Numbers at top indicate 10-fold serial dilutions. (C) Fluorescence micrographs showing colony growth of the indicated strains. The parental background for this experiment was PAO1 Δ*retS* attTn7::*gfp*. Growth of the Δ*tsi* strains was rescued by the addition of 1.0% w/v NaCl to the underlying medium. (D) Replication rates of the indicated *P. aeruginosa* strains in liquid medium of low osmolarity formulated as in (C). The parental strain used in this experiment was PAO1 Δ*retS*. Error bars ± s.d. (n=3).

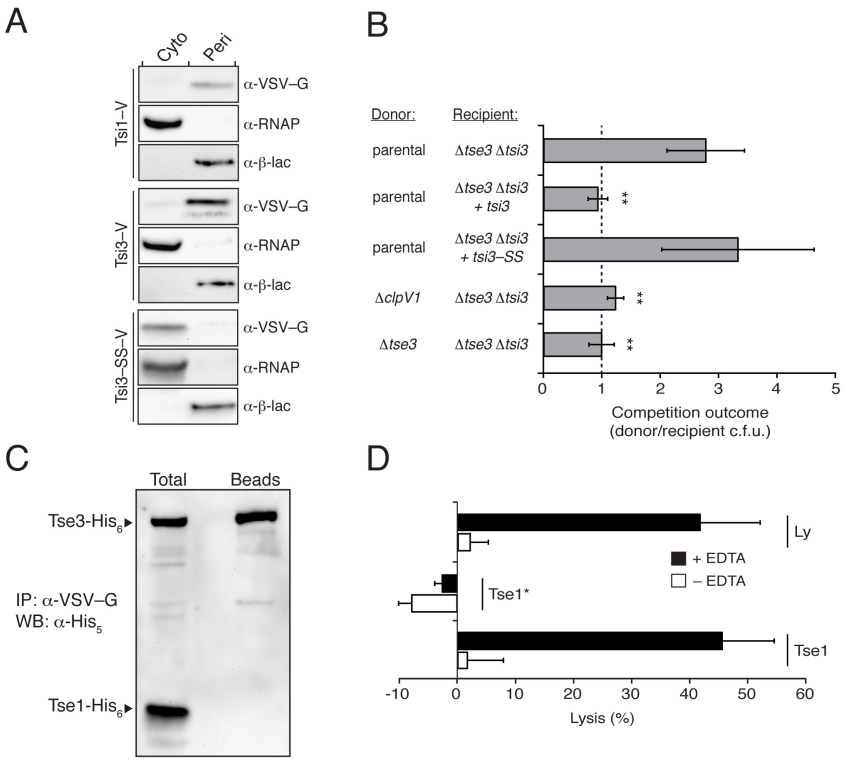

Figure 2.5: Tse1 and Tse3 delivered to the periplasm provide a fitness advantage to donor cells. (A) Western blot analyses of cytoplasmic (Cyto) and periplasmic (Peri) fractions of *P. aeruginosa* strains producing Tsi1–V, Tsi3–V or Tsi3–SS–V. Equivalent ratios of the Cyto and Peri samples were loaded in each panel. RNA polymerase (RNAP) and β-lactamase (β-lac) enzymes were used as cytoplasmic and periplasmic fractionation controls, respectively. The presence of Tsi3–a predicted outer membrane lipoprotein–in the periplasmic fraction is consistent with previous studies utilizing this method of fractionation (88). (B) Growth competition assays between the indicated donor and recipient strains under T6S-conducive conditions. Experiments were initiated with equal c.f.u. of donor and recipient bacteria as denoted by the dashed line. The parental strain used in this experiment was PAO1 Δ*retS*. All donor strains were modified at the attB site with *lacZ*. Asterisks indicate outcomes significantly different than parental versus Δ*tse3* Δ*tsi3*. Error bars ± s.d. (n=4). $^{**}P < 0.01$. (C) Western blot analysis of hexahistidine-tagged Tse proteins (–His6) in total and bead-associated fractions of an α-VSV–G immunoprecipitation of the VSV–G-fused Tsi3–SS protein from *E. coli.* (D) Lysis of EDTA-permeabilized or intact *P. aeruginosa* cells with equal quantities of Tse1, Tse1*, or Lysozyme (Ly). Lysis was normalized to a buffer control. Error bars ± s.d. (n=3).

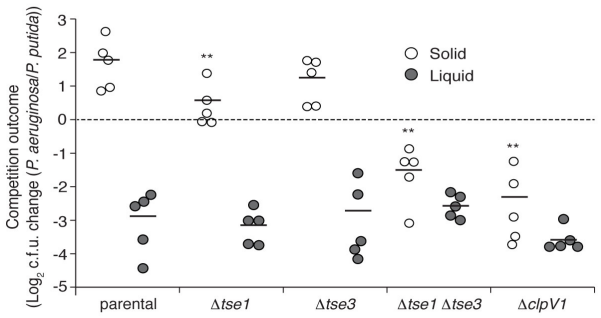

Figure 2.6: Tse1 and Tse3 contribute to *P. aeruginosa* fitness in polymicrobial growth. Competitive growth of *P. aeruginosa* against *P. putida* on solid (open circles) or in liquid (filled circles) medium. Competition outcome was defined as the c.f.u. ratio (*P. aeruginosa/P. putida*) divided by the initial ratio. The dotted line represents the boundary between competitions that increase in *P. aeruginosa* relative to *P. putida* (above the line) and those that increase in *P. putida* relative to *P. aeruginosa* (below the line). The parental strain used in this experiment was *P. aeruginosa* PAO1. Asterisks above competitions denote those where the outcome (*P. aeruginosa*/*P. putida*) was significantly less than the parental ($P < 0.05$). Horizontal bars denote the average value for each dataset (n=5).

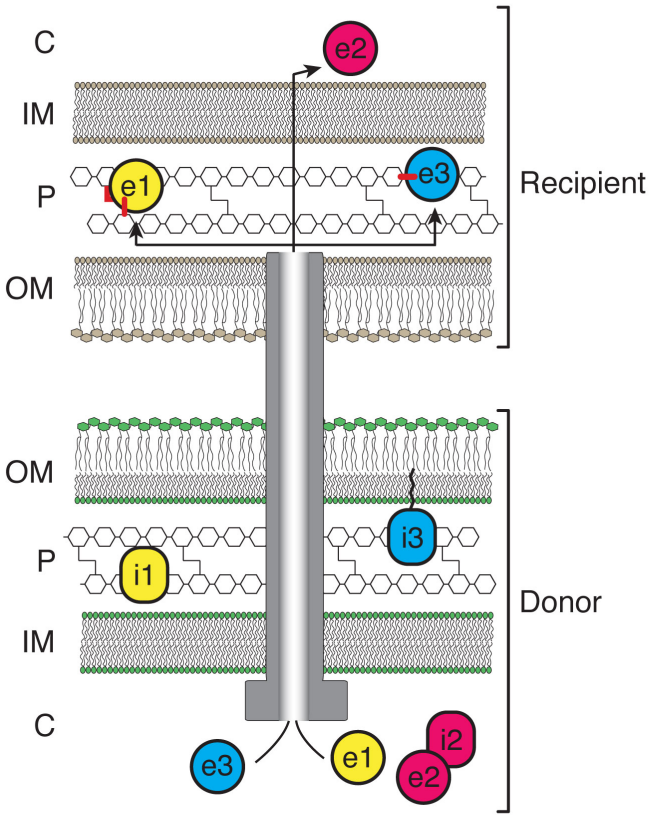

Figure 2.7: Proposed mechanism of T6S-dependent delivery of effector proteins. The schematic depicts the junction between competing bacteria, with a donor cell delivering the Tse effector proteins through the T6S apparatus (grey tube) to recipient cell periplasm. Effector and immunity proteins are shown as circles and rounded rectangles, respectively. Bonds in the peptidoglycan that are predicted targets of the effector proteins are highlighted (red). Cytoplasm (C), inner membrane (IM), periplasm (P), and outer membrane (OM) of both bacteria are shown.

CHAPTER III

A widespread type VI secretion effector superfamily identified using a heuristic approach

Published as: Russell, A.B., Singh, P., Brittnacher, M., Bui, N.K., Hood, R.D., Carl, M.A., Agnello, D.M., Schwarz, S., Goodlett, D.R., Vollmer, W., Mougous, J.D. 2012. *Cell Host & Microbe* 11, 538-549.

A.B.R. contribution: Working with J.D.M. conceived of study and wrote paper. Performed all informatic analyses of Tae proteins downstream of the application of heuristic values by M.B. (use of structural prediction servers, manual curation, alignments, phylogeny, genomic context, genetic context), *E. coli* toxicity experiments and expression analysis, *B. thailandensis* competition experiments, and experiments demonstrating *P. fluorecens* secretion of $Tae3^{PF}$. Generated a portion of the *E. coli* expression vectors, the *P. fluorescens* Δ*retS* suicide construct and resulting strain, and the *P. fluorescens* $tae3^{PF}$ expression vector.

ABSTRACT

Sophisticated pathways facilitate information exchange between interfacing bacteria. A type VI secretion system (T6SS) of *Pseudomonas aeruginosa* was shown to deliver cell wall-targeting effectors to neighboring cells. However, the generality of bacteriolytic effectors, and moreover, of antibacterial T6S, remained unknown. Here we discovered a phylogenetically disperse superfamily of T6S associated peptidoglycan-degrading effectors. These were identified informatically using parameters derived from experimentally validated members. The effectors separate into four families, which we demonstrate are composed of peptidoglycan amidase enzymes of differing specificities. We observe that effectors strictly co-occur with cognate immunity proteins, indicating that self-intoxication is a general property of antibacterial T6SSs and effector delivery by the system exerts a strong selective force in nature. The presence of antibacterial effectors in a plethora of organisms, including many that inhabit or infect polymicrobial niches in the human body, suggests that the system could mediate interbacterial interactions of both environmental and clinical significance.

INTRODUCTION

Bacteria are under immense competitive pressure for limited resources, which has shaped the evolution of a number of antagonistic antibacterial pathways (62, 99, 100). These pathways often target conserved processes that are not easily modified. One such target is bacterial cell wall peptidoglycan, a structure that is essential for maintaining osmotic stability and cell shape (18). Despite its many variations, the fundamental structure of peptidoglycan is highly conserved throughout the domain Bacteria. The Gram-negative cell wall is sequestered from the extracellular milieu by an outer membrane; nevertheless, some cell wall-targeting molecules can

overcome this barrier. For example colicin M, which degrades peptidoglycan precursors, or pesticin, which degrades the mature sacculus (65, 101).

The type VI secretion system (T6SS) of Gram-negative bacteria is a contact-dependent protein translocation apparatus that resembles an inverted bacteriophage puncturing device (57, 102-104). The system has recently been demonstrated to act as a pathway for the delivery of antagonistic effectors to adjacent bacteria (14, 105). This finding is consistent with the structural homology of the system to bacteriophage, as both effector delivery and phage entry appear to occur in an analogous fashion. Proteins delivered to bacteria by this system include Tse1-3 (type VI secretion exported 1-3), substrates of the hemolysin co-regulated protein secretion island I-encoded T6SS of *Pseudomonas aeruginosa* (H1-T6SS) (14). Tse1 and Tse3 are bacteriolytic enzymes that degrade the peptidoglycan of recipient bacteria, whereas Tse2 is bacteriostatic through an unknown mechanism (105).

Unlike other peptidoglycan-targeting molecules that affect Gram-negative bacteria, Tse1 and Tse3 have no intrinsic means of translocating the outer membrane. These effectors instead rely on the T6S apparatus for delivery to the periplasmic compartment of recipient cells. Within the periplasm, Tse1, as a cell wall amidase, cleaves the γ-D-glutamyl-L-*meso*-diaminopimelic acid bond, while Tse3, as a muramidase, hydrolyzes the β(1,4) linkage between *N*-acetylmuramic acid and *N*-acetyglucosamine (105). Both Tse1 and Tse3 appear to transit through the T6S apparatus in one step, bypassing the periplasmic space of the donor cell. This prevents the producing cell from intoxicating itself with Tse1 or Tse3 in transit. However, the H1-T6SS of *P. aeruginosa* can target neighboring, clonal, *P. aeruginosa* cells (14). Due to the ability of the H1-

T6SS to engage in self-targeting interactions, *P. aeruginosa* cells can intoxicate one-another via T6SS-delivered effectors. This intercellular self-intoxication is overcome through the production of specific cognate immunity proteins, Tsi1 and Tsi3, which reside in the periplasmic compartment and protect against the activities of Tse1 and Tse3, respectively (105, 106).

Thus far many of our mechanistic insights into bacteria-targeting T6S derive from the H1-T6SS and its substrates. Without further understanding obtained from the identification of other T6SS substrates, it remains unclear whether these insights are generally applicable. For example, our laboratory previously demonstrated that T6SS-1 of the soil saprophyte *Burkholderia thailandensis* provides cell contact-dependent fitness to the organism during growth competition assays against certain Gram-negative bacteria (58). The specific effector proteins utilized by T6SS-1, and for several other demonstrated antibacterial T6SSs, have yet to be defined (60, 107). Therefore, a major bottleneck in the study of bacteria-targeting T6S is the identification of the substrates that mediate T6S-dependent effects.

Both bioinformatic and traditional experimental approaches have been fruitful in the identification of novel proteins exported by alternative bacterial secretion pathways. However, the application of such approaches to the identification of T6S substrates is complicated by the fact that determinants for passage through the T6S apparatus are not currently apparent and the pathway is repressed under standard laboratory conditions in many organisms (108, 109). Here we sought to develop a general method for the identification of antibacterial T6S substrates. We initiated our study by defining substrates of *B. thailandensis* T6SS-1 using mass spectrometry (MS). Analysis of these data revealed characteristics shared between a *B. thailandensis* T6SS-1

substrate and proteins previously found to transit the H1-T6SS of *P. aeruginosa*. These commonalities were exploited to develop a heuristic informatic approach for the large-scale identification of T6S substrates. With this approach, we discovered a phylogenetically diverse and broadly distributed superfamily of T6S effectors. Our findings reveal a general paradigm describing the mechanism of interbacterial T6S, and suggest that it plays a broad role in shaping clinically- and environmentally-relevant microbial communities.

RESULTS

Identification and genomic analysis of T6SS-1 substrates

In an effort to deepen our understanding of interbacterial T6S effector function, we sought to define the substrates of *B. thailandensis* T6SS-1 (58). To this end, we first established a reference secretome using wild-type *B. thailandensis*. While the T6SS ultimately translocates proteins into a recipient cell, previous studies utilizing mass spectrometry have demonstrated that effector proteins are spuriously shed into the extracellular milleux. Using MS, we identified a total of 232 proteins in the supernatant fraction of log phase cultures. Of these, 114 were present in each of the three replicates conducted (Table 3.1). This variability stems from low-abundance proteins; the average spectral count of variably present proteins was < 20% (8 spectral counts (SC)) of those detected in all replicates (43 SC). Based on this correlation, we did not include variably present proteins in further analyses.

Next we determined the secretome of *B. thailandensis* ΔT6SS-1 and compared it to the wild-type reference. This analysis identified 13 proteins reproducibly absent from the ΔT6SS-1 secretome (Figure 3.1A and Table 3.1). The absence of these proteins appeared specific, as their average abundance was high (34 SC) and the secretion of the remaining reference secretome proteins was

largely unaffected in the mutant strain. Our observations also appeared relevant to T6S, as only two of the proteins are predicted substrates of alternative secretory pathways and four are VgrG homologs (Table 3.1). To determine the specificity of these proteins for export by T6SS-1, we also measured the secretome of a *B. thailandensis* strain with an inactivating mutation in another of its five T6SSs. We chose T6SS-5 for this experiment, as this system is the only other to have been linked to a phenotype – attenuated virulence in mammalian infection models – in *B. thailandensis* and closely related organisms (58, 110, 111). Notably, none of the 13 proteins dependent upon T6SS-1 for export were absent or found in significantly lower abundance in the ΔT6SS-5 secretome (Figure 3.1B). Finally, the secretome of a strain inactivated in all five T6SSs (ΔT6S) lacked only one protein in addition to those that were T6SS-1-dependent (Figure 3.1C). From these data, we conclude that T6SS-1 is specifically required for the export of at least 13 proteins from *B. thailandensis*. Furthermore, our analyses demonstrate that the remaining *B. thailandensis* T6SSs may be quiescent with regard to substrate export under *in vitro* conditions.

Substrate export via the T6SS is thought to occur in a Sec-independent fashion. Thus, the lack of two proteins, BTH_II0639 and BTH_I2723, containing predicted N-terminal signal peptides from the ΔT6SS-1 secretome is most likely explained by pleiotropic effects, potentially stemming from regulatory affects of effector retention in the cytoplasm or inability to assemble an active T6SS apparatus, rather than their direct reliance upon T6SS-1 for export. In light of these data, we do not classify these proteins as putative T6SS-1 substrates in this report.

The genes encoding the remaining 11 proteins requiring *B. thailandensis* T6SS-1 for export clustered non-randomly in the genome. Five are found within a single gene cluster, and four

others are distributed among the two copies of a region of the genome that apparently underwent a recent duplication event (Figure 3.1D). This duplication event gave rise to two *vgrG* genes encoding identical VgrG proteins, making it impossible to determine the relative contributions of these loci to the secreted protein we observe using MS (Table 3.1).

Several of the putative T6SS-1 substrates have predicted functions consistent with the known role of T6SS-1 in mediating interbacterial interactions. Structure-based algorithms predict extensive structural similarity between two of the proteins, BTH_II0310 and BTH_I2691, and bacteriocins LlpA and colicin Ia, respectively (112, 113). Although to our knowledge there is no prior experimental evidence for the secretion of a bacteriocin-like protein by a T6SS, predicted bacteriocins have been found in association with the T6SS (46). Particularly germane to our current study, we found that another putative substrate of T6SS-1, BTH_I0068, has predicted structural homology with peptidoglycan amidase enzymes (114). This is of interest, as our laboratory previously showed Tse1, an antibacterial effector of the H1-T6SS of *P. aeruginosa*, acts as a peptidoglycan-degrading amidase (105). Given the genetic linkage and predicted antibacterial properties of many of the putative *B. thailandensis* substrates, it is likely that these proteins are extracellular components or effectors of T6SS-1. In our effort to better understand the significance of cell wall targeting T6S effectors, we decided to focus further study on BTH_I0068.

BTH_I0068–BTH_I0069 are a T6S amidase effector–immunity pair

BTH_I0068 has a high degree of predicted structural similarity with the CHAP family of peptidoglycan amidases, including catalytic cysteine and histidine residues (Figure 3.2A) (115,

116). These residues are also conserved in Tse1, which has predicted structural homology with related group of peptidoglycan amidases (NlpC/P60) (114). We observed additional similarities between BTH_I0068 and Tse1 beyond predicted catalytic activity. Like Tse1, BTH_I0068 lacks a Sec signal peptide despite its predicted function in the periplasm. Also similar to Tse1, the *Burkholderia* protein lacks regulatory domains often associated with peptidoglycan amidases. Finally, both proteins are encoded in predicted bicistrons with a gene encoding a periplasmic protein (Figure 3.1D). In the case of Tse1, this periplasmic protein is Tsi1, an immunity protein that specifically prevents Tse1-dependent intoxication (105). Despite their lack of significant primary sequence homology, these observations led us to hypothesize that BTH_I0068–BTH_I0069 constitutes a T6S effector–immunity (EI) pair analogous to Tse1–Tsi1.

To determine the extent of functional similarity between BTH_I0068 and Tse1, we first sought to establish whether BTH_I0068 displays amidase activity. To test this, we incubated purified BTH_I0068 with peptidoglycan sacculi prepared from *E. coli*. Subsequent muramidase digestion followed by HPLC and MS analysis of soluble products indicated that BTH_I0068 cleaves peptidoglycan tetrapeptide-tetrapeptide crosslinks at the D,D amide bond between *meso*-diaminopimelic acid (*m*DAP) and D-alanine (Figure 3.2B). As certain species have higher degrees of the nascent crosslink form (tetrapeptide–pentapeptide), we also determined whether BTH_I0068 is able to process peptidoglycan crosslinks in this configuration. The activity of BTH_I0068 was not affected by the presence of the additional D-alanine residue, suggesting that BTH_I0068 could act broadly as an amidase to cleave peptidoglycan crosslinks (Figure 3.2C).

Overexpression of typical cell wall-degrading amidases is deleterious to *E. coli*. However, BTH_I0068 lacks a signal peptide and thus in the absence of the T6SS should only be toxic when directed to the periplasm through the addition of an N-terminal signal peptide. As predicted for a bacteriolytic T6S substrate analogous to Tse1, *E. coli* viability was reduced only when BTH_I0068 was artificially targeted to the periplasm (Figures 3.2D and E).

Next we asked whether the predicted periplasmic protein encoded adjacent to BTH_I0068, BTH_I0069, functions as a cognate immunity protein – analogous to Tsi1. Co-expression experiments in *E. coli* showed that BTH_I0069 provides significant rescue to cells expressing BTH_I0068, whereas Tsi1 failed to provide such rescue (Figure 3.2D). Taken together, we conclude that BTH_I0068–BTH_I0069 define an amidase–immunity pair analogous – and not homologous – to *P. aeruginosa* Tse1–Tsi1.

If BTH_I0068, like Tse1, is an effector, we reasoned that *B. thailandensis* should be able to intoxicate neighboring bacteria with the protein in a T6SS-dependent manner. We tested this by performing growth competition assays under cell contact-promoting conditions. These assays revealed that *B. thailandensis* recipient cells bearing a deletion of the BTH_I0068–BTH_I0069 bicistron display a fitness defect relative to wild-type donor strains (Figure 3.2F). Recipient fitness was rescued either through inactivation of T6SS-1 in the donor strain or by expression of BTH_I0069 in the recipient cell. Together with our *in vitro* studies, these data demonstrate that BTH_I0068–BTH_I0069 constitute a T6S EI pair. Furthermore, these data suggest the model for T6S interbacterial effector targeting derived from studies of *P. aeruginosa* H1-T6SS is

applicable to *B. thailandensis* T6SS-1. We propose the name Tae2 (type VI amidase effector) for BTH_I0068 and Tai2 (type VI amidase immunity) for BTH_I0069.

Identification of novel T6S EI pairs

All currently defined T6SS EI pairs lack identifiable primary sequence homology. In spite of an inability to link EI pairs phylogenetically, certain physical and contextual properties appear intrinsic to their function. We hypothesized that parameters describing these properties could be used in a heuristic informatic method for the *de novo* prediction of novel EI pairs from genomic sequences. Such an approach was previously successful in the identification of type III secretion effectors from the *Pseudomonas syringae* DC3000 genome (117, 118).

We initiated our search by developing a comprehensive set of parameters describing characterized T6S EI pairs. These include parameters common to all pairs (Figure 3.3A, orange), those indicative of periplasmically-targeted pairs (Figure 3.3A, blue), and those specific to amidase pairs (Figure 3.3A, brown). Individually, the parameters describing T6S EI pairs are weak in their discriminatory capacity. However, we reasoned that by restricting our search to amidase EI pairs, thus allowing the application of all parameters serially, we could achieve enrichment sufficient for computationally intensive secondary analyses.

To identify novel T6S amidase EI pairs, we applied our parameters as constraints to a set of 193 phylogenetically diverse organisms encoding T6SSs (Figure 3.3B). This procedure provided a group of 419 candidate EI pairs, a 99.9% reduction in the sample set. The extent of this reduction enabled detailed examination of each EI pair, including structure prediction analysis – already

established as a valuable means for identifying sequence divergent amidase effectors (105). This second step further reduced our set of candidate EI pairs to 16 non-orthologous pairs (Table 3.2). Based on genomic analyses, and biochemical and genetic experiments discussed in subsequent sections, we considered the pairs in this group as our set of high-confidence peptidoglycan amidase effectors. In the last step of our pipeline, we expanded the number of EI amidase pairs to 51 by searching for homologous sequences in the entire non-redundant sequence database (Figure 3.3B).

Although our search for EI pair homologs was conducted in an unbiased dataset, with only one exception, all homologous pairs we identified reside in Gram-negative organisms encoding T6SSs. This finding is unlikely to occur through chance, as even when we consider the phylogenetic group most enriched in T6S, the Proteobacteria, only a minority possess the system (17.6%, $p < 0.0001$) (6). Vertical inheritance is one factor that clearly contributes to the non-random association between EI pairs and the T6SS. However, we note that many homologous EI pairs are found both in distantly related organisms and in species with close-relatives that lack T6S. The only organism lacking a T6SS that we found to contain an EI pair is *Salmonella enterica* subspecies enterica serovar Paratyphi B (*S.* Paratyphi B); however, Blondel and colleagues noted the loss of T6S in this organism was a recent event (46). Importantly, all effector homologs in our expanded set contain sequence motifs characteristic of CHAP and NlpC/P60 amidase enzymes (71, 115).

EI pairs segregate into four families

The 51 putative effectors discovered in our screen segregate into four families based on overall primary sequence homology (Figure 3.4). These families are disparate, confounding attempts to place them in a phylogenetic context using full-length alignments. However, we did identify two relatively conserved motifs surrounding predicted catalytic residues (Figure 3.4). Phylogenetic analyses based on these regions, which owing to their involvement in catalysis are subject to less genetic drift, yielded a tree with family assignments matching those derived from full-length sequence homology (Figure 3.5).

The majority of the immunity proteins identified in our search mapped to EI bicistrons. Among these, homologous immunity proteins distribute with homologous effectors; therefore, we assigned immunity proteins into families reflecting their cognate effectors. Divergence within immunity protein families was considerably higher than that found within the effector families (Figure 3.6). This is not surprising, as functional constraints on immunity proteins (effector binding) are likely less restrictive than those on the effectors (immunity binding and catalysis). The remaining 23 immunity proteins group into two categories: those associated with EI pairs (3) and those coded for by orphan immunity genes (20). Immunity genes associated with EI pairs appear to have arisen through gene duplication events, as in each instance they belong to the same immunity family as the neighboring immunity gene. In summary, we have found that the putative T6S effectors identified in our screen distribute coincident with cognate immunity proteins into four phylogenetically discernable families. As expected based on results garnered from detailed studies in *P. aeruginosa* and *B. thailandensis*, this observation strongly implies coevolution of effector and immunity proteins (105).

Characterization of novel EI families

An important feature of the informatic approach we utilized for defining novel T6S effectors is its lack of reliance on primary sequence homology. While this non-sequence-biased approach allowed the discovery of four highly divergent families, it also increases the probability that one or more of these might include either peptidoglycan amidase effectors with novel catalytic specificity, effectors with unexpected activity, or false-positives not representing effector proteins.

To test whether putative effector families 3 and 4 include cell wall amidase enzymes, we purified one member from each family and ascertained its activity towards *E. coli* peptidoglycan sacculi. Similar to Tae2, the family 3 enzyme from *S.* Typhi ($Tae3^{TY}$) hydrolyses DD-crosslinks between D-*m*DAP and D-alanine (Figure 3.7A). In contrast, the family 4 enzyme from *S.* Typhimurium ($Tae4^{TM}$) hydrolyzes peptide crosslinks at the γ-D-glutamyl-*m*DAP LD-bond, like Tse1 (Figure 3.7A). However, unlike Tse1, $Tae4^{TM}$ cleaves acceptor and non-crosslinked tetrapeptide stems, and does not cleave the donor peptide stem (Figure 3.7B). While pentapeptide-enriched peptidoglycan is readily degraded by $Tae3^{TY}$, it is a poor substrate for $Tae4^{TM}$.

Having demonstrated that $Tae3^{TY}$ and $Tae4^{TM}$ are amidases, we next investigated whether these enzymes and their corresponding immunity proteins fit additional characteristics of T6S EI proteins that have emerged from studies of Tse1, Tse3, Tae2, and cognate immunity proteins. Consistent with previously validated effectors, we found that $Tae3^{TY}$ and $Tae4^{TM}$ are highly toxic when artificially directed to the periplasm of *E. coli*, but not when expressed in their native form

(Figures 3.7C and D). Also, we observed that the periplasmic proteins, Tai3^{TY} and Tai4^{TM}, encoded adjacent to *tae3*^{TY} and *tae4*^{TM}, respectively, could rescue this toxicity.

As a final means of functionally validating the EI pairs identified by our informatics approach, we tested the competency of one novel effector to serve as a T6S substrate. Since most T6SSs are repressed under *in vitro* cultivation condition and there is as yet no general means of T6S activation, we restricted our efforts to systems with known regulation. In Pseudomonads, certain T6SSs are posttranscriptionally regulated by the Gac/Rsm pathway (119-122). This pathway is modulated by two hybrid sensor kinases, LadS and RetS, which activate and repress T6S, respectively. In *P. aeruginosa*, deletion of *retS* leads to constitutive effector export by the H1-T6SS (14).

P. fluorescens Pf-5 is closely related to *P. aeruginosa* and encodes a single T6SS that is regulated by the Gac/Rsm pathway (121). Despite these similarities, *P. fluorescens* lacks homologs of H1-T6SS substrates, Tse1-3. Interestingly, our screen identified a family 3 EI pair in this organism (PFL_5498-PFL_5499, Tae3^{PF}-Tai3^{PF}), a family not represented in *P. aeruginosa.* While wild-type *P. fluorescens* did not secrete detectable amounts of Tae3^{PF}, an in-frame deletion of *retS* in this organism resulted in constitutive secretion of the putative effector (Figure 3.7E, data not shown). In order to determine if Tae3^{PF} export occurs in a T6S-dependent manner, we introduced an in-frame deletion of *clpV* into the *P. fluorescens* Δ*retS* background. This deletion abrogated secretion, demonstrating that Tae3^{PF} is a substrate of the *P. fluorescens* T6SS. In total, these data strongly suggest that the proteins identified in our screen include four

evolutionarily distinct amidase families that act, along with their cognate immunity proteins, as T6S EI pairs.

EI diversity reflects function

Immunity proteins from bacteria-targeting pathways such as bacteriocins and CDI systems tend to provide specific protection against only their cognate toxins (61, 123, 124). If immunity to effector Families 1-4 behaves in an analogous fashion we would expect that there would not be cross-complementation of immunity proteins between families, even for those effector families with overlapping enzymatic activity. When we test all combinations of confirmed EI pairs we observe that contrary to this model, one of the immunity proteins can provide significant protection against two effector families (Figure 3.8A). Specifically, the $Tai3^{TY}$ immunity protein protects against the *B. thailandensis* Tae2 ($Tae2^{BT}$) effector in addition to its cognate $Tae3^{TY}$ effector. The $Tai2^{BT}$ immunity protein does not protect against the $Tae3^{TY}$ effector, indicating that immunity does not hold for the inverse configuration.

As both $Tae2^{BT}$ and $Tae3^{TY}$ have identical activity, $Tai3^{TY}$ could be capable of broadly neutralizing all DD-endopeptidases. To examine this possibility we used another Tae2 homolog present in *S.* Typhi ($Tae2^{TY}$). $Tai3^{TY}$ is unable to rescue *E. coli* expressing periplasmic $Tae2^{TY}$, demonstrating that cross-family immunity between T6SS effector families can be specific (Figure 3.8B. The non-overlapping immunity spectra provided by $Tai2^{TY}$ and $Tai3^{TY}$ is consistent with the presence of both genes in *S.* Typhi; if $Tai3^{TY}$ provided immunity to both $Tae2^{TY}$and $Tae3^{TY}$ there would be no pressure to retain $Tai2^{TY}$. Furthermore, the finding that

immunity to effectors is specific demonstrates that even effector families that are identical in catalytic activity are not redundant in function.

As the differences between effector families are adaptive, we sought to determine whether the variation within effector families also represents functional diversity. Given the observation that Tai3^{TY} provides immunity differentially to Tae2^{BT} and Tae2^{TY} we began by testing whether the cognate immunity proteins of these two effector homologs have the capacity – unlike Tai3^{TY} – to neutralize the toxic activity of both effectors. Our data show that Tai2^{TY} does not provide immunity to Tae2^{BT}, and that Tai2^{BT} also does not protect against Tae2^{TY} (Figure 3.8C). This demonstrates that even though Tae2^{TY} and Tae2^{BT} are homologs, their neutralization pattern with respect to varying immunity proteins differs. However, we did observe instances of cross-reactivity of cognate immunity proteins between effectors within the same family. Both Tsi1 from *P. aeruginosa* (Tsi1^{PA}) and *Burkholdeira phytofirmans* Tsi1 (Tsi1^{BP}) can rescue cells from the toxicity of Tse1^{PA}, albeit rescue by the latter is less efficient (Figure 3.8D).

We have found that the diversity in effector sequence is adaptive, not only with regard to catalytic activity, but also in terms of immunity protein recognition. This observation extends from inter-family to intra-family diversity, indicating that there is not a stringent selection to maintain identical EI interactions. In contrast, the ability of one immunity protein to neutralize non-homologous effectors suggests that there has been selection for cross-immunity.

Distribution of effector and immunity proteins

The T6S amidase EI pairs are found among β-, δ-, and γ-proteobacteria. As depicted in Figure 3.9, they are particularly prevalent in the Enterobacteriaceae, Pseudomonadaceae, and the Burkholderiales. EI pairs appear to be inherited both vertically and horizontally within phylogenetic groups, resulting in a discontinuous distribution of the families. Although the pairs occupy a variety of genomic contexts, at least one member of Families 2-4 is encoded within a T6S gene cluster (Figure 3.10). Within T6S gene clusters, EI pairs are often encoded adjacent to *hcp* genes. For one family 4 pair, this association also extends to members encoded by genes outside of T6S gene clusters. Close association of *hcp* with EI pair loci is consistent with the previous finding that a T6S-exported protein of *Edwardsiella tarda*, EvpP, directly interacts with an Hcp protein (125).

Interestingly, certain homologous EI pairs appear to be recognized by disparate T6SSs. For example, $Tae2^{BT}$ has been experimentally demonstrated to require T6SS-1 for export (Figures 3.1 and 3.2), whereas $tae2^{TY}$ is located within Salmonella pathogenicity island 6 (SPI-6) – the only T6SS present in this organism (Figure 3.10). While the effectors belong to the same family, their associated T6SSs are distantly related. The secretion of multiple effector families by a single secretion system also appears to occur. The genomes of several *S. enterica* serovars containing only the SPI-6 T6SS encode EI pair Families 2-4 (46). In total, these data strongly suggests that a single effector family can be secreted by divergent T6SSs and that a single T6SS can utilize a diversity of amidase effectors.

A critical observation made in our study is that effector proteins strictly co-occur with cognate immunity proteins (Figure 3.9). As peptidoglycan amidase effectors are toxic only in the periplasm, and they access that space exclusively by intercellular transfer through the T6S apparatus, the co-occurrence of effectors with immunity proteins demonstrates a strong selection due to active self-intoxication. The only exception we observed is that in certain *B. mallei* strains Tai2 is encoded by an apparent pseudogene, while the adjacent *tae2* locus remains intact. Importantly, the T6SS responsible for intercellular delivery of Tae2, T6SS-1 (based on *B. thailandensis* orthologs), is mutationally inactivated in *B. mallei* (57, 58). This example further underscores the generality of selection for immunity via the process of self-intoxication.

In contrast to our observation that effector genes always co-occur with immunity genes, 27% of the immunity proteins we identified were not encoded adjacent to intact effector genes (Figure 3.10). This argues that there is a selective pressure to retain immunity even in the absence of cognate effectors, and thus supports a role for T6S in antagonistic interspecies interactions. Notable examples of this phenomenon are found in pathogens that inhabit polymicrobial environments at some stage of their life cycle, such as *Yersinia pestis* and *S.* Typhimurium.

DISCUSSION

We have developed and implemented a sequence homology-independent means for confidently identifying T6S effectors from bacterial genomes. Using this approach, we discovered four broadly distributed, phylogenetically distinct families of T6S amidase EI pairs. Given current limitations in identifying T6S effectors through strictly experimental means, this method stands to significantly increase our ability to study the functional significance of the system. Our

findings have already led to several key insights into the mechanism, function, and evolutionary significance of T6S. While our current approach enriches for effectors with amidase function, the heuristic nature of our method allows for the addition of parameters as they become known. This could allow the removal of constraints specific to enzymatic activity, thereby facilitating the discovery of novel effector types.

Structural variability in peptidoglycan can provide protection against lytic proteins (126). As Gram-positive organisms lack an outer membrane, this protection is considered critical to their survival in certain environments (127). Our work has demonstrated that the peptidoglycan of Gram-negative bacteria may also be subject to frequent attack via T6S. Thus, modifications to its structure, such as D-amino acid substitutions and changes to the crosslink position, might serve a protective role against T6S amidase enzymes (128-130). Interestingly, our analyses of T6S cell wall effectors have revealed distinct cleavage specificities against Gram-negative peptidoglycan. The selection for variable specificity could be indicative of a molecular arms race occurring between donor and recipient bacteria.

Thus far we cannot reliably predict non-cognate effector recognition by immunity proteins. We observe instances that violate the simple model that effector relatedness correlates to immunity recognition. This could be explained by a conserved interaction site on the effector protein that binds highly divergent immunity proteins. Alternatively, effector inactivation might proceed through non-conserved immunity protein interactions, and even through non-conserved mechanisms. In this case, homology may be a poor predictor of binding because residue positions participating in the EI interface could differ. Structural insights into EI interaction will

be critical for developing an accurate molecular model of the interplay between effector and immunity sequence variation.

A relatively non-discriminating interbacterial EI pathway such as the T6SS has the potential to assist in our comprehension of bacterial interaction networks and community structure. The implications of orphan immunity proteins might be most easily interpreted, as these proteins are presumably present only for defensive purposes. For example, the presence of an orphan immunity protein within one organism that has evolved to specifically recognize an effector encoded by a second organism, suggests that these two organisms compete and interface in their natural environment. Likewise, dissimilar organisms with a matching repertoire of T6S EI pairs might cooperate, and related organisms with incompatible pairs may not. At a cursory level, the distribution and diversity of T6S EI pairs is consistent with expectations. In general, we observe an enrichment of EI pairs in organisms that occupy habitats with relatively dense and rich populations of bacteria, such as the soil and the gastrointestinal tract (GI tract) (131, 132). This trend also holds for pathogens; EI pairs are overrepresented in pathogens that colonize polymicrobial sites such as the GI tract and chronic wounds in comparison to those that elicit disease from sterile sites. Whether the T6S EI pairs of pathogens are adaptive for life within the host, persistence in the environment, or a combination of these, remains to be determined.

The divergence of effector recognition by immunity proteins both within and between effector families suggests that T6S effector loci might drive speciation and kin-recognition. The evolution or acquisition of novel EI pairs, incompatible with the ancestral EI pair, would render strains incapable of cooperating in the formation of multicellular aggregates with those carrying

the ancestral locus. This would produce a barrier to the flow of genetic information between strains and potentially allow for the divergence of species (133, 134). EI loci might also function in kin discrimination, allowing bacteria to exclude non-kin organisms from their local environment and thus prevent those organisms from benefitting from the production of common goods (135). In either case further study will be required to ascertain the role of EI loci in sociomicrobiology and community organization.

MATERIALS AND METHODS

Bacterial Strains, Plasmids, and Growth Conditions

B. thailandensis strains used in this study were derived from the sequenced strain E264 (136). *B. thailandensis* strains were grown on either Luria-Bertani media (LB), or the equivalent lacking additional NaCl (LB low salt (LB-LS): 10 g bactopeptone and 5 g yeast extract per liter) at 37 °C supplemented with 200 μg ml^{-1} trimethoprim, 100 μg ml^{-1} ampicillin, 2000 μg ml^{-1} zeocin, or 25 μg ml^{-1} irgasan where necessary. For introducing in-frame deletions, *B. thailandensis* was grown on M9 minimal medium agar plates with 0.4% glucose as a carbon source and 0.1% (w/v) *p*-chlorophenylalanine for counter-selection (137). *P. fluorescens* strains used in this study were derived from the sequenced strain Pf-5 (138). *P. fluorescens* strains were grown on LB at 30 °C supplemented with 25 μg ml^{-1} irgasan, 10 μg ml^{-1} gentamycin, and stated concentrations of IPTG as required.

E. coli strains included in this study included DH5α for plasmid maintenance, BL21 pLysS for expression of effectors for toxicity assays, SM10 for conjugal transfer of plasmids into *P. fluorescens*, and Shuffle T7 pLysS Express (New England Biolabs), for purification of effectors.

All *E. coli* strains were grown on either LB or LB-LS at 37 °C supplemented with 150 μg ml^{-1} carbenicillin, 50 μg ml^{-1} kanamycin, 30 μg ml^{-1} chloramphenicol, 200 μg ml^{-1} trimethoprim, 0.1% rhamnose, and stated concentrations of IPTG as required.

Plasmid Construction

Plasmids used for expression were pSCrhaB2 for *B. thailandensis*, pPSV35CV for *P. fluorescens*, and pET29b+ (Novagen), pET22b+ (Novagen), and pSCrhaB2 for *E. coli* (84, 85). In-frame chromosomal deletions in *B. thailadensis* were made utilizing a previously-described suicide plasmid, pJRC115 (137). Strains bearing inactivating mutations in *B. thailandensis* T6SSs for secretome analysis and competition experiments were described in a previous study (58). In-frame chromosomal deletions in *P. flourescens* were made using the pEXG2 suicide vector as previously described for *P. aeruginosa* (42). The plasmids pJRC115, pSCrhab2, pPSV35-CV, and pEXG2 have been described previously (84, 137).

E. coli pET29b+ effector expression vectors were constructed by amplification of effector genes and subsequent cloning into NdeI/XhoI restriction sites, creating an in-frame C-terminal fusion with a His_5 epitope tag. *E. coli* pET22b+ expression vectors were constructed using BamHI/XhoI restriction sites creating an in-frame N-terminal fusion to the PelB signal peptide and a C-terminal fusion with a His_5 epitope tag. pSCrhaB2 immunity expression vectors were constructed by first cloning a VSV-G epitope linker into an XbaI site and subsequently cloning immunity genes into NdeI/XbaI sites, creating C-terminal fusions with the VSV-G epitope tag. The *P. fluorescens* PFL_5498 ($tae3^{PF}$) expression vector was generated through amplification of PFL_5498 and subsequent cloning into pPSV35CV using SacI/XbaI restriction sites, creating a

C-terminal fusion with a VSV-G epitope tag. Effector and immunity genes amplified from genomic DNA of *B. thailadensis* E264, *S.* Typhimurium LT2, *S.* Typhi Ty2, *P. aeruginosa* PAO1, and *P. fluorescens* PF-5. For the ΔBTH_I0068-BTH_I0069 (*tae2-tai2*^{BT}), ΔPFL_0664 (*retS*), and ΔPFL_6093 (*clpV*) deletion constructs 600 bp upstream and 600 bp downstream of the indicated genes was amplified and ligated together using SOE PCR (87). For the ΔBTH_I0068-BTH_I0069 construct this product was then cloned into pJRC115 using XbaI/HindIII restriction sites. For the ΔPFL_0664 and ΔPFL_6093 constructs products were cloned into pEXG2 using EcoRI/XbaI and HindIII/XbaI sites respectively.

Strain Construction

In-frame chromosomal deletions in *B. thailandensis* were made utilizing a previously-described suicide plasmid, pJRC115 (137). Strains bearing inactivating mutations in *B. thailandensis* T6SSs for secretome analysis and competition experiments were described in a previous study (58). In-frame chromosomal deletions in *P. flourescens* were made using the pEXG2 suicide vector as previously described for *P. aeruginosa* (42).

***E. coli* Toxicity Measurements**

Overnight cultures of *E. coli* BL21 pl*ysS* harboring expression constructs for native (pET29b+) or periplasmic (pET22b+) effector proteins and immunity (pSCrhab2) proteins as indicated were diluted in LB to 10^6 as 10-fold dilutions for pictures, or 2-, 3-, and 10-fold dilutions to 2^6, 3^6, and 10^6 respectively for plate counts. These dilutions were spotted on LB-LS 3% agar with either IPTG or IPTG and rhamnose. For comparisons of native expression to periplasmic expression, cells were induced with either 100μM (Tse1^{PA}, Tae2^{Ty}, Tae3^{TY}, Tae3^{TM}) or 40μM (Tae2^{BT})

IPTG. For effector–immunity assays cells were induced with 0.1% rhamnose and either 15μM (Figures 3.2D, 3.7C, 3.8A, and 3.8C), 50 μM (Figure 3.8B), 10 μM, or 25μM IPTG (Figure 3.8D). All pictures and plate counts were taken between 20 and 26 hours after plating. Statistical analyses performed using a one-tailed Student's T-test.

Bioinformatics Screen

A small set of predicted toxin/immunity gene pairs were used in a bioinformatics search of type VI secretion positive genomes for bicistronic operons that may encode EI pairs. The 193 genomes used in the initial steps of this screen consisted of sequenced strains of species whose genomes were previously confirmed to encode T6SSs (58). Annotation files from NCBI (ftp://ftp.ncbi.nih.gov/genomes/Bacteria/) were screened using a custom Perl script to find candidate effector/immunity pairs occurring as bicistronic genes. The properties of the candidate effector protein were (1) pI > 8, (2) a predicted signal sequence, (3) a sequence motif consisting of cysteine and histidine residues separated by 40 to 70 residues, and (4) a sequence length under 200 amino acid residues. The candidate immunity protein was required to have a predicted signal sequence and a sequence length under 200 residues. Criteria for what constituted a bicistronic pair of genes were empirically determined by selecting parameters that did not eliminate any of the initial set of positive candidates. The parameters used were two consecutive cistronic genes of length less than 600 nucleotides, separated by no more than 50 nucleotides and surrounded by genes no closer than 20 nucleotides for genes on the same strand. Signal sequence prediction was obtained using SignalP 3.0 (139). The isoelectric point was determined for the entire annotated protein sequence using Compute pI/Mw (http://web.expasy.org/compute_pi/pi_tool-doc.html). Protein sequences that met the effector gene criteria of this screen were evaluated for potential

amidase activity using Phyre 2 structure prediction or HHpred homology detection (70, 140). A tblastn search of the NCBI non-redundant nucleotide (nr) database (ftp://ftp.ncbi.nih.gov/blast/db/) for homologs of our initial sixteen candidate effector and immunity proteins was performed to expand families to include all unique instances of homologous effector and immunity proteins. A search for the prevalence of T6S in sequenced Proteobacterial genomes was performed on 1875 fully-sequenced and assembled genomes (ftp://ftp.ncbi.nih.gov/genbank/genomes/Bacteria/) using a pblast search for matches to TssK or TssJ from *P. fluorescens* Pf-5 with an expect value cutoff of 10^{-7}. Statistical analysis of the probability of the co-occurrence of T6SSs and EI pairs was performed assuming a binomial distribution of T6S in genomes containing EI pairs.

MS sample preparation and analysis

Three biological replicates of wild-type samples were used to establish the reference secretome of *B. thailandensis*. All T6S mutants were analyzed as biological duplicates. For proteomic analysis, samples were reduced, alkylated and trypsin-digested. Peptides were extracted and analyzed by LC-MS/MS on a LTQ-Orbitrap hybrid mass spectrometer (Thermo Fisher) as described elsewhere (14). Each biological sample was analyzed in triplicate. Data was searched against the *Burkholderia thailandensis* strain E264 database (www.burkholderia.com) using the Sequest algorithm (141). Search results were validated with PeptideProphet and ProteinProphet software programs. The relative abundance for each identified protein was calculated using the spectral counting technique (142). Spectral count for each protein was normalized to total spectral counts in the sample. Average spectral counts of values of all biological and technical

replicates were used for further analysis. An empirically determined threshold of 11 spectral counts was used to curate the reference *B. thailandensis* secretome.

Enzymatic Assay

Purified peptidoglycan sacculi (300 μg) from *E. coli* D456 (tetrapeptide enriched) (143), CS703-1 (pentapeptide enriched) (143), or MC1061 (only tetrapeptide) (94) were incubated with $Tae2^{BT}$, $Tae2^{TY}$, $Tae3^{TY}$ or $Tae4^{TM}$ (100 μg/ml) in 300 ml of 20 mM Tris/HCl, pH 8.0 for 4 h at 37°C. A sample with enzyme buffer instead of enzyme served as a control. The pH was adjusted to 4.8 and the sample was incubated with 40 μg/ml of the muramidase cellosyl (kindly provided by Höchst AG, Frankfurt, Germany) for 16 h at 37°C to convert the residual peptidoglycan or solubilized fragments into muropeptides. The sample was boiled for 10 min and insoluble material was removed by brief centrifugation. The reduced muropeptides were reduced with sodium borohydride and analysed by HPLC as described (94). Product fractions E and F (Fig. 4A) of the $Tae4^{TM}$ sample were collected, concentrated in a SpeedVac, acidified by 1% trifluoroacetic acid and analysed by offline electrospray mass spectrometry on a Finnigan LTQ-FT mass spectrometer (ThermoElectron, Bremen, Germany) as described (95) (data not shown).

Acknowledgements

The authors wish to thank Colin Manoil for sharing *B. thailandensis* transposon mutants, Joe Gray of the Pinnacle Laboratory of Newcastle University for MS analysis, Nels Elde for advice on sequence analysis, Ferric Fang and Larissa Singletary for insights pertaining to Salmonella, Sonya Heltshe for assistance with statistical analyses, Josie Chandler for critical review of the manuscript, and members of the Mougous laboratory for helpful discussions. Research was

supported by grants to J.D.M from the National Institutes of Health (AI080609 and AI057141) and W.V. from the European Commission within the DIVINOCELL programme. A.B.R. was supported by a grant from the National Science Foundation (DGE-0718124). J.D.M. holds an Investigator in the Pathogenesis of Infectious Disease Award from the Burroughs Wellcome Fund.

Table 3.1: Summary of proteins identified in the B. thailandensis secretome by mass spectrometry.

Locus Tag	Annotation	Unique peptides[a]	Average spectral count[b]				Signal sequence[c]
			Wild-type	ΔT6SS-1	ΔT6SS-5	ΔT6S	
BTH_I2962	Unnamed protein product; Similar to Hcp protein	13	418	16	491.5	28	N
BTH_II1925	Chitin binding domain protein	21	403.33	375.5	453	346.5	N
BTH_I2402	Chitinase family 18 (EC:3.2.1.14)	9	333.33	52.5	315.5	252.5	N
BTH_II1834	LasA protease precursor	15	205	32	161	86.5	Y
BTH_II1578	Microbial collagenase, putative	24	199.67	89	170	174.5	N
BTH_II0783	Hypothetical protein	13	186.33	44	133.5	109	N
BTH_II2112	Lipoprotein, putative	14	158.67	64	137	137	Y
BTH_I1515	Hypothetical protein	24	157	80.5	160	106	Y
BTH_I2945	Peptidase, M1 family	23	139	117	135.5	130	N
BTH_I1458	Chaperonin GroEL	21	112	89	75	123.5	N
BTH_I3070	Translation elongation factor Tu	17	109.33	71.5	95	147	N
BTH_II0380	Dipeptidyl-peptidase IV (EC 3.4.14.11). Serine peptidase. MEROPS family S15	19	88.33	47.5	77	76.5	N
BTH_I1933	Hypothetical protein	3	86.67	76.5	120	100.5	Y
BTH_I1421	Serine-type carboxypeptidase family protein	15	84.33	49.5	84	81.5	Y
BTH_II1306	Carbohydrate ABC transporter substrate-binding protein, CUT1 family (TC 3.A.1.1.-)	14	80	57.5	87.5	92	Y
BTH_II0517	Hypothetical protein	10	66.67	34.5	63.5	60.5	Y
BTH_I3071	Translation elongation factor 2 (EF-2/EF-G)	19	65.67	37	53	75.5	N
BTH_II0089[d,e]	**Rhs element Vgr protein, putative**	**19**	**62.67**	**0**	**69.5**	**0**	**N**
BTH_I3225	**Rhs element Vgr protein, putative**	**19**	**62.67**	**0**	**69.5**	**0**	**N**
BTH_II1851	Metallopeptidase domain protein	11	61	17	49.5	45	Y
BTH_II1872	Levansucrase	15	60.33	30.5	44	38	Y
BTH_I3226[f]	**Hypothetical protein**	**11**	**57.33**	**0**	**54**	**0**	**N**
BTH_II0090	**Hypothetical protein**	**11**	**57.33**	**0**	**54**	**0**	**N**
BTH_I2044	Serine protease, subtilase family	14	53	27	49	47	N
BTH_II1069	gp28	14	46	53	41	47.5	N
BTH_I2697	**Rhs element Vgr protein, putative**	**13**	**45.33**	**0**	**45.5**	**0**	**N**
BTH_II1544	Flagellar hook-associated protein 2	8	44.67	41.5	142	95.5	N
BTH_II0113	PqaA	17	44	11.5	49	42.5	Y
BTH_II1243	Putative ABC transporter ATP-binding protein	11	43.67	30	42	36	Y
BTH_I2693	**Rhs element Vgr protein, putative**	**12**	**39**	**0**	**30.5**	**0**	**N**
BTH_I2705	**Rhs element Vgr protein**	**13**	**38**	**0**	**26**	**0**	**N**
BTH_II1852	Leucyl aminopeptidase (EC 3.4.11.10). Metallo peptidase. MEROPS family M28E	11	37.33	17	94	45.5	Y
BTH_I0955	Heat shock protein HtpG	12	33.33	29.5	26.5	32	N
BTH_II0658	Malate dehydrogenase (NAD) (EC 1.1.1.37)	10	33	17.5	32	46.5	N
BTH_I0068	**Hypothetical protein**	**7**	**31.94**	**0**	**33.5**	**0**	**N**

BTH_I0646	Succinyl-CoA synthase, beta subunit	8	30	25.5	25.5	20.5	N
BTH_I0261	Hypothetical protein	8	30	35	24	42.5	Y
BTH_I3196	Flagellin	6	29.33	16	99	58	N
BTH_I0233	Lytic murein transglycosylase, putative	10	28.67	20	35	32.5	Y
BTH_I1633	Hypothetical protein	8	28.33	35.5	23.5	29	Y
BTH_I2092	Antioxidant, AhpC/Tsa family	6	27.67	25	23.5	32	N
BTH_I2691	**Hypothetical protein**	**9**	**27**	**0**	**22**	**0**	**N**
BTH_I1638	SSU ribosomal protein S1P	11	26.67	28	13	31	N
BTH_I2723	**Filamentous haemagglutinin**	**9**	**25.33**	**0**	**11.5**	**0**	**Y**
BTH_II0720	Hypothetical protein	6	25	6.5	19	19	Y
BTH_I0967	Cytochrome c family protein	5	23	37	26	21.5	Y
BTH_I1783	Amino acid ABC transporter substrate-binding protein, PAAT family (TC 3.A.1.3.-)	7	22.67	11.5	18.5	24.5	Y
BTH_I3308	ATP synthase F1 subcomplex beta subunit	9	22.67	27.5	12.5	46	N
BTH_I1830	**Hypothetical protein**	**4**	**22.33**	**0**	**17.5**	**0**	**N**
BTH_I1431	Hypothetical protein	6	21.33	17	21.5	12.5	Y
BTH_I1434	Activator protein, putative	3	21.33	28	23	15	Y
BTH_I1457	Chaperonin, 10 kDa	6	20.67	36	17.5	21.5	N
BTH_I3300	Amino acid/amide ABC transporter substrate-binding protein, HAAT family (TC 3.A.1.4.-)	7	20	25	14.5	32	Y
BTH_I1308	Chaperone protein DnaK	7	19	11.5	15.5	22	N
BTH_I2028	Tanslation elongation factor Ts (EF-Ts)	6	18.33	7	19.5	22.5	N
BTH_I0759	Isocitrate dehydrogenase (NADP) (EC 1.1.1.42)	6	18.33	17.5	11.5	20.5	N
BTH_I0643	RecA protein	5	18	5.5	21	14.5	N
BTH_I2231	Nucleoside diphosphate kinase	4	18	12	20	36	N
BTH_I3310	ATP synthase F1 subcomplex alpha subunit	6	18	16	18	19	N
BTH_II2339	Lipase	5	17.67	7	5.5	0	Y
BTH_II0227	Hypothetical protein	5	17.67	11	20	22.5	N
BTH_II1016	gp42	8	17.33	16	8.5	28	N
BTH_II1054	Phage tail assembly chaperone	5	17.33	29.5	11.5	23.5	N
BTH_II2037	Aromatic amino acid aminotransferase apoenzyme (EC 2.6.1.57)	7	16.33	0	14	0	N
BTH_I1654	Electron transfer flavoprotein, alpha subunit	5	16.33	11	15.5	19	N
BTH_II0639	**Lipase**	**5**	**16.33**	**20.5**	**18**	**23.5**	**Y**
BTH_II1224	CmaB	6	16.33	30	12	33.5	N
BTH_II1015	gp41	4	16	10.5	12.5	16.5	N
BTH_I0564	Acyl-CoA dehydrogenase domain protein	6	15	14	18	22	N
BTH_I0647	Succinyl-CoA synthetase (ADP-forming) alpha subunit (EC 6.2.1.5)	5	15	23	15	37	N
BTH_I2668	Beta-N-Acetylglucosaminidase	6	14.67	5	16	6.5	N
BTH_II0665	Citrate synthase (EC 2.3.3.1)	7	14.67	13	12	21.5	N
BTH_I1894	Enolase (EC 4.2.1.11)	6	14.33	10	7.5	27	N
BTH_I3078	LSU ribosomal protein L10P	4	14.33	12.5	9.5	13	N
BTH_I2182	LSU ribosomal protein L9P	6	14.33	20	5.5	31.5	N

BTH_I1196	Glyceraldehyde-3-phosphate dehydrogenase (EC 1.2.1.12)	4	14	8.5	12	18	N
BTH_I2118	Trigger factor	4	13.33	7.5	19.5	23.5	N
BTH_I1762	Phospholipase C	5	13.33	14.5	14	15	N
BTH_I1653	Electron transfer flavoprotein, beta subunit	4	13.33	16.5	7.5	22.5	N
BTH_I0473	LSU ribosomal protein L25P	3	13	7	9.5	8.5	N
BTH_I3075	DNA-directed RNA polymerase subunit beta' (EC 2.7.7.6)	7	13	22.5	8	24.5	N
BTH_II0310	**Antifungal protein precursor, putative**	**2**	**12.33**	**0**	**11.5**	**0**	**N**
BTH_I2218	Thioredoxin	4	12.33	12.5	7	11.5	N
BTH_II0213	Probable glucan 1,4- a-glucosidase	5	12	11	10.5	19.5	Y
BTH_II1520	Outer membrane porin OpcP	5	12	11.5	11	18.5	Y
BTH_II1047	Phage major capsid protein, HK97 family	4	12	18.5	20	15.5	Y
BTH_I2698	**Hypothetical protein**	**6**	**11.67**	**0**	**7.5**	**0**	**N**
BTH_I3042	DNA-directed RNA polymerase subunit alpha (EC 2.7.7.6)	6	11.67	11	23	33.5	N
BTH_II0654	Aconitase (EC 4.2.1.3)	6	11.67	12.5	7	17.5	N
BTH_II1926	Alkyl hydroperoxide reductase, subunit c	4	11	14	12	26.5	N

[a] Average of three biological replicates of the wild-type sample

[b] Average spectral count values obtained from biological triplicates within each sample.

[c] Signal peptide predictions were performed by SignalP 3.0 server using the default parameters

[d] Rows highlighted in yellow correspond to protein absent in ΔT6SS-1 secretomes samples.

[e] BTH_I3225 and BTH_0089 encode VgrG proteins with 100% sequence homology. Thus, it is not possible to distinguish between the two proteins using mass spectrometry.

[f] BTH_I3226 and BTH_II0090 encode proteins with 96% sequence homology. While the presence of both the proteins was confirmed by identification of unique peptides from the variable regions of the proteins, their relative contributions cannot be determined by mass spectrometry.

Table 3.2: Summary of proteins identified in informatic screen.

Organism	Effector Locus	Immunity locus	Effector PI[b]	Structural prediction of effector[a]		
				Structure	Confidence (%)	Coverage (%)
Pseudomonas aeruginosa	PA1844	PA1845	8.9	RipA[c]	95.5	58
Burkholderia phytofirmans	Bphyt_5187	Bphyt_5186	9.1	RipA	93.4	51
Burkholderia thailandensis	BTH_I0068	BTH_I0069	9.4	CHAP amidase	93.9	56
Burkholderia ambifaria	BamMC406_0673	BamMC406_0672	9.7	CHAP amidase	93.7	83
Salmonella Typhi	t2586	t2585	9	CHAP amidase	91.7	53
Cronobacter turicensis	CTU_33040	CTU_33030	9.6	CHAP amidase	90.6	70
Acidovorax citrulli	Aave_0030	Aave_0029	9.2	CHAP amidase	93.7	66
Acidovorax citrulli	Aave_1502	Aave_1501	9.2	CHAP amidase	93.7	66
Salmonella Typhi	t0489	t0488	9.4	CHAP amidase	97.4	72
Burkholderia xenovorans	Bxe_A2093	Bxe_A2092	8.7	RipB[d]	97.6	57
Pseudomonas fluorescens	PFL_5498	PFL_5499	9.6	CHAP amidase	97.4	61
Ralstonia pickettii	Rpic12D_3260	Rpic12D_3261	9.3	CHAP amidase	97.2	60
Delftia acidovorans	Daci_3854	Daci_3855	9.3	RipB	97.5	57
Cronobacter turicensis	CTU_30570	CTU_30560	9.7	NlpC/P60	99.7	68
Salmonella Typhimurium	STM0277	STM0278	9	Cysteine protease[e]	69.2	48
Erwinia tasmaniensis	ETA_06210	ETA_06220	9.2	Cysteine protease[f]	66.6	44

[a] Top hit when submitted to the PHYRE 2 structural prediction server (http://www.sbg.bio.ic.ac.uk/phyre2)
[b] Isoelectric point calculated using Compute pI/Mw (http://web.expasy.org/compute_pi/pi_tool-doc.html)
[c] RipA is a cell wall amidase from *Mycobacterium tuberculosis*
[d] RipB is a cell wall amidase from *Mycobacterium tuberculosis*
[e,f] Predictions made using the HHpred server (http://toolkit.tuebingen.mpg.de/hhpred)

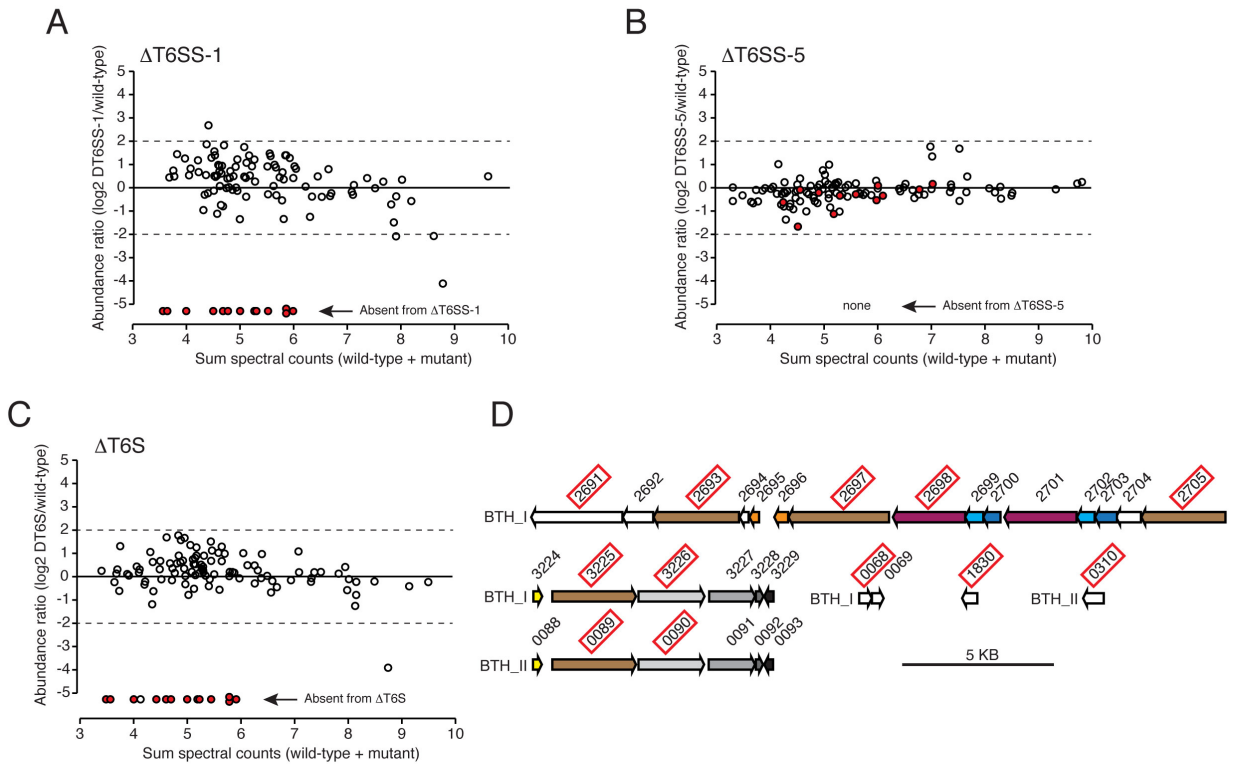

Figure 3.1: Identification of *B. thailandensis* T6SS-1 substrates. (A–C) Comparison of individual protein abundance in wild-type versus ΔT6SS-1 (A), ΔT6SS-5 (B), and ΔT6S (C) *B. thailandensis* secretomes. Proteins absent from ΔT6SS-1 are indicated in each panel by filled red spheres. (D) Organization of genes encoding *B. thailandensis* proteins (boxed red) that specifically require T6SS-1 for export. Color indicates homology.

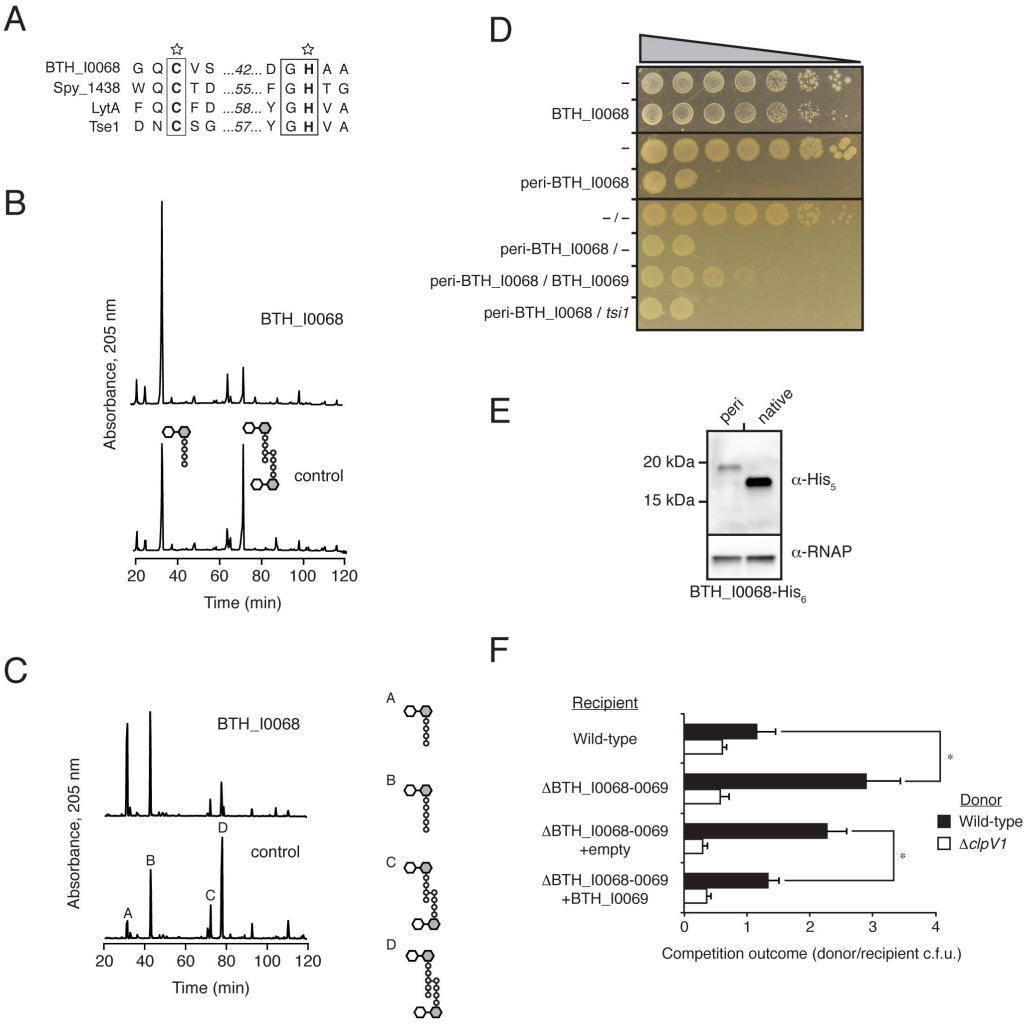

Figure 3.2: ***B. thailandensis*** **BTH_I0068 and BTH_I0069 are a T6S amidase effector–immunity pair.** (A) Sequence alignment of conserved catalytic motifs share between BTH_I0068 and characterized cell wall amidase enzymes. (B,C) Partial HPLC chromatograms of sodium borohydride-reduced soluble products resulting from digestion with BTH_I0068 and subsequent cleavage with cellosyl of tetrapeptide (B) or pentapeptide (C) -enriched *E. coli* peptidoglyan. (D) Growth of *E. coli* harboring one (top panels) or two (bottom panel) vectors expressing the indicated genes. A dash indicates the empty vector. From left to right are increasing serial ten-fold dilutions. (E) Western blot analysis of His-tagged effectors with native sequence or directed to the periplasm (peri) as expressed in (D). RNA polymerase (RNAP) was used as a loading control. (F) Growth competition assays between the indicated *B. thailandensis* donor and recipient strains under T6S-conducive conditions. The Δ*clpV1* strain is a T6S-deficient control. Asterisks mark significantly different competition outcomes ($p < 0.01$). Error bars ± s.d. n=6.

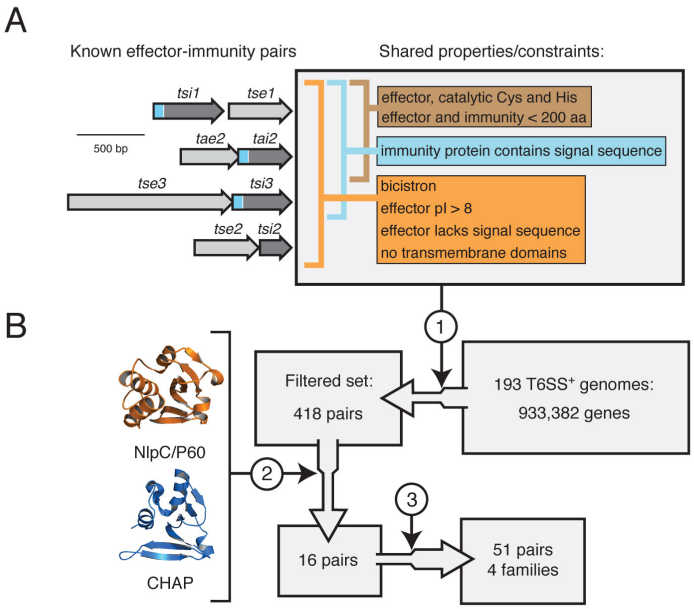

Figure 3.3: Identification of a T6S effector superfamily. (A) Overview of shared T6S EI pair properties. Depicted at left are the four bicistrons encoding all characterized EI pairs (this study and (14, 105)). Properties are divided among those shared by all EI pairs (orange), periplasmically-targeted pairs (blue), and amidase pairs (brown). Sequences encoding signal peptides within immunity proteins are represented in blue. (B) Schematic of informatic effector identification workflow. Key steps in the workflow are indicated: 1) filter by constraints depicted in (A), 2) application of structure prediction criteria, 3) expansion by homology searching of the non-redundant nucleotide database.

Family 1

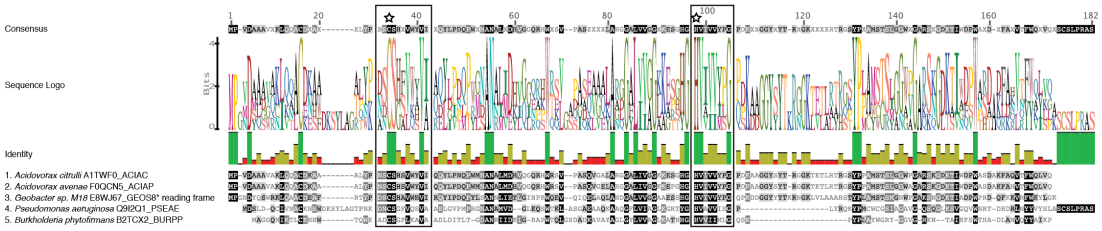

Family 2

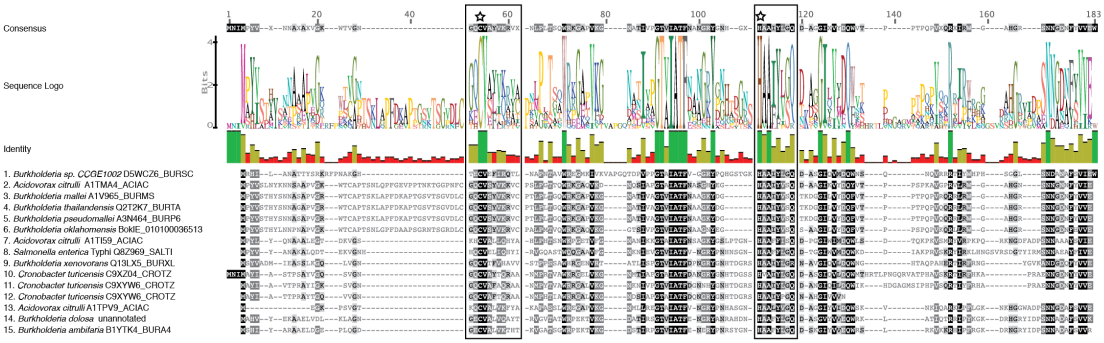

Family 3

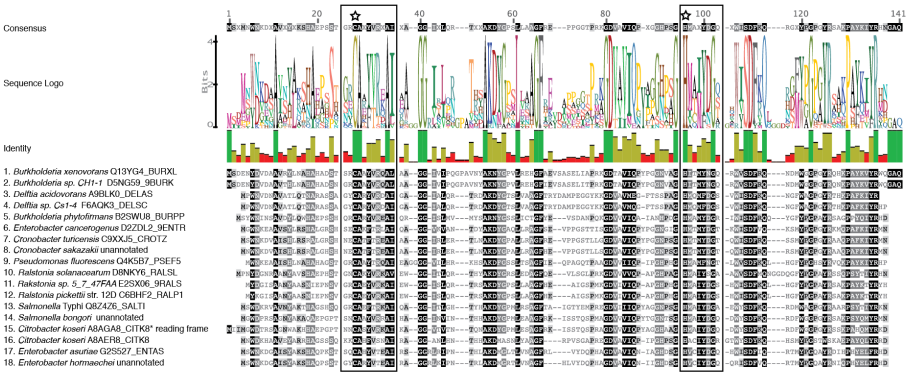

Family 4

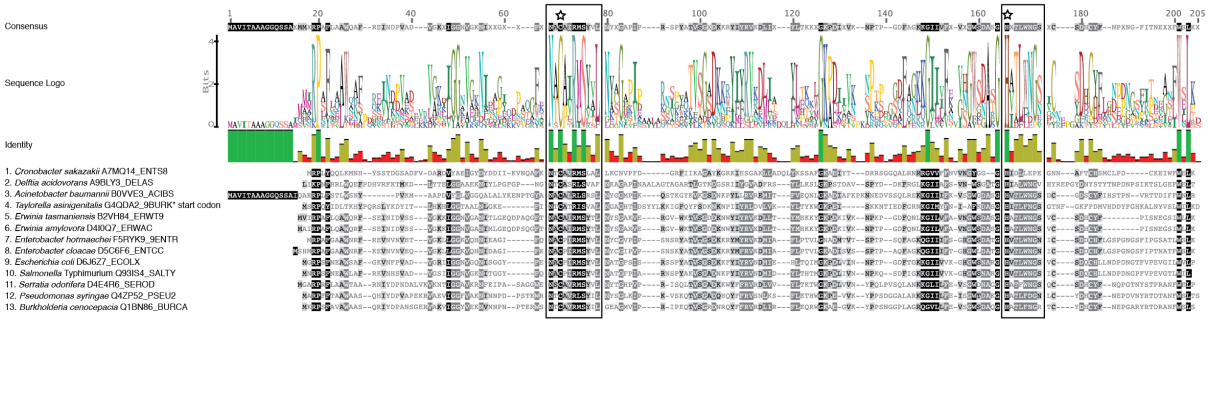

Figure 3.4. Full-length alignments of effector families.
Alignment of all sequences in each effector family. Alignments were generated from full-length sequences using Geneious software with the MUSCLE algorithm. Consensus, sequence logo, and identity were also generated with Geneious software. Shading of individual residues within sequences represents the similarity of that residue with all sequences at that position, with darker shading corresponding to greater similarity. Predicted catalytic cysteine and histidine residues are noted with a star. Family members are identified by the organism name followed by SWISS-PROT protein identification when available. Instances in which a protein differs from its SWISS-PROT entry are noted with an asterisk followed by the nature of the change (different start site, different reading frame). Unannotated proteins have no SWISS-PROT identifiers. Boxed residues denote regions used to generate the phylogenetic tree in Figure 3.5, using equivalent regions in the papain-like fold enzymes (Pfam clan, CL0125) as an outgroup.

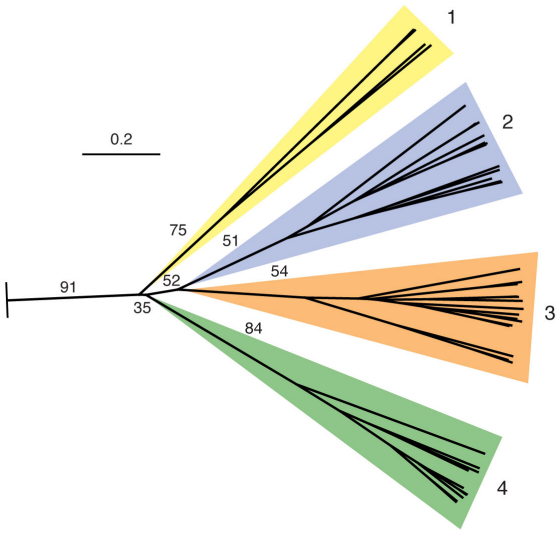

Figure 3.5: The Tae superfamily consists of four phylogenetically distinct subfamilies. Phylogenetic tree of novel T6S effectors identified by methods depicted in Figure 3.3. The tree was based on alignment of catalytic motifs (Figure 3.4). Effectors distribute into four branches, referred to as Families 1-4. The background colors assigned to the families are used henceforth. Critical boostrap values are indicated (n = 100). The tree was rooted using equivalent catalytic motifs of papain-like fold enzymes (Pfam clan, CL0125). Scale bar indicates evolutionary distance in amino acid substitutions per site.

Family 1

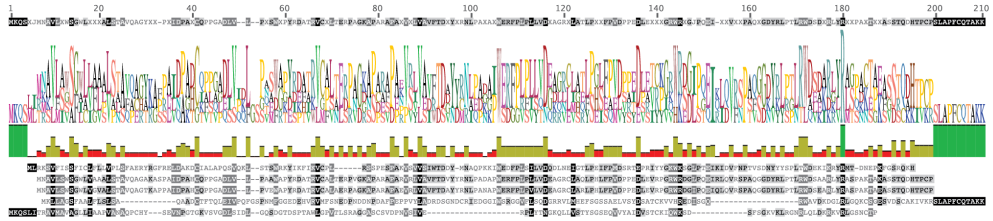

Family 2

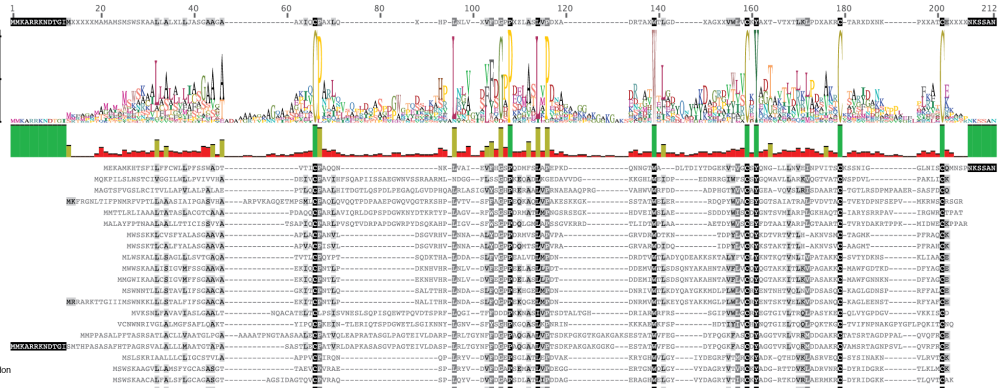

Family 3

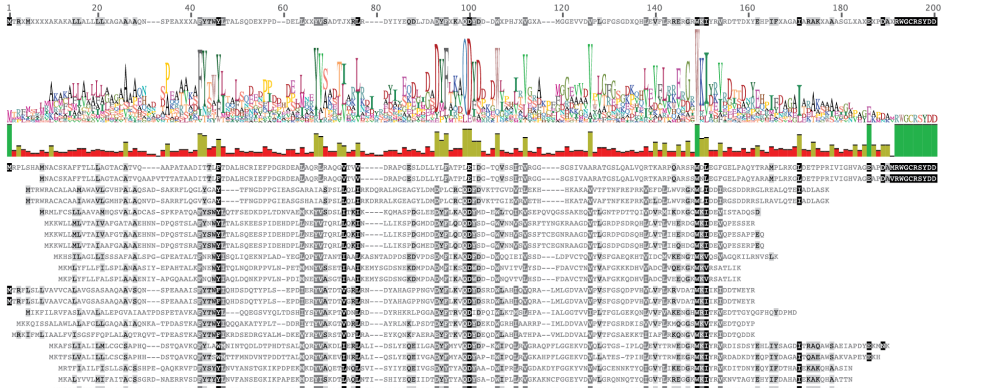

Family 4

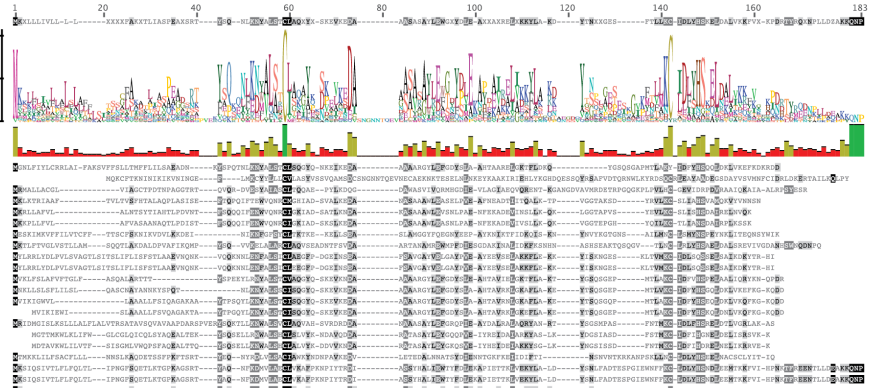

Figure 3.6. Full-length alignments of immunity proteins.
Alignment of all sequences in each immunity family. Alignments generated and displayed as in Figure 3.4.

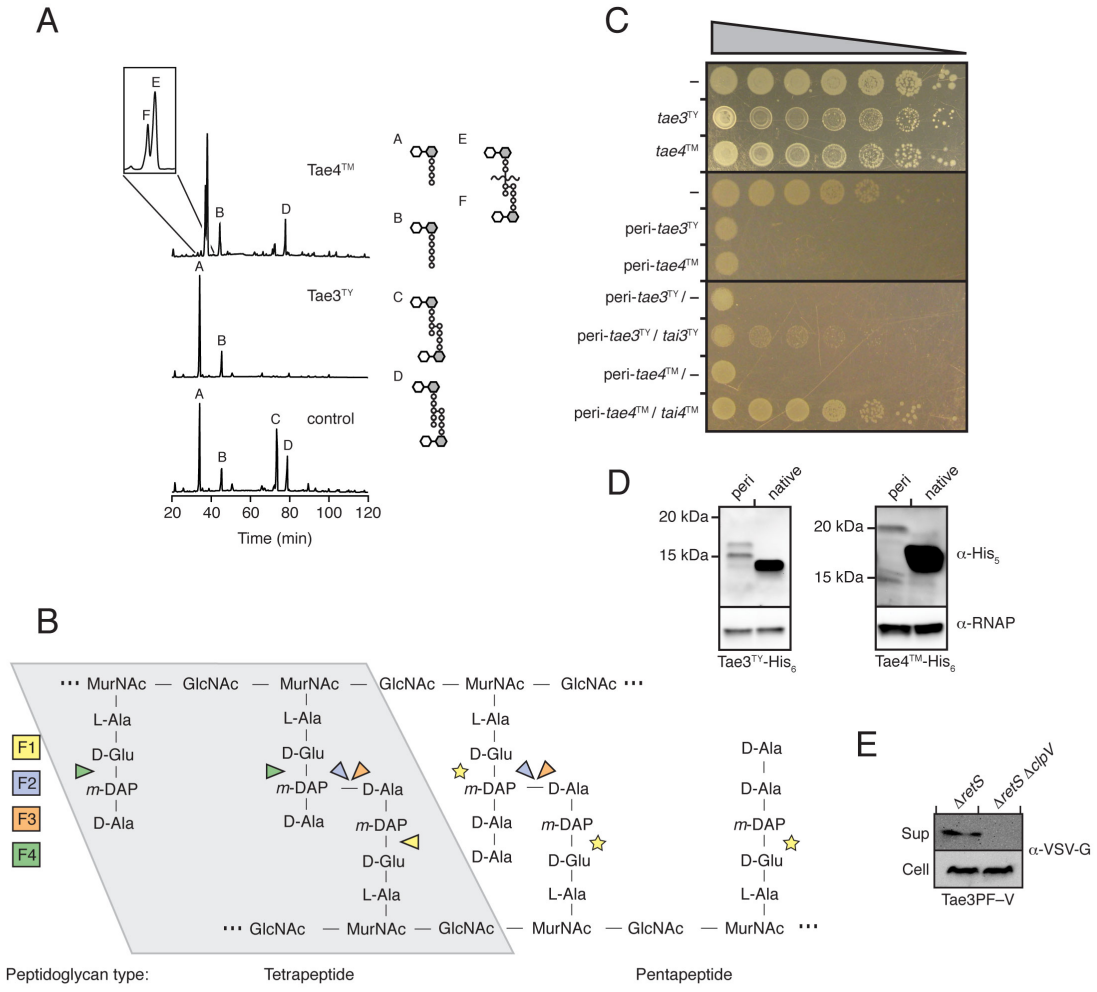

Figure 3.7: Representatives of Families 3 and 4 are T6S amidase EI pairs. (A) Partial HPLC chromatograms of sodium borohydride-reduced soluble *E. coli* peptidoglycan products resulting from digestion with Tae3^{TY} or Tae4^{TM} as in Figure 3.1A. B) Simplified representation of Gram-negative peptidoglycan showing cleavage sites of effector families 1-4 (F1-4). Cleavage specificity on peptidoglycan with tetrapeptide (left) and pentapeptide (right) stems are depicted. Tse1 activity against pentapeptide-rich peptidoglycan has not been tested, as indicated by yellow stars. Abbreviations: GlcNAc, *N*-acetyl-glucosamine, MurNAc, *N*-acetyl-muramic acid. (C) Growth of *E. coli* harboring one (top panels) or two (bottom panel) vectors expressing the indicated genes. A dash indicates the empty vector. From left to right are increasing serial ten-fold dilutions. (D) Western blot analysis of His-tagged effectors with native sequence or directed to the periplasm (peri) as expressed in (C). RNA polymerase (RNAP) was used as a loading control. (E)Western blot analysis of supernatant (Sup) and cell-associated (Cell) fractions of the indicated *P. fluorescens* strains expressing vesicular stomatitis virus glycoprotein (VSV-G) tagged Tae3^{PF} (Tae3^{PF}–V).

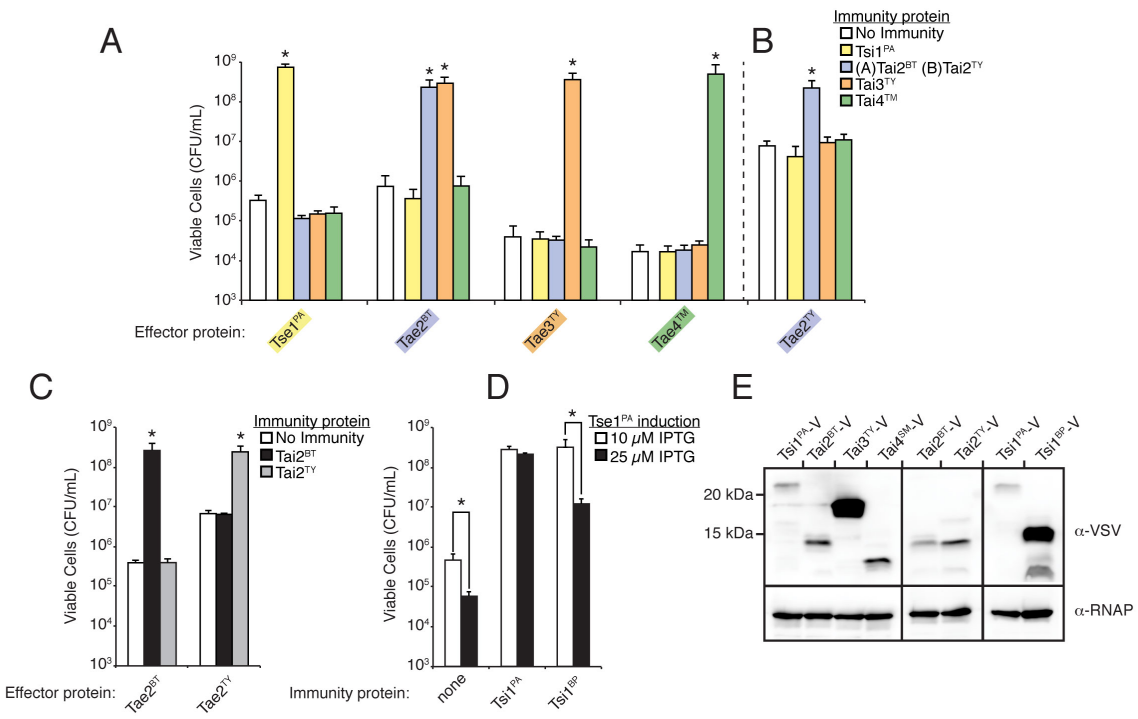

Figure 3.8: Immunity proteins display varying non-cognate effector neutralization. (A-D) All panels show the growth of *E. coli* harboring vectors co-expressing the indicated effector and immunity proteins. Immunity proteins were induced identically in all panels. Error bars represent ± s.d. (n=3). (E) Western blot analysis performed on *E. coli* bearing expression vectors for VSV-G (–V) tagged immunity proteins induced as in (A-D). RNA polymerase (RNAP) was used as a loading control.

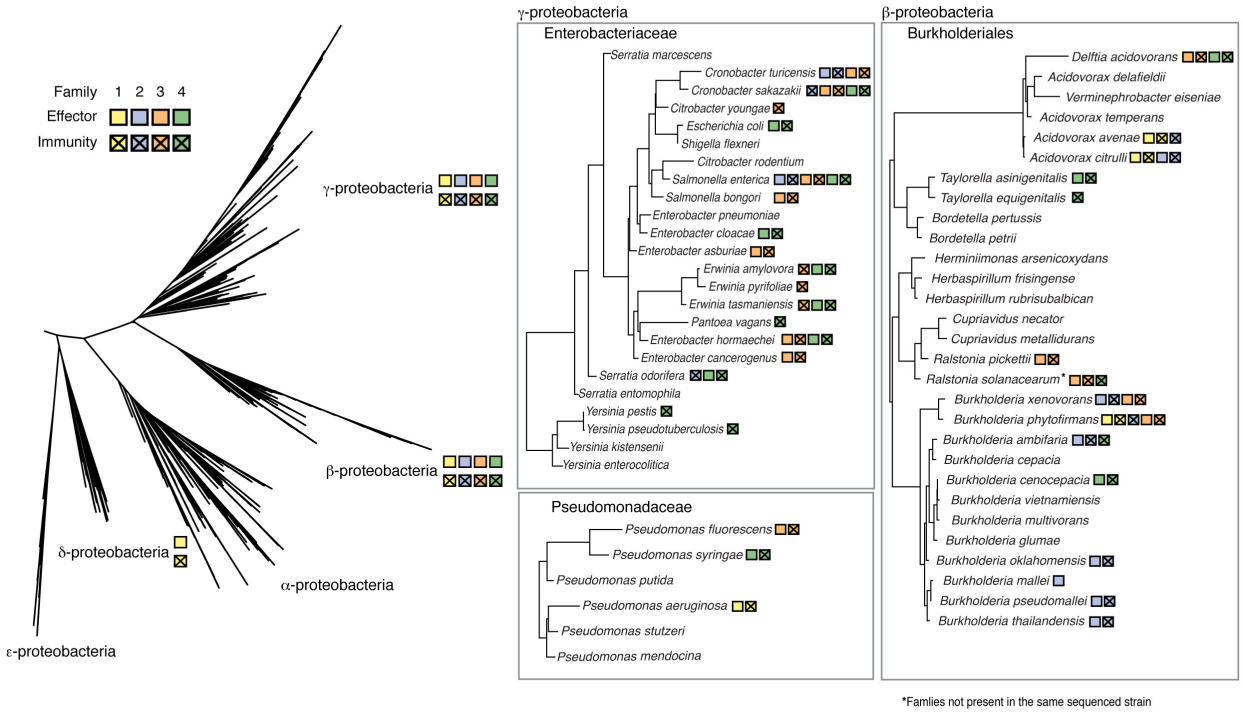

Figure 3.9: T6S cell wall amidase effector and immunity proteins are broadly distributed. Phylogenetic tree depicting the distribution of select effector and immunity proteins in Families 1-4. Trees are based on the 16s rRNA tree of life from Silva's Living Tree project (http://www.arb-silva.de/projects/living-tree/). For each species all effector and immunity proteins present in any genome are noted, however due to variability at the species level, not all members organisms in the group may have all effector and immunity proteins shown.

A

Salmonella Typhi str. Ty2

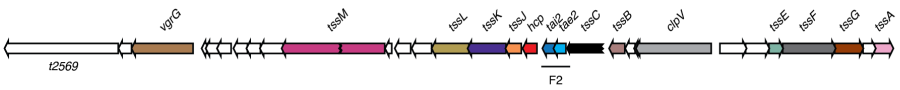

B

Burkholderia sp. CH1-1

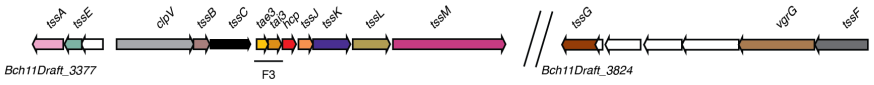

C

Erwinia tasmaniensis str. ET1/99

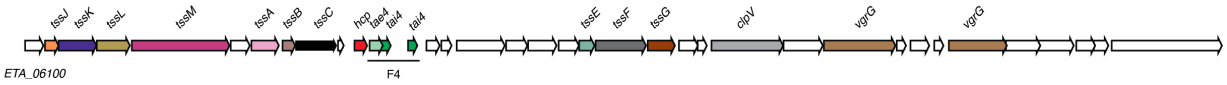

D

Salmonella Newport str. SL254

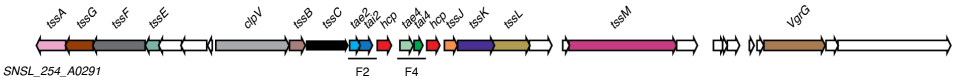

E

Acidovorax citrulli str. AAC00-1

Acidovorax avenae subsp. avenae str. ATCC 19860

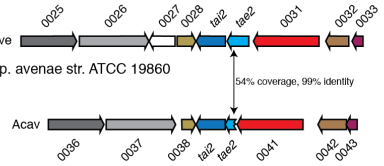

Salmonella Typhi str. Ty2

Salmonella Typhimurium str. LT2

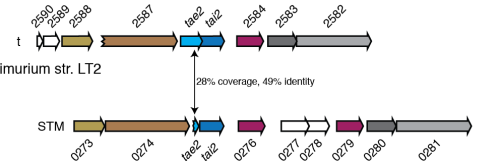

F

Salmonella Typhi str. Ty2

Salmonella Agona str. SL48

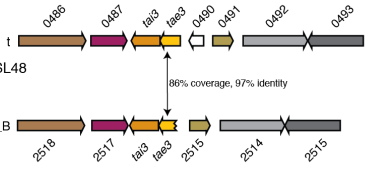

G

Pseudomonas syringae pv. syringae str. B728a

Ralstonia solanacearum str. IPO1609

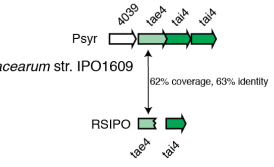

Erwinia amylovora str. CFBP1430

Yersinia pestis str. KIM10

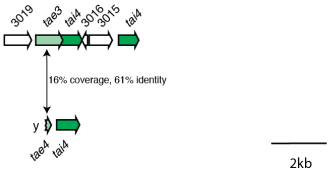

Figure 3.10. EI pairs of families 2-4 can be found in T6SS loci and immunity proteins can be found in the absence of intact effector genes. (A-D) Genomic organization of T6SS-encoding loci containing EI gene pairs of family 2 (A), family 3 (B), family 4 (C) and families 2 and 4 (D). Genes encoding conserved T6SS components (Tss genes) labeled. For Burkholderia sp. CH1-1 T6SS components are present at disperate loci. Frameshift mutations in the Salmonella Typhi marked as a break in the gene. Family 2-4 (F2-4) EI loci underlined. (E-G) Genomic organization of orphan immunity proteins (bottom of each alignment) and intact EI loci (top of each alignment) from family 2 (E), family 3 (F), and family 4 (G). Fragments of effectors found upstream of orphan immunity proteins are depicted as broken arrows and the percent coverage and identity at the residue level of those fragments with a closely related EI locus is shown. Homologous genes between intact EI loci and orphan immunity loci are colored identically.

CHAPTER IV

Diverse type VI secretion phospholipases are functionally plastic antibacterial effectors

Published as: Russell, A.B., LeRoux, M., Hathazi, K., Agnello, D.M., Ishikawa, T., Wiggins, P.A., Wai, S.N., Mougous, J.D. 2013. *Nature* 496, 508-512

A.B.R. contribution: Working with J.D.M. conceived of study and wrote paper. Carried out all informatic analyses of Tle proteins (alignments, genomic and genetic context, assignment of putative catalytic residues), *B. thailandensis* competition experiments, subcellular fractionation of *P. aeruginosa* cells expressing epitope-tagged Tle5 and Til5, immunoprecipitation experiments between Tle5 and Tli5, measurement of Tle5-induced lysis in *P. aeruginosa* competitions, *P. aeruginosa–P. putida* competition experiments, propidium-iodide analysis of isogenic intercellular intoxication in *P. aeruginosa*, purification of polar lipid samples for downstream analysis by the Kansis lipidomics core, generation of suicide constructs and subsequent mutant strains for *tle/i1* and *tle/i5*, generation of Tle1 wild-type expression construct for purification, Tli5 and Tli1 expression constructs for immnoprecipitation experiments, and all *B. thailandensis* and *P. aeruginosa* expression constructs, and, with J.D.M., analyzed phospholipase activity of Tle1,2, and 5 representatives.

ABSTRACT

Membranes allow the compartmentalization of biochemical processes and are therefore fundamental to life. The conservation of the cellular membrane, combined with its accessibility to secreted proteins, has made it a common target of factors mediating antagonistic interactions between diverse organisms. Here we report the discovery of a diverse superfamily of bacterial phospholipase enzymes. Within this superfamily, we defined enzymes with phospholipase A1 (PLA_1) and A2 (PLA_2) activity, which are common in host cell-targeting bacterial toxins and the venoms of certain insects and reptiles (144, 145). However, we find that the fundamental role of the superfamily is to mediate antagonistic bacterial interactions as effectors of the type VI secretion system (T6SS) translocation apparatus; accordingly, we name these proteins type VI lipase effectors (Tle). Our analyses indicate that PldA of *Pseudomonas aeruginosa*, a eukaryotic-like phospholipase D (PLD)(146), is a member of the Tle superfamily and the founding substrate of the haemolysin co-regulated protein secretion island II T6SS (H2-T6SS). While prior studies have specifically implicated PldA and the H2-T6SS in pathogenesis (146-148), we uncovered a specific role for the effector and its secretory machinery in intra- and inter-species bacterial interactions. Furthermore we find that this effector achieves its antibacterial activity by degrading phosphatidylethanolamine (PE), the major component of bacterial membranes. The surprising finding that virulence-associated phospholipases can serve as specific antibacterial effectors suggests that interbacterial interactions are a relevant factor driving the ongoing evolution of pathogenesis.

INTRODUCTION

Within proteobacterial genomes, predicted lipases are often encoded adjacent to homologs of the *vgrG* gene (50). The VgrG protein is strongly associated with, and functionally important for, the cell contact-dependent T6S protein delivery pathway (28). This pathway, which is distributed throughout all classes of Proteobacteria, can target both eukaryotic and bacterial cells; however, it is the specificity of its effectors that dictates the consequences of intoxication by the system. Known T6 effectors are few and include enzymes that either modify actin or degrade peptidoglycan – both domain-restricted molecules (9, 105). Thus, one would speculate that a barrier to the expansion or alteration of domain targeting would be the acquisition of a new effector or the evolution of one that is preexisting.

RESULTS

Informatic identification of T6SS lipase effectors (Tle)

To understand the significance of the T6S-associated lipases we undertook an informatic approach to examine their genetic context, sequence, and phylogenetic distribution. This analysis uncovered 377 putative lipases comprising five divergent families (type VI lipase effector 1-5, Tle1-5) that share no detectable overall sequence homology (Figure 4.1A). However, the families are united by a broad sporadic distribution pattern within Gram-negative bacteria and conserved putative catalytic motifs. Four of the families (Tle1-4) exhibit the GxSxG motif common in esterases and many lipases, while the fifth (Tle5) possesses dual HxKxxxxD motifs found in PLD enzymes (Figure 4.1B) (144). Outside of catalytic motifs, Tle1-4 members lack significant homology with known lipase enzymes, suggesting these proteins could represent previously uncharacterized diversity in the lipase superfamily.

Our prior work has shown that antibacterial T6S effectors are encoded adjacent to cognate immunity genes, which are essential due to the self-targeting activity of the T6S apparatus (105, 149). Moreover, due to a direct inactivation mechanism, the localization of the immunity protein indicates the cellular compartment targeted by the effector. Examination of the genomic context of the putative lipase-encoding genes revealed each is found adjacent to an open reading frame encoding a predicted periplasmic protein (Figure 4.1A). Thus, we hypothesize that contrary to prevailing views of bacterial lipase function, *vgrG*-associated lipase families could universally serve roles in interbacterial competition, possibly targeting phospholipids accessible from the periplasm. Consistent with our hypothesis, one of the putative lipase enzymes that we identified, *V. cholerae* VC1418 ($Tle2^{VC}$), was recently found to act as an effector in amoeba defense and intraspecies bacterial competition (47). Though the biochemical activity of $Tle2^{VC}$ was not elucidated, this suggests a capacity for Tle proteins to target a structure conserved in eukaryotes and bacteria.

Tle proteins are antibacterial phospholipases

To determine whether $Tle2^{VC}$ participates in interspecies bacterial antagonism, we tested its ability to provide fitness to *V. cholerae* in competition with *E. coli*. We observed *V. cholerae* strains lacking $tle2^{VC}$ display a striking impairment in their capacity to kill *E. coli*, approaching that of a strain lacking T6S function (Figure 4.2A). It is of note that a prior study probing the function of $Tle2^{VC}$ did not observe a contribution of the protein to fitness in an interspecies setting (47). This study was performed with strain V52, in which T6S-associated genes exhibit constitutively high expression (150). Therefore, a potential explanation for the apparent

discrepancy is that in a hyperactive state the absence of one effector is not sufficient to diminish antibacterial activity to a measurable level.

Tle2 represents only one of four divergent GxSxG families within the broader superfamily. As a first step toward understanding the functional significance of other GxSxG families, we examined *B. thailandensis* BTH_I2698 ($Tle1^{BT}$, Figure 4.1), which we previously demonstrated to be a substrate of an antibacterial T6SS (149). The $tle1^{BT}$ gene is found adjacent to genes encoding two homologous periplasmic lipoproteins, I2699 and I2700, which we posited could serve as $Tle1^{BT}$ immunity proteins. Additionally, $tle1^{BT}$, I2699, and I2700 appear to have been subject to a duplication event, with homologs of all three genes present immediately upstream. To simplify our analysis, we generated a mutant strain lacking one copy of this duplicated region. Using labeled derivatives of this strain co-cultured under T6S-conducive conditions, we found that recipient strains lacking $tle1^{BT}$ and its putative immunity determinants exhibit significantly decreased fitness in competition with donor strains possessing $tle1^{BT}$ and a functional T6SS, and that expression of I2699 in the recipient strain was necessary and sufficient to restore competitive fitness (Figure 4.2B). These data show that $Tle1^{BT}$ is an antibacterial effector delivered between cells by T6S, and that I2699, henceforth referred to as $Tli1^{BT}$ (type VI secretion lipase immunity 1), protects against $Tle1^{BT}$.

Having demonstrated that members of two GxSxG Tle families function as antibacterial T6S effectors, we next sought to investigate their biochemical activity. To characterize $Tle1^{BT}$ and $Tle2^{VC}$, we purified the proteins and catalytic nucleophile substitution mutant derivatives ($Tle1^{BT}$(S267A) and $Tle2^{VC}$(S371A)) as N-terminal fusions to hexahistidine-tagged maltose

binding protein (MH–), which we found necessary to generate and maintain soluble protein. Importantly, Tle1-4 possess a Ser-Asp-His catalytic triad utilized by a diversity of esterase enzymes, including thioesterases, acetylesterases, and assorted lipase and phospholipases (144). Given this wide range of potential activities, we asked whether MH–Tle1^{BT} or MH–Tle2^{VC} possess phospholipase activity. Using vesicle substrates doped with fluorescent phospholipid derivatives, we determined that MH–Tle1^{BT} acts specifically as a PLA_2, and MH–Tle2^{VC} as a PLA_1 (Figures 4.3A and B). Linking these activities to the antibacterial phenotypes we observed associated with the proteins *in vivo*, neither Tle1^{BT}(S267A) nor Tle2^{VC}(S371A), both catalytically inactive, serve as antibacterial effectors (Figure 4.2). Moreover, we found that the PLA_2 activity of MH–Tle1^{BT} is robustly inhibited by the addition of its immunity protein, Tli1^{BT} (Figure 4.3C).

If GxSxG family Tle proteins serve as antibacterial T6SS phospholipases, we reasoned that their activity against sensitive recipients should correlate with an increase in cellular permeability. To test these predictions, we performed single-cell measurements of propidium iodide (P.I.) uptake within interbacterial competitions of *B. thailandensis*. Consistent with our hypotheses, the lack of Tle1 immunity within cells corresponded to significantly increased P.I. uptake (Figure 4.4A). Using automated cell identity and tracking algorithms (151), we further demonstrated that the increase in P.I. uptake depended upon direct contact with donor cells possessing a functional T6SS (Figures 4.4B and C).

P. aeruginosa Tle5 is an antibacterial phospholipase D

With our data validating members of two GxSxG families as antibacterial phospholipase effectors, we explored whether these findings could be extended to the HxKxxxxD family (Tle5). This catalytic motif is strongly indicative of PLD activity (144), which has heretofore not been associated with an antibacterial enzyme. We choose *P. aeruginosa* PldA, henceforth referred to as $Tle5^{PA}$ (Figure 4.1), as a representative Tle5 family member. We began our study by confirming the enzymatic activity of the protein, as its function was previously studied in the context of cellular extracts (146). Consistent with prior observations, $Tle5^{PA}$ catalyzes the release of choline from phosphatidylcholine (PC), in a manner dependent upon a predicted catalytic histidine residue (His855) (Figure 4.5A). Under similar conditions neither $Tle1^{BT}$ nor $Tle2^{VC}$ showed appreciable activity in this assay, underscoring the diverse substrate specificity within the Tle superfamily.

A candidate $Tle5^{PA}$ periplasmic immunity protein is not readily apparent, as the adjacent gene, PA3488, is predicted to encode a cytoplasmic protein. However, expression of PA3488 from a second, upstream, predicted start site yields a periplasmically-localized protein, henceforth referred to as $Tli5^{PA}$, that binds specifically to $Tle5^{PA}$ (Figures 4.5B and C). To probe the role of $Tle5^{PA}$ and $Tli5^{PA}$ in interbacterial interactions, we generated a lysis reporter strain bearing a deletion of the *tle5*^{PA} *tli5*^{PA} bicistron. Lysis of this strain was highly elevated when co-cultured with a wild-type, but not a Δ*tle5*^{PA} donor strain (Figure 4.5D). Additionally, expression of *tli5*^{PA} in the recipient was sufficient to protect from $Tle5^{PA}$-dependent lysis. Together, these data demonstrate $Tle5^{PA}$ acts as an antibacterial toxin and that $Tli5^{PA}$ is its cognate immunity determinant.

The *P. aeruginosa* genome encodes three T6SSs, the H1-3-T6SSs. The H1-T6SS is the only system with known substrates and a demonstrated role in interbacterial interactions (42). To define the T6SS involved in $Tle5^{PA}$ transport, we constructed strains bearing individual in-frame deletions of the critical ATPase genes, *clpV1-3*, associated with the H1-3 systems, respectively. Specific inactivation of the H2-T6SS in a donor strain abrogated $Tle5^{PA}$-dependent toxicity, indicating that this system is responsible for $Tle5^{PA}$ delivery (Figure 4.5D).

The finding that $Tle5^{PA}$ transits the H2-T6S pathway is interesting in light of data that implicate this T6SS as a virulence factor in plant, mammalian cell culture, worm, and mouse models of infection (147, 148). To more thoroughly explore the role of $Tle5^{PA}$ and the H2-T6SS in interbacterial interactions, we measured their influence on competition outcomes between *P. aeruginosa* and a model T6S target, *P. putida* (105). Our results showed that both $Tle5^{PA}$ and the H2-T6SS significantly contribute to the fitness of *P. aeruginosa* in interspecies competition under T6S-conducive conditions (Figures 4.5E and F). These findings show that $Tle5^{PA}$ is a potent antibacterial effector delivered by the H2-T6SS.

While our data thus far show that $Tle1^{BT}$, $Tle2^{VC}$, and $Tle5^{PA}$ possess phospholipase activity *in vitro*, this did not allow us to definitively assign the toxic consequences of these effectors to membrane destruction. The phospholipase activity of the effectors could be accessory to a second toxicity mechanism found in these large, multidomain proteins. To resolve this remaining ambiguity concerning Tle function, we focused our studies on $Tle5^{PA}$. Since a mixture of healthy and intoxicated cells could complicate our measurements, we decided to assay $Tle5^{PA}$

effects in self-intoxicating monocultures of Δ*tli5*^{PA}, wherein each cell serves both as a donor and a sensitive recipient. As expected, this strain exhibited increased membrane permeability in a manner dependent on an active H2-T6SS and Tle5^{PA} (Figure 4.6A).

Under conditions promoting intercellular delivery of Tle5^{PA}, we harvested lipids of both non-intoxicated (wild-type) and intoxicated (Δ*tli5*) cells and quantified their phospholipid composition using mass spectrometry. This analysis revealed that the unchecked action of Tle5^{PA} leads to a severely perturbed membrane phospholipid composition. Strikingly, phosphatidic acid (PA), a product of PLD activity and a minor constituent of wild-type membranes (0.17%), was present at 8.1% in Δ*tli5*^{PA} – a 48-fold enrichment (Figure 4.6B). The increased PA appeared to derive primarily from PE, as it underwent a concomitant decrease of similar magnitude. Finally, we noted that phosphatidylglycerol (PG) increased slightly in Δ*tli5* relative to the wild-type. We speculate this latter result either derives from a compensatory effect or from Tle5^{PA} activity against cardiolipin, a minor component of *P. aeruginosa* membranes not detectable by the analysis method we used. Taken together, these data strongly suggest that Tle5^{PA}-imposed cell death occurs through PA accumulation via PLD activity, primarily directed against PE. The precise physiological consequences of massive PA accumulation in bacterial cells are not known, however the strong negatively charged character of the molecule is likely to have a detrimental impact on both integral and peripheral membrane-associated proteins. It is known that PA induces membrane curvature that can promote fusion and fission events (152); therefore, Tle5^{PA} activity might also lead to generalized membrane destabilization, membrane blebbing and depolarization. Interestingly, the *in vivo* specificity of Tle5^{PA} for PE, the major phospholipid constituent of most bacterial membranes, affords *P. aeruginosa* the capacity to use this enzyme against a vast array of competitors.

DISCUSSION

The discovery of T6SS-delivered phospholipase effectors has many implications. Critically, their biochemical activity does not intrinsically limit their toxicity to bacterial cells (Figure 4.6C). Indeed, two specificities now ascribed to Tle superfamily members, PLD and PLA_2, are both highly represented in host cell-targeting bacterial toxins (145). As these effectors are found in numerous established and emerging opportunistic pathogens, our work highlights the need to understand the biochemical, genetic, and evolutionary basis of inter-domain targeting by the T6SS. Such knowledge may ultimately become a component of a larger strategy to develop predictive algorithms for the evolution of bacterial pathogens. In addition, our findings add a new dimension to our understanding of the mechanisms employed during bacterial competition. Based on our data it appears that membrane targeting evolved independently on multiple occasions as an antibacterial strategy. This convergent evolution underscores the susceptibility of the bacterial membrane to attack, a theme mirrored by the prior observation that bacteriolytic T6S effectors likewise degrade an essential, conserved bacterial structure (105). The continued discovery of antibacterial effectors promises to illuminate additional vulnerabilities of the bacterial cell, and thus may aid our efforts to define promising therapeutic targets.

MATERIALS AND METHODS

Bacterial strains and growth conditions

B. thailandensis strains used in this study were derived from the sequenced strain E264 (136). *B. thailandensis* strains were grown on either Luria-Bertani media (LB), or the equivalent lacking additional NaCl (LB low salt (LB-LS): 10 g bactopeptone and 5 g yeast extract per liter) at 37°C supplemented with 200 μg ml^{-1} trimethoprim and 25 μg ml^{-1} irgasan where necessary. For

introducing in-frame deletions, *B. thailandensis* was grown on M9 minimal medium agar plates with 0.4% glucose as a carbon source and 0.1% (w/v) *p*-chlorophenylalanine for counter-selection (137). *V. cholerae* strains used in this study were derived from the O1 El Tor strain A1552 (153). *V. cholerae* was grown on LB or LB with 340 nM NaCl at 37°C or 30°C supplemented with 100 μg/ml rifampin, 100μg/ml carbenicillin and stated concentrations of arabinose as needed. In order to introduce in-frame deletions *V. cholerae* was grown on LB supplemented with 10% (w/v) sucrose at 30 °C for counter-selection (154, 155). *P. aeruginosa* strains used in this study were derived from the sequenced strain PAO1 (83). *P. aeruginosa* strains were grown on LB at 37 °C supplemented with 25 μg ml^{-1} irgasan, 30 μg ml^{-}gentamycin, and stated concentrations of IPTG as required. To generate in-frame deletions *P. aeruginosa* was grown on LB-LS supplemented with 5% (w/v) sucrose at 30 °C for counter-selection (86). For intra- and inter-species competition *P. aerguinosa* was grown on synthetic cystic fibrosis sputum media (SCFM) at 23°C (156). *P. putida* used in this study was the sequenced strain, KT2440 (76). *P. putida* was grown on LB at 30°C or on SCFM at 23°C. *E. coli* strains included in this study included DH5α for plasmid maintenance and production of $Tli1^{BT}$ immunoprecipitate, SM10 λ*pir* for conjugal transfer of plasmids into *B. thailandensis*, *V. cholerae,* and *P. aeruginosa*, MC4100 for competition assays with *V. cholerae,* BL21(DE3) p*lysS* for $Tle5^{PA}$ immunoprecipitation studies, and Shuffle T7 p*lysY* Express (New England Biolabs), for purification of Tle proteins. All *E. coli* strains were grown on LB or 2xYT at 37 °C supplemented with 150 μg ml^{-1} carbenicillin, 50 μg ml^{-1} kanamycin, 30 μg ml^{-1} chloramphenicol, 200 μg ml^{-1} trimethoprim, 50μg/ml streptomycin, 15μg/ml gentamycin, 0.1% rhamnose, and 100 mM IPTG as needed.

DNA manipulations

The creation, maintenance, and transformation of plasmid constructs followed standard molecular cloning procedures. All primers used in this study were obtained from Integrated DNA Technologies. DNA amplification was carried out using either Phusion (New England Biolabs) or Mangomix (Bioline). DNA sequencing was performed by Genewiz Incorporated. Restriction enzymes were obtained from New England Biolabs. SOE PCR was performed as previously described (87).

Plasmid construction

Plasmids used for expression in this study were pET28b:His_6-MBP-TEV-His_6 (157), pET22b+ (Novagen), and pSCrhaB2 (84) for *E. coli*, pPSV35CV (85) for *P. aeruginosa*, and pBAD24 (158) for *V. cholerae*. Complementation in *B. thailandensis* was performed using the Tn7-based integration vector pUC18T-miniTn7T-Tp::PS12 (111). In-frame deletions were generated utilizing the suicide vectors pJRC115 for *B. thailandensis* (137), pVCD442 for *V. cholerae* (159), and pEXG2 for *P. aeruginosa* (86). For the production of deletion constructs either 600 bp (*B. thailandensis* and *P. aeruginosa*) or 500 bp (*V. cholerae*) regions flanking the deletion were amplified, ligated together using SOE PCR, and subsequently cloned into pJRC115, pEXG2, or pVCD442 respectively. To generate the $tle1^{BT}_{S267A}$ *B. thailandensis* mutation construct, 600 bp regions flanking the mutation with an additional overlapping extension consisting of the desired mutation were amplified and ligated together using SOE PCR and subsequently cloned into pJRC115. For *B. thailandensis* complementation constructs genes were amplified along with predicted ribosomal-binding sites and cloned into pUC18T-miniTn7T-Tp::P12. For *P. aeruginosa* complementation and expression constructs, genes were amplified with their native

ribosomal binding sites into pPSV35CV with a 3' fusion to the VSV–G (vesicular stomatitis virus glycoprotein) epitope tag. To further generate the pPSV35CV::*tle5*$^{PA}_{H167R}$ and $_{H855R}$–V constructs, the entire *tle5*^{PA} gene was amplified from pPSV35CV::*tle5*^{PA} and SOE PCR was used to introduce the desired base pair mutations. For pSCrhaB2 *E. coli* expression constructs and pBAD24 *V. cholerae* expression and complementation constructs, genes were cloned downstream of the optimized ribosomal binding site already present in these vectors with a fusion to a 3' VSV–G-linker. To further generate the pBAD24::*tle2*$^{VC}_{S371A}$–V construct, the entire *tle2*^{VC} gene was amplified from pBAD24::*tle2*^{VC}–V and SOE PCR was used to introduce the desired base pair mutations. This product was subsequently cloned into pBAD24. For the Tle purification constructs *tle* genes were amplified and cloned into pET28b:His_6-MBP-TEV-His_6 to generate an N-terminal fusion to an MBP protein and a hexahistadine purification tag. SOE PCR was then used to generate the desired catalytic nucleophile substitution mutants. For the Tle5^{PA} periplasmic expression construct, *tle5*^{PA} was amplified and cloned into pET22b+ to generate an N-terminal fusion to the PelB leader peptide and a C-terminal fusion to a hexahistidine epitope tag.

Informatic identification of Tle proteins

All sequences were obtained from NCBI (http://www.ncbi.nlm.nih.gov). BTH_I2698 from *B. thailandensis* E264, PA0260, PA1510, PA3487, and PA5089 from *P. aeruginosa* PAO1, and VC1418 from *V. cholerae* V52, all encoded adjacent to *vgrG* genes, were identified as putative lipases utilizing the PHYRE 2 structural prediction server (70). Using the amino acid sequences of these predicted lipases, blastp analyses were performed against the non-redundant protein database (ftp://ftp.ncbi.nih.gov/blast/db/) to identify unique instances of their homologs.

Homology identified by the blast server was used to distribute these proteins into five distinct Tle families. Each family was aligned using the MUSCLE algorithm and phylogenetic trees were generated using the PHYML 3.0 method with bootstrap analysis of 1000 replicates (160, 161). Proteins encoded by the genes shown in Figure 4.1A were analyzed for subcellular localization utilizing the SignalP 3.0 and TMHMM 2.0 servers, and VgrG proteins were identified utilizing blastp (139, 162). Regions depicted in Figure 4.1A were extracted based on boundaries defined by the presence of a *tle*, *tli*, or *vgrG* gene. Figure 4.1B catalytic residues were determined both by PHYRE 2 structural alignment with known lipase enzymes and conservation of those residues within the Tle family alignments. Sequence logos were generated from a manual alignment of conserved catalytic motifs utilizing Geneious software.

Western blot analyses

Whole cell fractions were prepared as described previously (85). Anti-RNA polymerase, anti-VSV–G, anti-beta-lactamase, anti-His_5, and anti-CRP Western blot analyses were performed utilizing previously-defined methods (105, 155, 163). Subcellular localization of epitope-tagged $Tle1^{PA}$ and $Tli1^{PA}$ in *P. aeruginosa* was performed identically to previous localization studies of Tsi1 and Tsi3 (88, 105). For immunoprecipitation experiments, BL21(DE3) p*lysS* cells co-expressing periplasmic hexahistidine-tagged $Tle5^{PA}$ from a pet22b+ vector and VSV–G tagged immunity proteins from pSCrhaB2 vectors were pelleted and resuspended in lysis buffer (20 mM Tris-Cl pH 7.5, 50 mM KCl, 8.0% (v/v) glycerol, 1.0% (v/v) triton, supplemented with DNase I (Roche), lysozyme (Roche), and 200µM PMSF). Cells were disrupted by sonication and the solution clarified by centrifugation. A sample of supernatant was then taken for analysis of total protein. The remainder of the supernatant was incubated with anti-VSV–G agarose beads

(Sigma) for 1 h at 4°C. Beads were washed four times with IP-wash buffer (100 mM NaCl, 25 mM KCl, 0.1% (v/v) triton, 20 mM Tris-Cl pH 7.5, and 2% (v/v) glycerol). Proteins were removed from beads with SDS loading buffer (125 mM Tris, pH6.8, 2% (w/v) 2-mercaptoethanol, 20% (v/v) glycerol, 0.001% (w/v) bromophenol blue and 4% (w/v) SDS) and analyzed by Western blot.

Bacterial competition experiments

Burkholderia competition experiments were performed as described previously (149). Recipient strains (Figure 4.2B, left), or donor strains (Figure 4.2B, right) were labeled with a GFP-expression constructed integrated into the attTn7 site, allowing the disambiguation of donor and recipient colonies through fluorescence imaging (58). For *V. cholerae* competition experiments with *E. coli*, both strains were grown to an OD_{600} of 0.5 in LB before being mixed 1:1 by volume. This mixture was then spotted on a nitrocellulose membrane on a 1.5% (w/v) agar LB plate containing 300 mM NaCl and 0.002% (w/v) arabinose. Competitions were incubated for 5 h at 37°C. Cells were then harvested and competitions analyzed. Initial and final colony-forming units (CFUs) of *V. cholerae* and *E. coli* were enumerated on LB plates supplemented with rifampin and streptomycin respectively. For *P. aeruginosa* competitions with *P. putida*, strains were grown overnight on solid LB media at 37 °C (*P. aeruginosa*) or 30 °C (*P.* putida) and resuspended in water to an OD_{600} of 0.3. Cells were mixed 1:1 and spotted on 1.5% (w/v) agar SCFM media plates, or inoculated into liquid media of the same. After 23 h of incubation at 23°C, a temperature previously demonstrated conducive to H2-T6SS and $Tle5^{PA}$ expression under *in vitro* conditions (164), cells were harvested and relative numbers of bacteria determined. Both initial and final counts of *P. aeruginosa* and *P. putida* were determined by

plate counts. *P. aeruginosa* self-intoxication assays were performed under identical conditions to solid media competition assays, save for the addition of 1 mM IPTG. After 23 h of growth, cells were stained with 5 μg ml^{-1} propidium iodide in PBS pH 7.0 for 10 minutes and washed prior to fluorescence measurements at an excitation/emission of 535/617 nm. Values shown were corrected for cellular density as measured by OD_{600}. Competition results for *B. thailandensis* and *P. aeruginosa* experiments are the change in ratio of donor cells to recipient cells, competition results from *V. cholerae* represent the final ratio alone. Data from all competitions were analyzed by a two-tailed Student's T-test, and data from monoculture experiments were analyzed by a one-tailed Student's T-test for a significant increase in P.I. staining.

Enzymatic assays of lipase activity

Fluorescence assays for phospholipase A activity were performed utilizing PED-A1 (*sn1*-labeled) and PED6 (*sn2*-labeled) fluorescent substrates according to manufacturer's directions (Invitrogen). Activity of $Tle1^{PA}$ and $Tle2^{VC}$ on these substrates was measured at an enzyme concentration of 300 nM ($Tle1^{PA}$) or 30 nM ($Tle2^{VC}$) at 28°C. For $Tle1^{BT}$-inhibition assays, immunoprecipitate was obtained as detailed under Western blot analyses from *E. coli* DH5α bearing a pSCrhaB2::$tli1^{BT}$–V expression construct or the equivalent empty vector control, with the modification that proteins were eluted from anti-VSV–G agarose beads by the addition of VSV–G peptide at a concentration of 100 μg ml^{-1} and no PMSF was used. After the addition of immunoprecipitate to $Tle1^{BT}$ enzymatic reactions, samples were incubated for four minutes after which the first reading was normalized to the measurement immediately prior to treatment. Fluorescent assays for phospholipase D activity were performed by measuring the production of peroxide by choline oxidase through the generation of the fluorescent molecule resorufin from

Amplex red reagent (Invitrogen) according the manufacturer's directions with the following modifications: reactions were performed in a buffer consisting of 50 mM Tris-Cl pH 7.2, 100 mM NaCl, 5 mM $CaCl_2$, and 2 mM $MgCl_2$, and vesicles consisting of equal amounts dioleoylphosphatidylcholine and dioleoylphosphatidylglycerol were used as a substrate at a final reaction concentration of 16.7 μM for each lipid species. Activity was measured at an enzyme concentration of 130 nM at 28°C. In all assays fluorescent values were corrected for fluorescence as measured in a buffer-only control.

Competitive lysis assays

The lysis of *P. aeruginosa* reporter strains was determined by the relative partitioning of LacZ to the supernatant. Lysis reporter strains were generated by the chromosomal integration of a previously-described miniCTX vector containing *lacZ* under the expression of a constitutive promoter (165). Lysis reporter strains and unmarked donor strains were grown overnight on solid LB media at 37°C and then resuspended in water to an OD_{600} of 0.3. Donor and recipient strains were mixed 1:1 and spotted on 1.5% (w/v) agar SCFM plates supplemented with 1 mM IPTG and incubated at 23°C for 23 h. Relative levels of supernatant LacZ activity as compared to total LacZ activity were then determined as previously described (45). Data were analyzed using a two-tailed Student's T-test.

Microscopic analyses of interbacterial competitions

Time-lapse fluorescence microscopy sequences were acquired with a Nikon Ti-E inverted microscope fitted with a 60X oil objective, automated focusing (Perfect Focus System, Nikon), a Xenon light source (Sutter Instruments), a CCD camera (Clara series, Andor), and a custom

environmental chamber. NIS Elements (Nikon) was used for automated image acquisition. Overnight cultures of recipient (*B. thailandensis* ΔBTH_I2698-I2703 attTn7::*gfp*) and donor (either *B. thailandensis* wild-type, ΔBTH_I2698 ΔBTH_I2701-3, or ΔBTH_I2598) strains were mixed 1:1 and diluted 2-fold with LB. The resulting bacterial suspension (~2 μL) was spotted onto growth pads made with LB broth, 2.5% (w/v) agarose, 0.2% (w/v) sodium nitrate, and 2.5 μg mL^{-1} propidium iodide. Automated image acquisition was performed at 5-min intervals for 6-8 h at 30°C. Cell identification, cell linking, and donor-contact analyses were performed using customized Matlab-based software (2012a, Mathworks) as described previously (151). Donor (unlabeled) and recipient (GFP-labeled) populations were identified using an empirically determined green fluorescence gate. A P.I. uptake event was defined as the first frame in which a cell achieved an empirically determined mean red fluorescence intensity threshold. Counting error was calculated as the square root of measurable events. Results represent two fields of view from a single experiment; each experiment was independently repeated at least three times.

Protein purification

For purification, Tle proteins were expressed from pET28b:His_6-MBP-TEV-His_6 in Shuffle T7 pLysY Express cells (New England Biolabs). Proteins were purified to homogeneity using nickel chromatography followed by size-exclusion chromatography using previously-reported methods, with the exception that reducing agents were excluded (91).

Lipidomic analyses

Wild-type and *tli5* mutant *P. aerguinosa* strains were grown as 20 individual 10 μl spots on 1.5 % (w/v) agar SCFM plates for 23 h at 23°C. These spots were then resuspended in PBS and

lipids were extracted using the Bligh-Dyer method (166). Purified lipid samples were analyzed for PE, PC, PG, and PA content by the Kansas State Lipidomics Research Center. An automated electrospray ionization-tandem mass spectrometry approach was used, and data acquisition and analysis were carried out as described previously (167, 168) with modifications. The lipid samples were dissolved in 1 ml chloroform. An aliquot of 50 µl of extract in chloroform was used. Precise amounts of internal standards, obtained and quantified as previously described (169), were added in the following quantities (with some small variation in amounts in different batches of internal standards): 0.6 nmol di12:0-PC, 0.6 nmol di24:1-PC, 0.6 nmol 13:0-lysoPC, 0.6 nmol 19:0-lysoPC, 0.3 nmol di12:0-PE, 0.3 nmol di23:0-PE, 0.3 nmol 14:0-lysoPE, 0.3 nmol 18:0-lysoPE, 0.3 nmol di14:0-PG, 0.3 nmol di20:0(phytanoyl)-PG, 0.3 nmol di14:0-PA, and 0.3 nmol di20:0(phytanoyl)-PA. The sample and internal standard mixture was combined with solvents, such that the ratio of chloroform/methanol/300 mM ammonium acetate in water was 300/665/35, and the final volume was 1.4 ml. Unfractionated lipid extracts were introduced by continuous infusion into the ESI source on a triple quadrupole MS/MS (4000QTrap), Applied Biosystems, Foster City, CA). Samples were introduced using an autosampler (LC Mini PAL, CTC Analytics AG, Zwingen, Switzerland) fitted with the required injection loop for the acquisition time and presented to the ESI needle at 30 µl/min. Sequential precursor and neutral loss scans of the extracts produce a series of spectra with each spectrum revealing a set of lipid species containing a common head group fragment. Lipid species were detected with the following scans: PC and lysoPC, $[M + H]^+$ ions in positive ion mode with Precursor of 184.1 (Pre 184.1); PE and lysoPE, $[M + H]^+$ ions in positive ion mode with Neutral Loss of 141.0 (NL 141.0); PG, $[M + NH_4]^+$ in positive ion mode with NL 189.0 for PG; and PA, $[M + NH_4]^+$ in positive ion mode with NL 115.0. The collision gas pressure was set at 2 (arbitrary units). The

collision energies, with nitrogen in the collision cell, were +28 V for PE, +40 V for PC, +25 V for PA, and +20 V for PG. . Declustering potentials were +100 V for all lipids. Entrance potentials were +15 V for PE and +14 V for PC, PA, and PG. Exit potentials were +11 V for PE and +14 V for PC, PA, and PG. The scan speed was 50 or 100 u per sec. The mass analyzers were adjusted to a resolution of 0.7 u full width at half height. For each spectrum, 9 to 150 continuum scans were averaged in multiple channel analyzer (MCA) mode. The source temperature (heated nebulizer) was 100 °C, the interface heater was on, +5.5 kV were applied to the electrospray capillary, the curtain gas was set at 20 (arbitrary units), and the two ion source gases were set at 45 (arbitrary units). The background of each spectrum was subtracted, the data were smoothed, and peak areas integrated using a custom script and Applied Biosystems Analyst software, and the data were isotopically deconvoluted. The first set of mass spectra were acquired on the internal standard mixture only. Peaks corresponding to the target lipids in these spectra were identified and molar amounts calculated in comparison to the two internal standards on the same lipid class. To correct for chemical or instrumental noise in the samples, the molar amount of each lipid metabolite detected in the "internal standards only" spectra was subtracted from the molar amount of each metabolite calculated in each set of sample spectra. The data from each "internal standards only" set of spectra was used to correct the data. Values expressed are the percentage of the total polar lipid signal detected. Statistical significance analyzed by a two-tailed Student's T-test.

Acknowledgements

We thank H. Kulasekara, B.E. Uhlin, and members of the Mougous and Wai laboratories for insightful discussions, J. Woodward for sharing chemistry expertise, the Manoil lab for sharing

B. thailandensis transposon mutants, and the Parsek laboratory and K. Korotkov for sharing reagents. This work was supported by grants from the National Institutes of Health (AI080609, AI057141, and AI105268), Cystic Fibrosis Foundation (CFR565-CR07), National Science Foundation (PHY-084845 and MCB-1151043), the Swedish Research Council (2010-3073, 2007-8673 UCMR Linnaeus, 2006-7431 MIMS), and the Faculty of Medicine, Umeå University. A.B.R. was supported by a Graduate Research Fellowship from the National Science Foundation (DGE-0718124), M.L. was supported by the NIH Cellular and Molecular Training Grant (GM07270), P.A.W. received support from the University of Washington Royalty Research Fund and the Sloan Foundation, and J.D.M holds an Investigator in the Pathogenesis of Infectious Disease Award from the Burroughs Wellcome Fund.

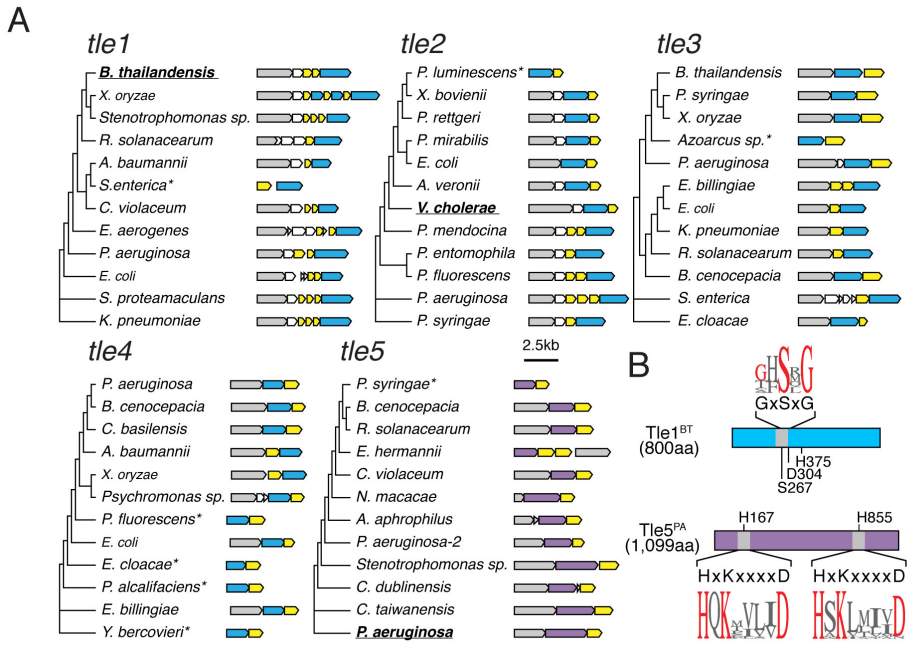

Figure 4.1: Overview of the Tle superfamily. (A) Evolutionary trees, genetic organization, and phylogenetic distribution of select Tle family members. Genes are colored by their predicted protein product (blue, Tle proteins with a GxSxG catalytic motif; purple, Tle proteins with dual HxKxxxxD catalytic motifs; grey, VgrG proteins; yellow, putative periplasmic immunity proteins). Branch lengths are not proportional to evolutionary distance. Asterisks denote *tle* genes without an apparent adjacent *vgrG* gene. (B) Domain organization of a single member of the GxSxG and dual HxKxxxxD catalytic classes of Tle proteins. Regions comprising these catalytic motifs are labeled in grey, and positions of all putative catalytic residues are denoted. Sequence logos were generated from alignments of the catalytic motif from Tle1-4 (GxSxG) and catalytic motifs from Tle5 (HxKxxxxD).

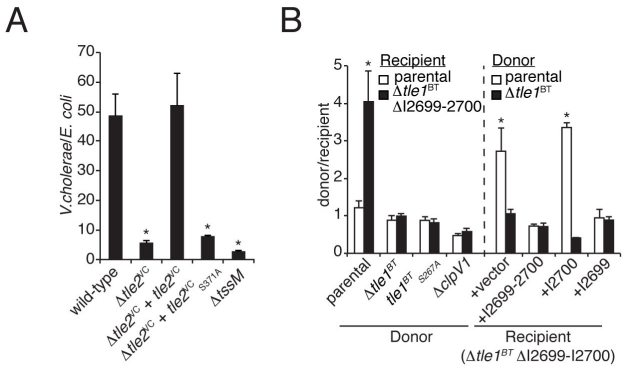

Figure 4.2: Tle GxSxG-type proteins are antibacterial effectors delivered by the T6SS. Error bars for all panels ± s.d. (A) Outcome of growth competitions between the indicated *V. cholera* strains and *E. coli*. The Δ*tssM* strain is inactive for T6S. Asterisks denote competitive outcomes significantly different than those obtained with wild-type ($P<0.05$, n=3). (B) Growth competition assays between the indicated *B. thailandensis* donor and recipient strains. The Δ*clpV1* strain is inactivated for T6SS-1, required for $Tle1^{BT}$ export (149). The parental strain for all experiments in this panel is ΔI2701-2703. Asterisks denote competition outcomes significantly different between indicated recipient strains (left) or indicated donor strains (right) ($P<0.05$, n=3).

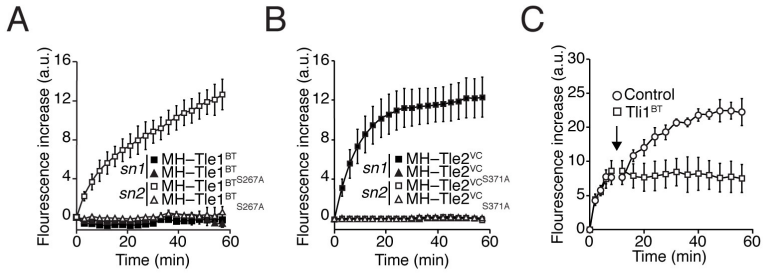

Figure 4.3: Tle GxSxG-type effectors possess phospholipase activity. (A,B) Enzymatic activity of the designated proteins against vesicles containing phospholipid derivatives with fluorescent moieties at the *sn1* or *sn2* positions (n=4). (C) Enzymatic activity of MH–Tle1^{BT} on *sn2*-labeled phospholipids as measured in (c) upon the addition of the indicated immunoprecipiate (arrow) (n=5).

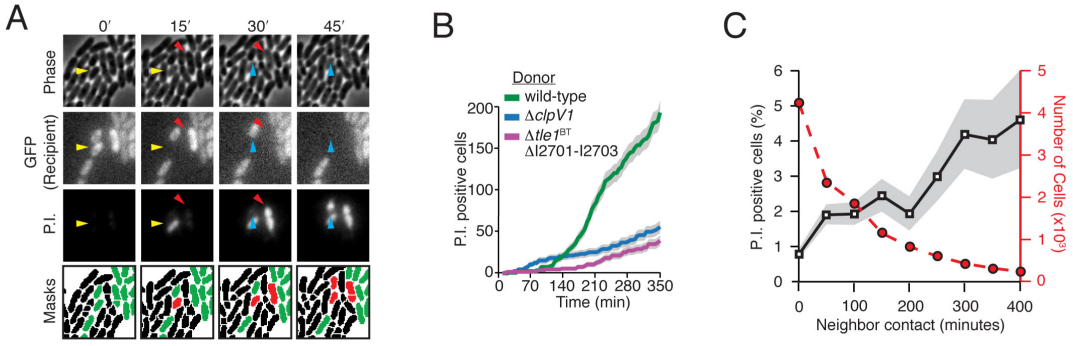

Figure 4.4: Tle1^{BT} induces permeability in sensitive recipients in a T6SS- and contact-dependent fashion. (A) Representative cropped micrograph series displaying three propidium iodide (P.I.) uptake and subsequent lysis events in a growth competition experiment between *B. thailandensis* wild-type and a Tle1^{BT}-sensitive recipient, ΔI2698-I2703. Each event spans two frames and is highlighted by arrowheads. The mask frames depict cell assignments made by gating cells based on fluorescence (black, donor; green, recipient; red, P.I.-positive). (B,C) Quantitation of P.I. staining events from *B. thailandensis* growth competitions as a function of time (B) or contact (C) using automated custom software. The recipient strain was the same as used in (B). Shading indicates counting error.

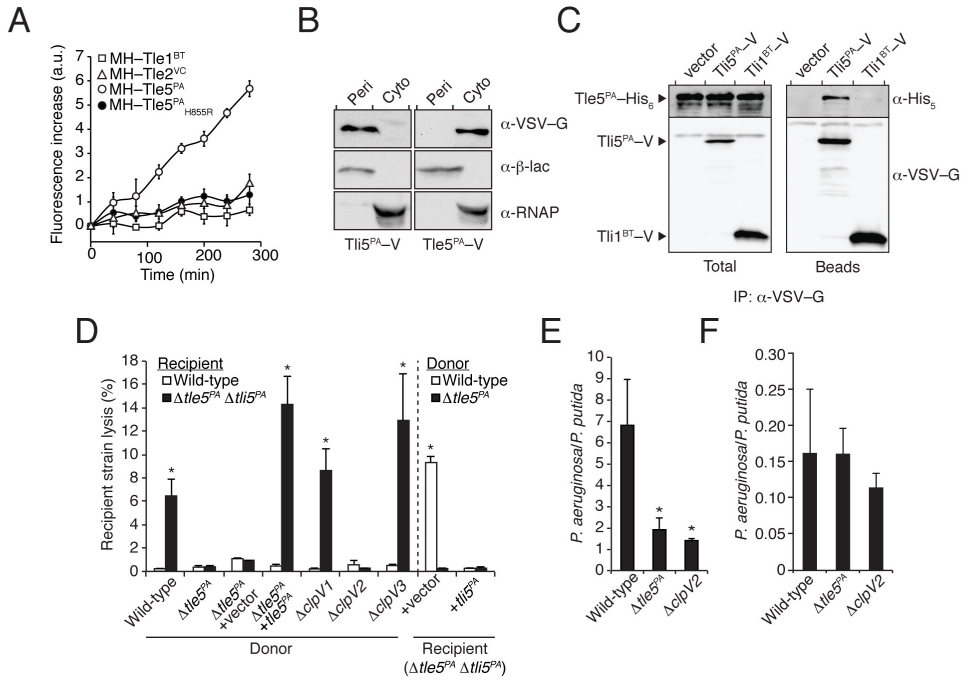

Figure 4.5: Tle5^{PA} is an HxKxxxxD-type interspecies antibacterial phospholipase effector delivered by the H2-T6SS of *P. aeruginosa*. Error bars for all panels ± s.d. (A) PC-specific PLD activity of the indicated proteins against mixed lipid vesicles (n=3). (B) Western blot analysis of subcellular distributions of Tli5^{PA} and Tle5^{PA} in *P. aeruginosa* grown in liquid LB media. Equivalent fractions of cytoplasmic (Cyto) and periplasmic (Peri) samples were loaded in each panel. Tli5^{PA} and Tle5^{PA} were expressed as fusions to a C-terminal VSV–G tag (–V), and detected with an anti-VSV–G antibody. RNA polymerase (RNAP) and β-lactamase (β-lac) enzymes were used as cytoplasmic and periplasmic fractionation controls, respectively. (C) Western blot analysis of total and bead-associated fractions from an α-VSV–G immunoprecipitation of the indicated VSV–G-tagged immunity proteins (–V) co-expressed in E. coli with periplasmically-localized Tle5^{PA} bearing a C-terminal hexahistidine epitope tag. (D) Lysis of recipient strains grown in co-culture with the indicated donor strains. Asterisks mark experiments wherein recipient lysis is significantly different between indicated recipients (left), or between indicated donors (right) ($P<0.05$, n=3). (E,F) Competitive growth of indicated *P. aeruginosa* strains against *P. putida* under T6SS-conducive (solid growth, E) or non-conducive (liquid growth, F) conditions. Asterisks denote competition outcomes significantly different than those obtained with wild-type *P. aeruginosa* ($P<0.05$, n=3).

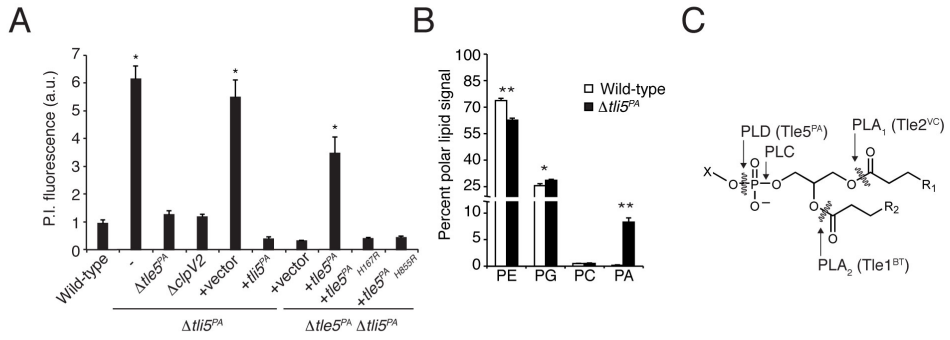

Figure 4.6: Tle5^{PA} targets phosphatidylethanolamine *in vivo*. (A) Membrane permeability of the indicated *P. aeruginosa* strains grown in monoculture as measured by propidium iodide (P.I.) staining. Asterisks denote significantly increased P.I. staining above wild-type levels. Error bars + s.d. ($P<0.05$, n=3). a.u., arbitrary units. (B) Summary of phospholipid profiles of the indicated *P. aeruginosa* strains grown as in (A). Statistical significance noted (n=4, * $P<0.01$, ** $P<0.001$). (C) Generalized schematic of a phospholipid indicating the activities defined in this study.

CHAPTER V

Bacterial antagonism in Bacteroidetes mediated by a type VI secretion-related interbacterial effector delivery pathway

Published as: Russell, A.B., Wexler, A.G., Harding, B.N., Whitney, J.C., Bohn, A.J., Goo, Y.A., Tran, B.Q., Barry, N.A., Peterson, S.B., Chou, S., Gonen, T., Goodlett, D.R., Goodman, A.L., and Mougous, J.D. 2014. *Cell Host & Microbe* 16, 227-236

A.B.R. contribution: Working with J.D.M. conceived of study and wrote paper. Performed all informatic analyses (identification of T6S clusters in the Bacteroidetes, assignment of gene identity within those clusters, identification of twelve genes conserved between T6SS^{iii} loci, phylogenetic analyses of TssC and TssK, genomic and genetic context of T6SS^{iii} systems, and identification of critical residues of *F. johnsoniae* ClpV, Fte1, and Fjoh_3274), *E. coli* toxicity experiments and expression analysis, propidium iodide measurements in *F. johnsoniae* isogenic intercellular intoxication experiments, microscopic analysis of ClpV-GFP foci in *F. johnsoniae*, generation of all mutant *F. johnsoniae* strains and all constructs used in *F. johnsoniae* or *E. coli* except for the *clpV-GFP* and Δ*tssN* allelic replacement vectors, and, with J.D.M and B.N.H., performed *F. johnsoniae* competition experiments with *P. putida* and *B. thailandensis*.

ABRSTRACT

Bacteroidetes are a diverse phylum of Gram-negative bacteria abundant in environmental and mammalian-associated polymicrobial communities often characterized by high cell density. However, cell contact-dependent mechanisms of interbacterial antagonism, such as the type VI secretion system (T6SS), have not been characterized in this phylum. Herein we report the bioinformatic and functional characterization of a T6SS-like pathway in diverse Bacteroidetes. Using prominent human gut commensal and soil-associated species, we demonstrate that these systems localize dynamically within the cell, export antibacterial proteins, and mediate interbacterial antagonism. The Bacteroidetes system is a distinct pathway with marked differences in gene content and a high degree of evolutionary divergence from the canonical T6S pathway. Our findings offer a potential molecular explanation for the abundance of Bacteroidetes in polymicrobial environments, the observed stability of Bacteroidetes strains in healthy humans, and the barrier presented by the microbiota against pathogen invasion.

INTRODUCTION

The Bacteroidetes are a phylum of Gram-negative bacteria that can be isolated from diverse natural habitats (170). Though they include agriculturally and medically relevant pathogens, as well as representatives that play important roles in critical environmental processes such as bioremediation, the phylum is relatively poorly studied. Bacteroidetes are perhaps most appreciated for their intimate association with humans and other mammals, as abundant residents of the gastrointestinal (GI) tract. In this ecosystem, bacteria form dense microbial communities that can exceed 10^{13} cells per milliliter (78, 171, 172). Bacteroidetes constitute 20-80% of the fecal microbiota of most adult humans and are largely represented by two genera, *Bacteroides*

and *Prevotella* (173). Members of this phylum generally act as mutualists by aiding in the digestion of complex carbohydrates, promoting gut development, modulating the immune system, and protecting against colonization by pathogens (170, 172, 174). As metabolically pliable organisms, Bacteroidetes also help to support a diverse gut community through syntrophic interactions with other microbes (175, 176).

Evidence suggests that the capacity of a bacterium to survive in a polymicrobial environment is related to the elaboration of interbacterial antagonistic factors. Studies performed primarily on Proteobacteria have shown that Gram-negative organisms can utilize soluble products as well as contact-dependent mechanisms to compete with other bacteria (61, 177). Although Bacteroidetes occupy numerous polymicrobial niches, including the human gut, to our knowledge contact-dependent antagonistic pathways have not yet been characterized in this phylum.

The type VI secretion system (T6SS) is a pathway that grants Gram-negative bacteria the capacity to translocate substrates to a wide range of recipient cells (2). Initially speculated to participate strictly in host cell interactions, it is now clear that the more common function of the system is to deliver proteins from the cytoplasm of a donor cell to the periplasm of a Gram-negative recipient (57). Substrates transported in a T6S-dependent manner include antibacterial effectors with diverse activities such as phospholipases, peptidoglycan hydrolases, nucleases, and membrane pore-forming proteins (1, 3). The pathway appears to lack a mechanism for discriminating self from non-self; thus, bacteria with active T6SSs possess immunity proteins that interact with, and inactivate, the effector molecules (14, 105). These interactions are allele

specific, and cognate effector–immunity (E–I) pairs are generally encoded adjacently within predicted operons (149, 178).

The T6S pathway requires the functions of 13 core proteins; unique subsets of these appear to have evolutionary relatedness to type IV secretion system (T4SS) components or to bacteriophage (6, 179). Proteins within the subsets are generally encoded adjacent to each other and interact extensively, suggesting that although each of the 13 core genes is essential, the complete system may be composed of modular, functionally distinct sub-complexes. The T4S-related components, TssL and TssM, are integral membrane proteins that form a trans-envelope complex with an outer-membrane lipoprotein, TssJ (33, 180, 181). The bacteriophage-like protein TssC, in conjunction with TssB, forms a dynamic filamentous assembly with gross structural similarity to the bacteriophage sheath complex (38, 39). Two other bacteriophage-related proteins, VgrG and Hcp, interact with non-overlapping sets of effectors, forming the basis for genetically distinct pathways for T6S-dependent substrate export (44, 48, 51). VgrG is a phage tail spike-like protein that interacts with effectors via conserved adaptor domains, whereas Hcp is ring-shaped, bears structural homology to the major phage tail tube protein gpV, and interacts with effectors within its pore. Supporting the relationship of Hcp to gpV, Hcp rings have been observed to form higher order head-to-tail stacked structures *in vivo*, analogous to those observed in bacteriophage (43).

Here, we report the bioinformatic and functional characterization of a T6S-like pathway in the phylum Bacteroidetes. We demonstrate that this pathway has the capacity to mediate cell contact-dependent intra- and inter-phyla bacterial antagonism. Although the pathway lacks

conserved elements essential to the well characterized Proteobacterial T6SS, and components that are shared with Proteobacteria display considerable sequence divergence, we provide evidence that they function in a mechanistically similar manner. Several genera that possess the Bacteroidetes T6S-like pathway, including *Bacteroides*, *Prevotella*, and *Porphyromonas*, are abundant members of human-associated polymicrobial communities, suggesting that the pathway may have an important role in defining the composition of the microbiome (182).

RESULTS

Bioinformatic characterization of a T6S-like gene cluster in Bacteroidetes

A generally applicable diagnostic secretion signal for T6S effectors is not available; however, genes encoding these proteins can often be identified by sequence-based approaches. Our group and others have noted that in many cases T6S effector and *vgrG* genes occur proximally and co-directionally on bacterial chromosomes (50, 183, 184). We recently exploited this observation to identify a large superfamily of T6S-exported phospholipases. Interestingly, a search for homologs of this class of effectors revealed their presence in Bacteroidetes – a bacterial phylum that does not possess a characterized T6S pathway (183). Moreover, like the Proteobacterial effectors, those found in the Bacteroidetes reside in close proximity to apparent *vgrG* genes and adjacent to open reading frames (ORFs) encoding predicted periplasmic immunity determinants. Our observations concerning phospholipase effector distribution are supported by an exhaustive study of polymorphic toxin domains conducted by Aravind and colleagues, which found genes encoding putative T6 effectors of various catalytic classes represented in Bacteroidetes (184).

Given the abundance and widespread nature of antibacterial T6S effector genes in Bacteroidetes, we postulated that these proteins participate in interbacterial interactions via a yet

uncharacterized T6S-like pathway. Proteobacterial T6S gene clusters often include effector loci; thus, to identify a T6S-like pathway in Bacteroidetes, we searched in the vicinity of putative effector genes for elements that could constitute a secretion system. This led to the identification of a cluster of twelve genes, including *vgrG*, with orthologs invariantly found in species with predicted effectors (Figures 5.1A-C and Table 5.1). Supporting the hypothesis that this gene cluster encodes a T6-like pathway, among the products of the twelve genes, we found a predicted ATPase with domain architecture similar to the Proteobacterial T6S core ATPase, ClpV (Figure 5.1D) (40).

Homology searches of the remaining conserved elements of the Bacteroidetes gene cluster failed to identify corresponding Proteobacterial T6S proteins. Given the evolutionary distance between Bacteroidetes and Proteobacteria, we posited that conservation between the constituents of this putative secretion system and the Proteobacterial T6SS might be below the detection limit of non-iterative approaches. By applying iterative search algorithms such as jackHMMER and PSI-BLAST (185, 186), we found that six additional genes in the Bacteroidetes cluster encode proteins bearing distant homology to core elements of the Proteobacterial T6SS, TssB, C, E, F, G, and K (Figure 5.1C).

In total, our sequence-based searches identified eight of the thirteen putative functional orthologs of the Proteobacterial T6SS encoded within the Bacteroidetes gene cluster (Table 5.1). Included in these eight components are each of the identified proteins of the bacteriophage-like module of the T6SS, with the exception of Hcp. In the Proteobacterial T6SS, Hcp proteins are required for effector recognition and export, thus the apparent absence of this conserved component was

unexpected (44). To ensure we had not overlooked a cryptic Hcp functional ortholog, we turned to structural prediction algorithms, which can identify highly divergent proteins, or convergent proteins, by their common folds. Indeed, using the Phyre remote homology modeling server, we found that one of the remaining four conserved genes in the Bacteroidetes cluster is predicted to encode a protein that adopts a structure with a high degree of similarity to Proteobacterial Hcp proteins (>90% confidence) (70). To further probe this predicted relatedness, we heterologously expressed and purified a member of this putative Hcp-like protein family encoded within the T6S-like gene cluster of *Flavobacterium johnsoniae*, a soil-dwelling member of the Bacteroidetes phylum (Figure 5.1E) (187). Visualization of this protein by negative stain transmission electron microscopy demonstrated that it adopts the characteristic ring shape and approximate dimensions of Proteobacterial Hcp proteins (Figure 5.1F). Together, our data suggest that a conserved gene cluster within the Bacteroidetes phylum encodes a T6S-like pathway. Henceforth, we refer to this pathway as T6SS subtype 3 ($T6SS^{iii}$), with the intent to distinguish it from the general Proteobacterial and Francisella pathogenicity island-like systems, herein constituting subtypes 1 and 2 ($T6SS^{i,ii}$), respectively (Figures 5.1A-C) (6, 188).

In order to better understand the relationship of the three T6SS groups, we performed phylogenetic analyses on the shared elements TssC and TssF. Phylogenetic trees generated from conserved regions of these proteins exhibited similar topologies, suggesting that the genes encoding them have been co-inherited (Figures 5.2A and B). In each tree, all Bacteroidetes components comprise a unique clade, distinct from Proteobacterial T6S homologs (Figure 5.2C). While some proteins encoded by species in the phylum Acidobacteria are also found in this clade, analysis of the genomic context of these homologs indicates they reside in gene clusters

that lack conserved Bacteroidetes components (Figure 5.3). We therefore restrict our definition of T6SS^{iii} to those systems that reside in Bacteroidetes. Interestingly, T6SS^{iii} gene clusters lack homologs of the T6SS^{i} proteins, TssA, L, M, and J. A gene encoding a putative TssM protein was recently suggested to reside in a *B. cellulosilyticus* T6S gene cluster (189). However, we note that homologs of this gene are neither generally found within or adjacent to T6SS^{iii} clusters across the Bacteroidetes phylum, nor are they encoded in the genomes of all organisms that possess the T6SS^{iii} pathway (data not shown). Our data suggest the entirety of the T6SS^{i} trans-envelope sub-complex – including *tssM* – is absent from T6SS^{iii}. In summary, our data suggest that a phylogenetically distinct T6S-like pathway – composed of an assemblage of proteins distinct from those required for the function of Proteobacterial T6SSs – is found within members of the phylum Bacteroidetes.

A T6SS^{iii} pathway exports antibacterial effectors

T6SSs are functionally versatile and can deliver effectors to other bacteria, to eukaryotic host cells, or to both of these cell types. We identified a number of predicted antibacterial effectors associated with T6SS^{iii} gene clusters in Bacteroidetes, suggesting that this system might possess the capacity to mediate interbacterial antagonism (data not shown). To first establish whether the T6SS^{iii} gene cluster encodes a secretory pathway responsible for the export of effector proteins, we conducted secretome measurements using *F. johnsoniae*. We chose this organism because it is genetically tractable, easily maintained under aerobic conditions in the laboratory (187, 190), and it possesses a T6SS^{iii} gene cluster that is highly representative of the system in other Bacteroidetes, including the human gut-associated commensal species *B. fragilis*, *B. vulgatus*, and *B. eggerthii* (Figure 5.2C).

To determine the contribution of the T6SS^{iii} pathway to the secretome of *F. johnsoniae*, we compared the culture supernatant of a strain bearing an in-frame deletion of its predicted *tssC* homolog, Fjoh_3266, to the wild-type parental strain using mass spectrometry. This analysis identified six proteins that were undetected in *F. johnsoniae* Δ*tssC*, but met our criteria for inclusion in the wild-type secretome (Table 5.2). Strikingly, the two most abundant of these proteins were Fjoh_3262 and Fjoh_3260, the Hcp and VgrG homologs encoded within the T6SS^{iii} gene cluster, respectively (Figure 5.1C). This finding parallels similar secretome studies of T6SS^{i} pathways, which generally find Hcp- and VgrG-family proteins as the major components of the T6SS-dependent substrate pool (14, 149, 191).

Of the remaining four proteins, two are encoded by hypothetical ORFs present within the T6SS^{iii} gene cluster (Fjoh_3257 and Fjoh_3274), whereas the remaining two are implicated in gliding motility and possess predicted signal sequences (Figure 5.1C, Table 5.1) (190). While the latter may have yet unrecognized roles relevant to T6SS^{iii}, for the purposes of identifying secreted effectors we focused on Fjoh_3257 and Fjoh_3274, which do not contain predicted signal peptides. Notably, these proteins both possess domains found in known or predicted T6SS^{i} effectors. Fjoh_3257 contains an HEXGH motif found in zinc metalloproteases fused to T6SS^{i}-exported VgrG proteins and Fjoh_3274 contains both a central glycoside hydrolase domain and a C-terminal zinc-dependent peptidoglycan endopeptidase motif (Figure 5.4A) (9, 149). Based on these data, we hypothesized that Fjoh_3257 and Fjoh_3274 are T6SS^{iii}-exported effectors that exert toxicity in the periplasm of target cells.

To test the hypothesis that the T6SS^{iii} pathway exports antibacterial effectors, we further investigated Fjoh_3257. When directed to the periplasm of *Escherichia coli*, Fjoh_3257 induced significant cell lysis, whereas the native protein – predicted to localize to the cytoplasm – did not exhibit apparent toxicity (Figure 5.4B,C). T6SS^{i} delivers effectors directly to the periplasm of recipient cells. If T6SS^{iii} functions similarly, our data suggest Fjoh_3257, henceforth referred to as *Flavobacterium* type VI secretion effector 1 (Fte1), could promote intercellular toxicity and thus necessarily associate with a cognate immunity determinant. Moreover, we would expect this immunity protein to reside in the periplasmic compartment, as T6SS^{i} effector inactivation invariably occurs via direct interaction with immunity (105, 192-194). We identified a gene encoding a protein matching the predicted immunity criteria directly downstream of *fte1*, Fjoh_3256 (hereafter referred to as *Flavobacterium* type VI secretion immunity 1, or *fti1*). Co-expression of Fti1 specifically abrogated the lytic effects of Fte1, indicating that Fte1-Fti1 comprise an antibacterial effector–immunity pair of T6SS^{iii} in *F. johnsoniae* (Figure 5.4D).

To test whether Fte1 exerts antibacterial activity in a T6SS^{iii}-dependent manner, we measured the cellular integrity of *F. johnsoniae* strains lacking *fti1*. When propagated on a solid substratum, a condition conducive to prolonged cell contact, we observed increased membrane permeability in the Δ*fti1* strain (Figure 5.4E). This phenotype was abrogated by concomitant deletion of *tssC*, *fte1*, or by growth in liquid media. Together with our secretome studies, these data strongly suggest the capacity of T6SS^{iii} to participate in interbacterial interactions through the export of antibacterial effectors.

T6SS^{iii} mediates interspecies bacterial antagonism

Interbacterial T6SS^{i} has been observed to be a crucial determinant of fitness during polymicrobial growth. Under contact-promoting conditions, its inactivation generally leads to significant defects in the capacity to outcompete other organisms in co-culture. To determine whether T6SS^{iii} also functions in interspecies antagonism we grew wild-type *F. johnsoniae* and derivative strains with either *Burkholderia thailandensis* or *Pseudomonas putida* under T6-conducive conditions. The inactivation of T6SS^{iii} by a deletion of *tssC* in *F. johnsoniae* greatly impacted the outcome of these growth competitions, allowing for significant expansion of the competitor population (Figures 5.5A and B). This phenotype could be complemented by the introduction of an extra-chromosomal copy of *tssC*, demonstrating that the observed change in fitness was not due to mutant polarity. Moreover, wild-type and Δ*tssC* displayed equal fitness in liquid growth medium, consistent with the known requirement for intimate cell–cell contact in T6S-dependent interactions. We further examined interspecies co-cultures containing *F. johnsoniae* lacking the T6SS^{iii}-restricted component, *tssN* (Fjoh_3277, Table 5.1). *F. johnsoniae* Δ*tssN* antagonized *B. thailandensis* and *P. putida* to an equivalent degree as Δ*tssC* or a strain bearing deletions in both *tssC* and *tssN*, consistent with our hypothesis that these genes encode essential elements of the same pathway (Figures 5.5A and B). Overall, our data strongly suggest that the T6SS^{iii} pathway mediates interbacterial antagonism in a manner analogous to T6SS^{i}, yet using a distinct complement of proteins.

The T6SS^{iii} apparatus exhibits dynamic behavior

Antibacterial effectors released by the T6SS^{i} pathway are operative on Gram-negative recipients only if they are delivered across the outer membrane by the translocation machinery. Owing to

this feature of the system, the apparatus must behave dynamically in order to sample localizations that orient the system toward competitor cells. Green fluorescent protein (GFP) fusions to the C-terminus of ClpV proteins have served as a convenient means to visualize this behavior of T6SS^{i} systems. Since an apparent ClpV ortholog is identifiable in T6SS^{iii} gene clusters, we sought to monitor the subcellular localization and dynamic behavior of this protein as a way to further interrogate the mechanistic similarity between T6SS^{i} and T6SS^{iii} pathways. We began by generating a strain of *F. johnsoniae* bearing a functional *clpV–gfp* fusion at the native *clpV* locus (Figure 5.5C). Visualization of this strain using time-lapse fluorescence microscopy revealed punctate foci appearing, disappearing, and frequently reappearing at different subcellular locations, on a rapid time scale (Figure 5.5D). Inactivation of the system in *F. johnsoniae* through the deletion of *tssC* abrogated these foci, similar to what has been observed in the T6SS^{i} pathway. It is worth noting that T6SS^{iii} ClpV exhibits punctate localization and dynamic behavior in the absence of an apparent TssM homolog, whereas in T6SS^{i} systems, TssM proteins are required for ClpV dynamics. Taken together with our bioinformatic, secretomic, and phenotypic data, these findings strongly suggest that the T6SS^{iii} pathway functions in a manner mechanistically similar to T6SS^{i} despite a highly divergent and unique assemblage of core components.

Bacteroides fragilis targets *B. thetaiotaomicron* via T6SS^{iii}

Motivated by our characterization of the T6SS^{iii} pathway in *F. johnsoniae*, we sought to explore the relevance of our findings to human-associated Bacteroidetes. Our analyses indicate T6SS^{iii} gene clusters are present in many members of the genus *Bacteroides*, including numerous prominent human gut residents (Figure 5.2C). To probe the potential for the T6SS^{iii} pathway to

influence the behavior of these organisms in a physiological setting, we colonized germfree mice with a community containing *B. fragilis*, *B. eggerthii*, and the Proteobacterium *E. coli*, and measured T6SS^{iii} expression. Quantitative reverse transcriptase (RT)-PCR of the cecal contents from these mice revealed the *tssC* gene in both *Bacteroides* species is expressed, at levels approaching (*B. eggerthii*) or exceeding (*B. fragilis*) the housekeeping transcript *rpoD* (Figure 5.6A).

Expression of *tssC* in the mammalian gut environment led us to hypothesize that the T6SS^{iii} pathway could be employed by *Bacteroides* to target other Gram-negative human gut microbes, including other species of *Bacteroides*. To test this hypothesis, we assessed the ability of wild-type *B. fragilis* to inhibit growth of the prominent human gut commensal *B. thetaiotaomicron*, which lacks a T6SS. Growth competition experiments revealed that *B. fragilis* reduces *B. thetaiotaomicron* growth by approximately two orders of magnitude (Figure 5.6B). Strikingly, this activity is almost entirely T6SS^{iii}-dependent, as an in-frame, unmarked deletion of *tssC* (BF9343_1941) in *B. fragilis* renders this species largely unable to reduce *B. thetaiotaomicron* growth. These data demonstrate the capacity of T6SS^{iii} to act between prominent human gut-associated members of the genus *Bacteroides*.

DISCUSSION

With the bioinformatic and functional characterization of T6SS^{iii}, it is now evident that the Bacteroidetes possess a means for contact-dependent interbacterial antagonism. This is in-line with the observation that Bacteroidetes frequently occupy contact-promoting, polymicrobial niches (170). Indeed, many of the organisms we identify the T6SS^{iii} pathway within, including

Porphyromonas, *Prevotella* and *Bacteroides* spp, are highly adapted host-associated obligate anaerobes that predominate – as pathogens or commensals – within the most densely populated polymicrobial sites in the human body (172, 182). Thus, within sites such as the GI tract, oral cavity, and the vagina, where bacteria with T6SS^{iii} are abundant, the pathway may play a broad role in defining community composition.

By analogy with T6SS^{i} and T6SS^{ii}, it is reasonable to speculate that T6SS^{iii} has the capacity to mediate host cell interactions in addition to its now established role in interbacterial antagonism. Certain T6SS^{i} and T6SS^{ii} pathways appear to specialize in either bacterial or host cell targeting, whereas others can act on both cell types (9, 14, 58, 60, 195, 196). Target range appears to be dictated, at least in part, by the specific complement and corresponding activities of the effectors transported by a system. For example, recent reports suggest that by virtue of structural conservation among the phospholipid constituents of cellular membranes, T6S effectors belonging to the Tle phospholipase superfamily can confer both anti-bacterial and anti-eukaryotic activity (47, 183, 197). While members of the Tle superfamily are among the many apparent effectors of T6SS^{iii}, the preponderance of predicted effectors that target peptidoglycan, a molecule found exclusively in bacteria, indicates that interbacterial antagonism is likely the basal function of the T6SS^{iii} pathway.

Despite lacking several T6SS^{i} core components, including TssJ, L, and M, our observations suggest that T6SS^{iii} functions in a fundamentally analogous manner. Both systems exhibit dynamic behavior, target effectors to the periplasm of recipients, and abundantly export VgrG and Hcp-family proteins. There are several conceivable explanations for these observations. One

possibility is that the unique T6SS^{iii} components, TssN, TssO, and TssP functionally substitute for the missing components. This model is supported by the prediction that these components, like TssL and M, are integral membrane proteins (33) (198). However, TssJ is a predicted lipoprotein that requires localization to the outer membrane for function, and so far a T6SS^{iii}-conserved predicted outer membrane-localized protein has not been identified. It is worth noting that TssJ, L, and M interact stably to form a trans-envelope complex (179). While it has been postulated that this complex facilitates the passage of bacteriophage-like proteins and effectors out of the recipient cell, there are little experimental data to support this notion. It is therefore not yet possible to rule out a model whereby the components shared between T6SS$^{i\text{-}iii}$ – namely those belonging to the bacteriophage-like sub-complex – represent the minimal structural assemblage of the T6SS. Distinguishing essential structural components from proteins with critical regulatory roles, for example, can be challenging (85, 108). Understanding the functional significance of the varied complement of core elements associated with T6SS$^{i\text{-}iii}$ will ultimately require both detailed biochemical approaches aimed at defining more precisely the roles of the individual proteins and ultra-structural characterization of the system.

While T6SS^{i} and T6SS^{iii} are divergent, predicted effector proteins in T6SS^{iii}-encoding organisms are often closely related to homologs in organisms possessing T6SS^{i}. For example, homologs of Fte1 are readily identified in *Acinetobacter* spp as well as strains of *E. coli*. These homologs, like Fte1, are encoded adjacent to predicted periplasmic immunity proteins as well as VgrG, suggesting that they likely possess common modes of toxicity and export. The relative ease with which homologs of effectors that transit the T6SS^{i} and T6SS^{iii} pathways can be identified is

further indicative of the similarity between these two systems and suggests they might share a common pool of potential effectors exchanged through horizontal gene transfer.

The gene encoding one of the putative substrates identified in our study, Fjoh_3274, is found adjacent to a locus that encodes a small protein possessing a DUF4280 domain (Fjoh_3275). In Fjoh_3274 homologs found in other species, these open reading frames are often fused, suggesting their function is linked. Structure prediction algorithms indicate a strong likelihood that DUF4280 adopts a fold closely related to the PAAR domain, which forms a pyramidal structure that is thought to recruit effector proteins to the apparatus via interaction with VgrG (48). Interestingly, proteins bearing DUF4280 are found in Gram-positive bacteria, a division of bacteria not known to possess a T6S-like pathway. Moreover, the genes encoding these proteins are often found adjacent to VgrG-like proteins. Our finding herein that the T6S pathway extends to the Gram-negative phylum Bacteroidetes raises the possibility that other organisms, even Gram-positive bacteria, may also possess related systems that have yet to be identified. By analogy, the antibacterial nature of the C-terminal polymorphic toxin domains of YD-repeat proteins was initially discovered in Gram-negative bacteria; however, more recent studies have found homologs of these toxin domains participate in interbacterial antagonism in Gram-positive organisms (199, 200).

Colonization resistance is a property of the gut microbiota whereby it acts as a coherent, resilient entity that exhibits resistance to invading microbes (201). The importance of this property is exemplified by the enhanced susceptibility to pathogens observed following either depletion or dysbiosis of the gut microbial community during antibiotic treatment (202). Notably, recent

studies have also shown that individuals carry the same commensal strains in their gut microbiomes for years or decades, and that members of the Bacteroidetes exhibit the greatest stability (203). A complete molecular explanation for these observations will likely include metabolic exclusion (204), colonization of critical niches (205), and the production of diffusible antimicrobials such as bacteroicins (206). We posit that antagonistic contact-dependent interactions mediated by the T6SS^{iii} pathway are another important contributor to colonization resistance and commensal stability. Interestingly, Turnbaugh and colleagues recently identified a transcript corresponding to a core T6SS^{iii} element (*vgrG*) derived from Bacteroidales in a metatranscriptome of fresh human fecal samples (207). Moreover, another study showed that the physical environment of the gut is conducive to T6S-mediated interbacterial interactions (208). While experiments involving T6SS^{iii} mutants within gut colonization models will be needed in order to directly establish its role in this environment, taken together with our demonstration of the antibacterial nature of the system, these findings are consistent with the hypothesis that contact-dependent interbacterial interactions occur among commensals in the human gut.

MATERIALS AND METHODS

Bacterial strains and growth conditions

F. johnsoniae, *B. thailandensis*, *P. putida*, *B. fragilis*, *B. eggerthii*, and *B. thetaiotaomicron* used in this study were derived from the sequenced strains UW101, E264, KT2440, NCTC 9343, ATCC 27754, and VPI-5482 respectively (76, 136, 187, 209). *E. coli* strains used in this study included DH5α for plasmid maintenance and tri-parental conjugation of plasmids into *F. johnsoniae* and *B. fragilis*, Rosetta 2(DE3) (EMD Millipore) for toxicity experiments, BL21(DE3) pLysS for the expression and purification of Fjoh_3262, and Nissle 1917 for mouse

colonization experiments. *F. johnsoniae* was grown on modified tryptone yeast extract media (TYE, 10g tryptone, 5g yeast extract, and 1g $MgSO_4$ per liter supplemented with 10 mM Tris-Cl pH 7.5) (210), PY2 (2g peptone, 0.5g yeast extract per liter) (211), synthetic CF sputum media (SCFM) (156), or Luria-Bertani media (LB) at 23 °C. *B. thailandensis*, *E. coli*, and *P. putida* were grown on LB at 37 °C or 30 °C (*P. putida*). All *Bacteroides* strains were cultured in liquid TYG medium (212) at 37 °C in a flexible anaerobic chamber (Coy Laboratory Products) containing 20% CO_2, 10% H_2, and 70% N_2. *B. eggerthii* and *B. fragilis* were additionally cultured on either brain heart infusion (BHI; Becton Dickinson) agar supplemented with 10% horse blood (Colorado Serum Co. or Quad Five), or BHI supplemented with 50 μg/mL hemin (Sigma-Aldrich) and 0.5 μg/mL menadione (MP Biomedicals), respectively. Media were supplemented with antibiotics as needed for the following organisms at the indicated concentrations: *F. johnsoniae* – erythromycin (100μg ml^{-1}), streptomycin (100 μg ml^{-1}), and kanamycin (25 μg ml^{-1}), *P. putida* – gentamycin (30 μg ml^{-1}) and irgasan (25 μg ml^{-1}), *Bacteroides* – gentamycin (200 μg ml^{-1}), tetracycline (2μg ml^{-1}), and erythromycin (10 μg ml^{-1}), and *E. coli* – carbenicillin (150 μg ml^{-1}), kanamycin (50 μg ml^{-1}), streptomycin (50 μg ml^{-1}), chloramphenicol (30 μg ml^{-1}), and trimethoprim (200 μg ml^{-1}) Isopropyl-b-D-thiogalactoside (IPTG) and rhamnose were added in stated concentrations to media to induce expression in *E. coli*. Fluorescently labeled *B. thailandensis* and *P. putida* strains possessed GFP expression cassettes integrated into the *attTn7* site as described previously (58, 213). A marked strain of *B. thetaiotaomicron* Δ*tdk* was generated by the introduction of a tetracycline resistance gene in a pNBU2 vector as previously described (214). Allelic exchange in *F. johnsoniae* was performed utilizing the method developed by McBride and colleagues, with streptomycin counter-selection performed on PY2 media instead of CYE media and all other growth steps on TYE rather than

CYE (190). The *B. fragilis* Δ*tssC* strain was constructed using the mobilizable *Bacteroides* suicide vector pNJR6 (215). *B. fragilis* cointegrants were selected using erythromycin, grown under non-selective conditions to allow merodiploid resolution, and individual colonies were tested for erythromycin sensitivity and subsequently screened for the mutation by PCR. The deletion was confirmed by sequencing.

DNA manipulations

The creation, maintenance and transformation of plasmid constructs followed standard molecular cloning procedures. All primers used in this study were obtained from Integrated DNA Technologies. DNA amplification was carried out using Phusion (New England Biolabs) in HF buffer with the addition of 1mM $MgCl_2$. DNA sequencing was performed by Genewiz Incorporated. Restriction enzymes were obtained from New England Biolabs.

Plasmid construction

Plasmids used in this study included pRR51 and PNJR6 for the introduction of non-polar mutations into *F. johnsoniae* and *B. fragilis*, respectively (190, 215), pCP11 for complementation (210, 216), pR600 for mobilizing plasmids into *F. johnsoniae*, R751 for plasmid mobilization into *B. fragilis*, pScrhab2 for the expression of immunity proteins (84), pET29b+ (Novagen) for the expression of proteins with a C-terminal His-tag, and pET22b+ (Novagen) for the expression of proteins directed to the periplasmic space with a C-terminal His-tag. For the generation of deletion and genomic fusion constructs for *F. johnsoniae*, 2.2 kb regions flanking the locus of interest were amplified and serially cloned into pRR51 using BamHI, XbaI, and SphI sites. Similarly, the *B. fragilis* Δ*tssC* deletion construct was created by

amplifying two 1.5 kb flanks upstream and downstream of the gene, joining these regions by splicing by overlap extension PCR (217), and ligating the resulting product into pNJR6 after a SalI/BamHI digest. For the *fte1* pET29b+ expression construct, the gene was cloned using NdeI/XhoI as fusion to the C-terminal His_6 tag, and for the pET22b+ expression construct cloning was performed using BamHI/XhoI to generate a fusion to the PelB leader peptide and C-terminal His_6 tag. For the *fti1* immunity expression construct, the gene was cloned without a stop codon into pScrhaB2 with an NdeI/XbaI digest and subsequently a linker region encoding a VSV-G epitope tag and a stop codon was introduced at the 3' end of the gene. The construct for the expression of *tsi1* was described previously (105). In order to complement Fjoh_3266 (*tssC*), the predicted promoter region of the $T6SS^{iii}$ operon containing this gene was first cloned into BamHI-digested pCP11 using a BamHI/BglII digest to generate pCP11–pT6S. Into this vector, *tssC* and a 39 base pair upstream region that includes its ribosomal-binding site was cloned using a SacI/SmaI digest.

Informatic analyses

ClpV- and VgrG-like proteins from the Bacteroidetes were identified by automated annotation from NCBI blast servers (http://blast.ncbi.nlm.nih.gov/Blast.cgi) (218). Hcp-like proteins were initially found within *F. johnsoniae* by PHYRE 2.0 (http://www.sbg.bio.ic.ac.uk/phyre2), and were thereafter identified by homology using blastp analysis (70). Other T6SS homologs were identified in $T6SS^{iii}$ gene clusters by the application of the iterative search algorithm jackHmmer (http://hmmer.janelia.org/search/jackhmmer) on the RefSeq protein database using seed proteins obtained from *F. johnsoniae* (186, 219). After manual removal of sequences likely to represent non-T6SS components, partial sequences, bacteriophage, or pseudogenes, sequences were

aligned utilizing MAFFT within Geneious set to automated strategy choice (220). These sequences were then clustered using the Geneious UPGMA algorithm and representative proteins were chosen by excluding related sequences with a calculated distance of less than 0.08 residue differences per site. This representative set was then aligned using an online MAFFT server (http://mafft.cbrc.jp/alignment/server/) using the E-INS-i strategy, a BLOSUM62 scoring matrix, and a gap open penalty of 1.53 (220). For TssC and TssF trees these alignments were then trimmed using TrimAl set to the automated approach optimized for maximum-likelihood (ML) trees, and then further manually trimmed at ends to bound the alignment with regions of relatively high conservation (221). From these alignments ML trees were generated using a PHYML 3.0 server (http://www.atgc-montpellier.fr/phyml/), with the LG model of substitution (161). For the TssC ML tree consisting of only T6SS^{iii} members, the original set of sequences obtained from jackHMMER before subsequent steps was filtered to remove all proteins not resident in T6SS^{iii} clusters except for Acidobacterial sequences in T6SS^{iii}-like clusters which were maintained for use as an outgroup. This subset was then aligned using the MAFFT G-INS-i strategy. This alignment was trimmed using TrimAl, and used to generate an ML tree using PHYML 3.0 as before. All tree branch supports were generated using the aBayes method within PHYML 3.0 (222).

Domain prediction for Fjoh_3281 (*clpV*), Fjoh_3257 (Fte1), and Fjoh_3274 relied on automated prediction from NCBI, structure prediction from PHYRE 2.0, and hidden-markov model prediction by HMMscan and HHpred (70, 140, 219). The PAAR-like region of Fjoh_3257 was further identified through HHpred analysis performed on an alignment of proteins bearing

Fjoh_3257-like sequences at their N-termini. Predicted subcellular localization was obtained through use of SignalP 4.1 and TMHMM 2.0 (223, 224).

Preparation of samples for secretome analysis

Mid-log cultures of *F. johnsoniae* UW101 and *F. johnsoniae* UW101 Δ*tssC* grown in 2ml of SCFM were pelleted, washed, and used to inoculate 215 ml of SCFM to an OD_{600} of 0.001. Cells were then grown at 23 °C to an OD_{600} of 0.3-0.4 before being pelleted by centrifugation at 6000 g for 15 min at 4 °C. To ensure complete removal of cells, the supernatant fractions were collected and spun again at 6000 g for 15 min at 4 °C. Deoxycholic acid was then added to the sample supernatants to a final concentration of 0.2 mg/mL followed by incubation on ice for 30 min. Trichloroacetic acid (TCA) was then added to a final concentration of 8% (*v*/*v*) and the samples were incubated overnight at 4 °C. Precipitated proteins were pelleted by centrifugation at 18000 *g* for 30 min at 4 °C, dissolved in 4 mL ddH_20, and re-precipitated by the addition of 32 mL of pre-chilled 100% acetone followed by incubation at -20 °C for 2 h. The precipitate was spun at 18,000 *g* for 30 min at 4 °C, the supernatants discarded, and the pellets dried by evaporation. Samples were dissolved in 100 mM ammonium bicarbonate, 8 M urea and reduced by the addition of 1 mM Tris(2-carboxyethyl)phosphine (TCEP) followed by incubation for 1 h at 37 °C. Free cysteine residues in the protein samples were alkylated by adding iodoacetamide to a final concentration of 10 mM and incubated for 30 min at room temperature in the dark. Following quenching of iodoacetamide with 12 mM *N*-acetylcysteine, samples were diluted with 100 mM ammonium bicarbonate to lower the urea concentration to 1.5 M before treating with sequencing grade trypsin (Promega) overnight at 37 °C. Peptides were diluted with 100% acetonitrile and 10% (*w*/*v*) trifluoroacetic acid (TFA) to a final concentration of 5% (*v*/*v*) and

0.1% (*w*/*v*) and applied to C18 spin columns (Pierce) that had been charged with two washes of 100% acetonitrile followed by one wash with ddH_2O. Bound tryptic peptides were washed twice in 5% (*v*/*v*) acetonitrile, 0.1% (*w*/*v*) TFA before elution with 70% (*v*/*v*) acetonitrile, 25 mM formic acid.

MS analysis of tryptic peptides

Peptide digests were analysed by electrospray ionization in the positive ion mode on a hybrid quadrupole-orbitrap mass spectrometer (Q Exactive™, Thermo Fisher, San Jose, CA). The Q Exactive was equipped with a nanoflow HPLC system (NanoAcquity; Waters Corporation, Milford, MA) fitted with a home-built helium-degasser. Peptides were trapped on a homemade 100 μm i.d. × 20 mm long pre-column packed with 200 Å particles (5μm, C18AQ; Michrom BioResources, Auburn, CA, USA). Subsequent peptide separation was performed on an in-house constructed 75 μm i.d. × 180 mm long analytical column pulled using a Sutter Instruments P-2000 CO_2 laser puller (Sutter Instrument Company, Novato, CA) and packed with 100 Å particles (5 μm, C18AQ: Michrom). For each injection, an estimated amount of 1 μg of peptide mixture was loaded onto the pre-column at 4 μL min^{-1} in water/acetonitrile (95/5) with 0.1% (*v*/*v*) formic acid. Peptides were eluted using an acetonitrile gradient flowing at 250 nL min^{-1} using mobile phase consisting of: A, water, 0.1% formic acid; B, acetonitrile, 0.1% formic acid with a total gradient time of 95 min. Ion source conditions were optimized using the tuning and calibration solution recommended by the instrument provider. Data were acquired using MS survey scans in the Orbitrap followed by data-dependent selection of the 20 most abundant precursors for tandem mass spectrometry. Singly charged ions were excluded from analysis. Data redundancy was minimized by excluding previously selected precursor ions for 60 s

following their selection for tandem mass spectrometry. Data were acquired using Xcalibur, version 2.2 (Thermo Fisher). Samples were analyzed in triplicate.

Tandem mass spectra were searched for sequence matches against the UniProt *F. johnsoniae* UW101 database using MaxQuant v1.4.1.2 (225). The following modifications were set as search parameters: peptide mass tolerance at 6 ppm, trypsin digestion cleavage after Lys or Arg (except when followed by Pro), allowed missed cleavage site, carbamidomethylated cysteine (static modification), oxidized methionine, and protein N-term acetylation (variable modification/differential search option). Relative abundance of proteins was assessed using spectral counting (142). Proteins were filtered such that all had at least two unique peptides detected and possessed an average of three spectral counts in wild-type replicates.

Protein expression and purification

E. coli BL21 (DE3) cells (Novagen) harboring pET29b::Fjoh_3262 were grown in LB broth supplemented with kanamycin. Cells were grown at 37 °C to an OD_{600} of 0.6 before protein expression was induced with 1 mM IPTG for 4 h. Pelleted cells were then resuspended in 50 mM Tris-HCl, pH 8.0, 300 mM NaCl, 5 mM imidazole and lysed by sonication. Following centrifugation, the cleared cell lysates were passed over a Ni^{2+}-nitrilotriacetic acid affinity column using a linear gradient of 5–400 mM imidazole. The Fjoh_3262-containing fractions were then pooled and concentrated by spin ultrafiltration (10 kDa molecular weight cutoff, Amicon) before being further purified by size exclusion chromatography in 20 mM Tris-HCl, pH 8.0, 150 mM NaCl.

Negative stain electron microscopy

Purified Fjoh_3262-His_6 was negatively stained by 0.75% uranyl formate using standard procedures (226). Images were collected on a transmission electron microscope T12 (FEI) at room temperature operating under 120 kV and recorded at a magnification of 68,000X on a 4k X 4k Teitz CCD. The size of a pixel on the displayed image is 1.50Å.

***E.coli* growth curves**

Overnight LB cultures of *E. coli* Rosetta cells bearing the indicated plasmids were diluted 1:40 v/v in LB low salt (LB-LS, 10 g tryptone, 5 g yeast extract) without antibiotics (Figure 5.4B) or LB-LS supplemented with 0.1% w/v rhamnose (Figure 5.4D). Cells were then grown at 37 °C with shaking and measurements were taken of the optical density at 600 nm (OD_{600}) every 30 minutes. At 120 minutes cells were induced to express putative antibacterial proteins with the addition of 1 mM (Figure 5.4B) or 50 μM (Figure 5.4D) IPTG. Growth continued to be monitored every 30 minutes until the end of the experiment. Whole cell fractions for the measurement of Fte1-His_6 and peri-Fte1-His_6 expression were prepared 120 minutes after induction as described previously (85). Western blot analysis of these fractions using anti-RNA polymerase and anti-His_6 was performed using previously defined methods (105).

Fte1 self-intoxication experiments

F. johnsoniae strains bearing the indicated mutations were streaked onto 1.5% w/v agar TYE plates 24 hours prior to the experiment. Concomitantly, 2% w/v PY2 plates were produced. On the day of the experiment PY2 plates were dried for 30 minutes open to the air and a nitrocellulose membrane was placed on the surface. *F. johnsoniae* strains were then resuspended

in ddH2O to a final OD_{600} of 0.3 and 5 µl of this mixture was placed on the nitrocellulose surface. After 20 h of incubation at 23 °C cells were resuspended in ddH2O and stained with propidium iodide at final concentration of 5 µg ml^{-1} for 10 minutes. Cells were then pelleted and washed with ddH2O and readings were taken of turbidity (OD_{600}) and propidium iodide fluorescence (excitation/emission at 535/617 nm). Experiments in liquid culture were performed identically with the modification that 1 µl of cell suspension was used to inoculate 1 ml of PY2 liquid media, and after 20 h of growth 500 µl of culture was pelleted and washed in ddH2O prior to staining.

Bacterial competition experiments

For *F. johnsoniae* competition experiments, *F. johnsoniae* strains were streaked onto 1.5% w/v agar TYE plates 48 hours prior to the experiment. Cells grown from these plates were then resuspended to an OD_{600} of 0.06 in LB and 80 µl of this suspension was plated on a 1.5% w/v agar TYE plate 24 hours prior to the experiment. Concurrently, competitor cells bearing constitutive GFP reporters were streaked on LB 1.5% w/v agar plates and grown at 37 °C (*B. thailandensis*) or 30 °C (*P. putida*), and 2% agar w/v PY2 plates were generated. On the day of the experiment, the 2% agar w/v PY2 plates were dried for 30 minutes open to the air and nitrocellulose was placed on the agar surface. *F. johnsoniae* strains were respuspended from the TYE plates in ddH_2O to an OD_{600} of 3.0, and *B. thailandensis* and *P. putida* were similarly resuspended to an OD_{600} of 0.3. Suspensions were mixed at a 4:1 v/v ratio of *F. johnsoniae*:competitor and 5 µl of this solution was spotted on the nitrocellulose surface. After 20 h of growth at 23 °C competitions were harvested in 200 µl of LB and serial dilutions were generated. To obtain both initial and final counts of *F. johnsoniae* strains, dilutions were plated

on TYE plates and grown at 23 °C and colonies displaying clear *F. johnsoniae* morphology were enumerated. To obtain counts of *B. thailandensis* and *P. putida*, dilutions were plated on either LB or LB supplemented with irgasan and gentamycin, and grown at 37 °C or 30 °C, respectively, selecting against *F. johnsoniae* growth. For liquid competitions, steps were performed identically except that the competition was performed in 2 ml of PY2 liquid media inoculated with either 5 µl (*B. thailandensis*) or 2.5 µl (*P. putida*) of cell suspension, and *F. johnsoniae* counts were obtained from *P. putida* co-cultures by plating on TYE supplemented with kanamycin. Visualization of competitions by photography and GFP fluorescence was performed 48 hours after the start of the experiment to allow for robust growth of GFP-labeled strains.

For *Bacteroides* growth competition experiments, all strains were grown to stationary phase in TYG medium at 37˚C anaerobically. Optical densities were adjusted to 6.0 for *B. fragilis* strains and 0.6 for the *B. thetaiotaomicron* Δ*tdk* strain bearing a tetracycline resistance gene. Cells were mixed at a 1:1 v/v ratio, pelleted, resuspended in ddH_2O, and 5 µl of each mixture was spotted onto nitrocellulose squares placed on BHI agar supplemented with 50 µg/mL hemin and 0.5 µg/mL menadione. After incubation at 37˚C anaerobically for 24 h, competition mixtures were resuspended in TYG medium and serial dilutions were plated on BHI agar supplemented with 10% horse blood, 200 µg/mL gentamicin, and 2 µg/mL tetracycline to select for *B. thetaiotaomicron*.

Microscopic analyses of dynamic ClpV foci

Time-lapse fluorescence microscopy sequences were acquired with a Nikon Ti-E inverted microscope fitted with a X60 oil objective, automated focusing (Perfect Focus System, Nikon), a

Xenon light source (Sutter Instruments), a CCD camera (Clara series, Andor), and a custom environmental chamber as described previously (151). NIS Elements (Nikon) was used for automated image acquisition. *F. johnsoniae* cells were prepared similarly to bacterial competition experiments with the modifications that the initial OD_{600} used was 0.75 and cells were harvested after 18h of growth as monocultures. After harvesting, cells were placed on 1.5 % w/v agarose phosphate-buffered saline pads and visualized. Automated image acquisition was performed at 5s intervals for 6 minutes.

Genomic DNA extraction

B. eggerthii and *B. fragilis* were each grown to stationary phase in 5 mL liquid TYG medium. Genomic DNA was extracted by phenol-chloroform extraction and bead-beating as described (227).

Gnotobiotic animal studies

All animal experiments were performed using protocols approved by the Yale University Institutional Animal Care and Use Committee. Germ-free Swiss Webster mice were maintained in flexible plastic gnotobiotic isolators with a 12-hour light/dark cycle. Mice were individually caged (n = 5/group) and were provided with standard autoclaved mouse chow (5K67 LabDiet, Purina) ad libitum. On day 0, mice were gavaged orally with $2x10^8$ CFU of each strain (*B. fragilis*, *B. eggerthii*, and *E. coli*). Animals were sacrificed on day 7 and samples were collected along the length of the gut. All samples were snap-frozen in liquid nitrogen and stored at -80˚C. To obtain RNA, mouse cecum samples were resuspended in RNAprotect Bacteria Reagent (Qiagen), and subjected to bead beating for two one-minute cycles. RNA was then extracted and

purified using the Trizol reagent (Invitrogen) according to the manufacturer's instructions. Contaminating genomic DNA was removed by treating RNA preparations with Turbo DNase (Invitrogen) for one hour, followed by a second Trizol purification. Prior to cDNA synthesis, RNA samples were checked for DNA contamination with PCR. From RNA samples in which no PCR product was detected after 35 cycles using primers targeting *rpoD* of *B. fragilis,* cDNA was synthesized using the iScript cDNA synthesis kit (Biorad). Quantitative PCR to measure gene expression was performed on cDNA samples using the SsoAdvanced™ Universal SYBR® Green Supermix (Biorad), and expression for each T6SS gene was normalized to *rpoD* expression levels in the same organisms.

Acknowledgments

We thank M. McBride and L. Comstock for sharing reagents and protocols necessary for generating the *F. johnsoniae* and *B. fragilis* mutants used in our study, M. LeRoux and R. Kirkpatrick for assistance with fluorescence microscopy, and members of the Mougous and Goodman laboratories for helpful discussions. This work was supported by grants from the National Institutes of Health (NIH) (AI080609 and AI105268 to J.D.M.; DK089121, GM103574, and GM105456 to A.L.G). Research in the Gonen laboratory is supported by the Howard Hughes Medical Institute. Mass spectrometry analyses were supported by the University of Maryland Baltimore, School of Pharmacy Mass Spectrometry Center (SOP1841-IQB2014). A.B.R. was supported by the Josephine de Karman Fellowship Trust and the University of Washington Department of Microbiology Helen Whiteley Award. J.C.W. was supported by a postdoctoral research fellowship by the Canadian Institutes of Health Research. A.J.B. was supported by a grant from the National Science Foundation (DGE-1256082). S.C. was supported

by a Howard Hughes Medical Institute Life Sciences Research Foundation Fellowship. J.D.M. holds an Investigator in the Pathogenesis of Infectious Disease Award from the Burroughs Wellcome Fund.

Table 5.1: Summary of elements conserved in T6SS^{iii} gene clusters.

Name	*F. johnsoniae* locus[a]	*B. fragilis* locus	Predicted Localization[b]	Present in T6SS^{i}	Pfam annotation[c]
VgrG	Fjoh_3260	BF9343_1930	Cytoplasmic	Yes	Phage GPD, Phage base V
ClpV	Fjoh_3281	BF9343_1940	Cytoplasmic	Yes	AAA, AAA-2, ClpB D2-small
TssB	Fjoh_3267	BF9343_1942	Cytoplasmic	Yes	None
TssC	Fjoh_3266	BF9343_1941	Cytoplasmic	Yes	DUF877
TssE	Fjoh_3263	BF9343_1932	Cytoplasmic	Yes	GWP gp25
TssF	Fjoh_3254	BF9343_1931	Cytoplasmic	Yes	None
TssG	Fjoh_3278	BF9343_1923	Cytoplasmic	Yes	DUF1305
TssK	Fjoh_3269	BF9343_1924	Cytoplasmic	Yes	None
TssN	Fjoh_3277	BF9343_1925	Inner-membrane	No	None
TssO	Fjoh_3268	BF9343_1921	Inner-membrane	No	None
TssP	Fjoh_3280	BF9343_1920	Inner-membrane	No	PKD domain
Hcp	Fjoh_3262	BF9343_1935	Cytoplasmic	Yes	None

[a]Locus tag within *F. johnsoniae* UW101 or *B. fragilis* NCTC 9343. If paralogs exist only one is indicated.
[b]Predicted localization derived from SignalP 4.1 and TMHMM 2.0 analysis of *F. johnsoniae* proteins.
[c]Analysis of *F. johnsoniae* proteins by the Pfam server (http://pfam.xfam.org/)

Table 5.2: Secreted proteins not detected the *F. johnsoniae* Δ*tssC* secretome

Locus Tag[a]	Name	Abundance[b]	Unique peptides detected	Signal peptide[c]	T6SS^{iii} cluster[d]	Molecular weight	Predicted/determined function
Fjoh_3262	Hcp	133 ± 3.5[e]	10	N	Y	14.5	Secreted T6S structural component
Fjoh_3260	VgrG	13.3 ± 1.5	5	N	Y	66.0	Secreted T6S structural component
Fjoh_3206	RemH	11.7 ± 2.3	4	Y	N	16.9	Gliding motility
Fjoh_0984	RemF	5 ± 1.0	4	Y	N	16.8	Gliding motility
Fjoh_3274	–	4 ± 1.0	3	N	Y	102	T6SS^{iii} effector
Fjoh_3257	Fte1	3 ± 1.7	2	N	Y	62.7	T6SS^{iii} effector

[a] Locus tags derived from *F. johnsoniae* UW101 (NCBI Accession NC_009441.1).
[b] Average spectral counts of three technical replicates.
[c] Signal peptide predicted using SignalP 4.1 (http://www.cbs.dtu.dk/services/SignalP).
[d] The T6SS^{iii} gene cluster comprises two apparent divergently transcribed operons (Fjoh_3254-Fjoh_3281), with the terminal gene of each operon encoding a conserved T6SS^{III} element.
[e] Standard deviation of three technical replicates.

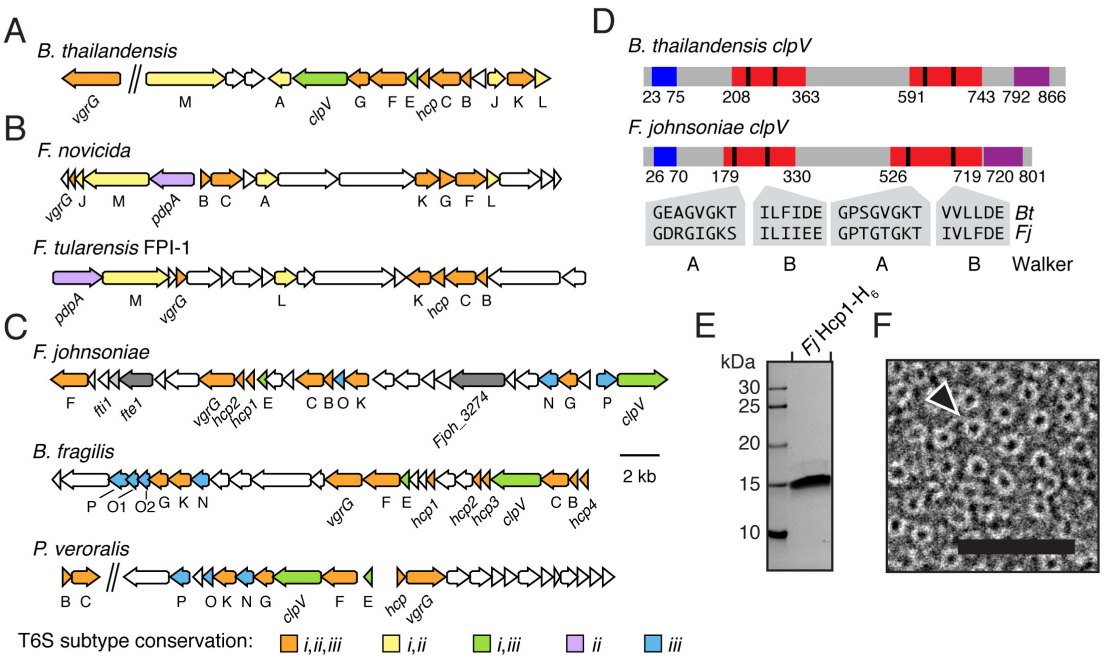

Figure 5.1: T6S-like gene clusters are found within the Bacteroidetes. (A-C) Gene content and conservation both within and between selected representative members of T6SS^{i} (A), T6SS^{ii} (B), and T6SS^{iii} (C). Genes with commonly used *tss* nomenclature are abbreviated to a single letter. The *Francisella tularensis* FPI is depicted owing to its status as the only T6SS^{ii} to be characterized; however, this system lacks clear homologs of *tssA* and *tssJ*, which are present in representative T6SS^{ii} systems such the *F. novicida* gene cluster shown. Locus tags of the regions shown: *B. thailandensis* E264 BTH_I2705 and BTH_I2954-2968 (A); *F. novicida* U112 FTN_0037-0054, *F. tularensis* SCHU FTT_1344-1361c (B); *F. johnsoniae* UW101 Fjoh_3254-328, *B. fragilis* NCTC 9343 BF9343_1918-1943, *P. veroralis* F0319 HMPREF0973_02422-02423 and HMPREF0973_02441-02466. Genes encoding *F. johnsoniae* T6SS^{iii} substrates identified in this study (dark grey) and a validated immunity locus (light grey) are labeled. (D) Comparison of domain organization of ClpV homologs from T6SS^{i} (*B. thailandensis*, *Bt*) and T6SS^{iii} (*F. johnsoniae*, *Fj*) pathways. Colors denote homologous domains: blue, Clp N; red, AAA+; purple, ClpB D2. Sequences highlight the conservation of motifs implicated in ATP binding and hydrolysis within the Walker A and B motifs. (E) SDS-PAGE analysis of purified Fjoh_3262 bearing a C-terminal hexahistidine tag (*Fj* Hcp1–H_6). Proteins were visualized by Coomassie Blue staining. (F) *F. johnsoniae* Hcp1 is a ring-shaped molecule with dimensions similar to Proteobacterial Hcp proteins. Transmission electron micrograph of purified *Fj* Hcp1–H_6 (E) negatively stained with uranyl formate. The arrowhead indicates a typical ring-like assembly. Scale bar, 40 nm.

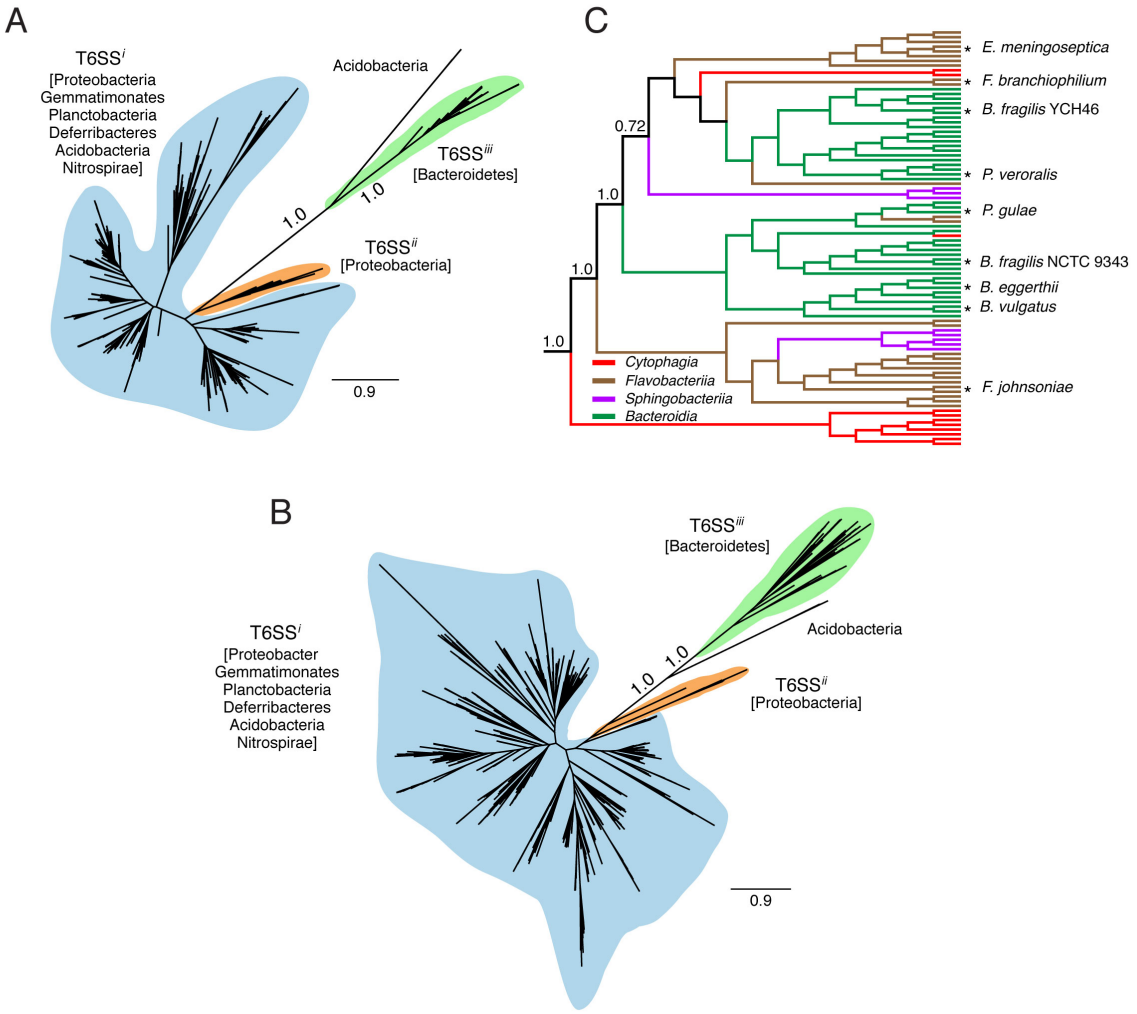

Figure 5.2: T6SS^{iii} is phylogenetically distinct from T6SS^{i} and T6SS^{ii}.
(A,B) Maximum likelihood (ML) phylogenetic trees generated from a partial alignment of (A) 686 representative TssC sequences or (B) 881 representative TssF sequences spanning the diversity present in T6SS^{i}, T6SS^{ii}, and T6SS^{iii} gene clusters. Phyla represented by each system are indicated. Branch support values derived from aBayes analysis for the T6SS^{iii} clade are shown. Scale bar represents amino acid changes per site. (C) ML tree created from a partial alignment of TssC sequences found within T6SS^{iii} gene clusters. The tree is rooted with Acidobacterial TssC sequences. Lengths do not reflect evolutionary distance. Colors trace the Class from which each sequence is derived. Nodes representing TssC sequences of organisms discussed in the text and those of particular significance are marked with an asterisk. Branch support values were generated by aBayes analysis.

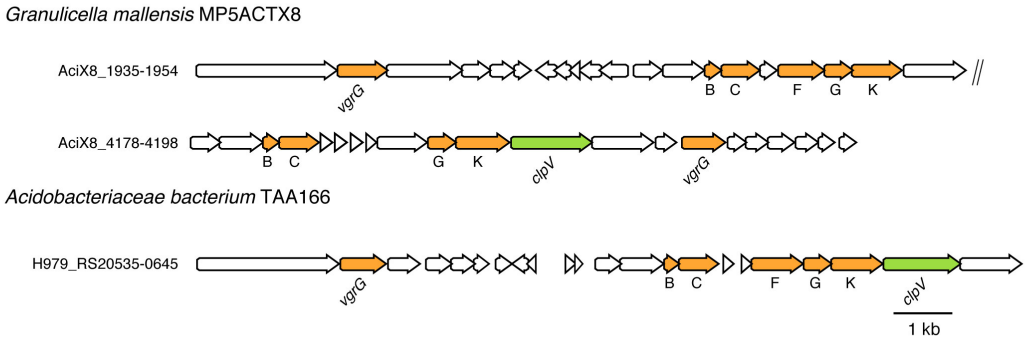

Figure 5.3: Acidobacterial homologs to Bacteroides T6SS components do not reside in T6SS^{iii} gene clusters. Genomic context of Acidobacterial proteins closely homologous to T6SS^{iii} components. Genes with commonly used *tss* nomenclature are abbreviated to a single letter, and are colored identically to Figure 5.1A.

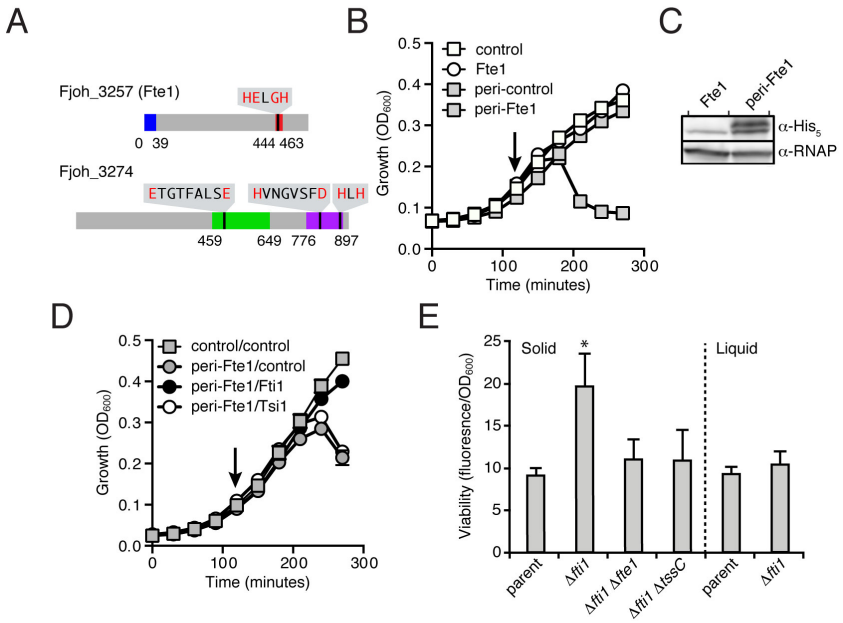

Figure 5.4: *F. johnsoniae* T6SS^{iii} exports an antibacterial protein that is encoded adjacent to a cognate immunity determinant. (A) Domain organization of the putative substrates of *F. johnsoniae* T6SS^{iii}. PAAR-like (blue), zinc-dependent metalloprotease (red), glycoside hydrolase (green), and zinc-dependent peptidoglycan amidase (purple) domains are indicated. Expanded amino acid sequences in each domain correspond to conserved motifs and invariant or critical catalytic residues (red). (B,D) Growth of *E. coli* strains harboring the indicated expression vectors. Empty vectors (control) and vectors that introduce an N-terminal Sec signal peptide (peri) are indicated. Cells were induced to express predicted immunity proteins (D) at time 0 and Fte1 at the indicated time point (arrow). Type VI secretion immunity protein 1 (Tsi1) is used as a non-cognate immunity control. Error bars represent ± standard deviation (SD) (n = 3). (C) Western blot analysis performed on *E. coli* containing expression vectors for Fte1–H_6 or Fte1–H_6 directed to the periplasm (peri) under induction identical to (B). RNA polymerase (RNAP) was used as a loading control. (E) Intercellular self-intoxication of the indicated *F. johnsoniae* strains as measured by propidium iodide staining. Liquid cultures were grown with vigorous shaking, which inhibits the formation of the prolonged cell–cell contacts required for T6-mediated interactions (14, 151). Error bars represent ± standard deviation (SD) (n = 3). Samples differing significantly from parent as measured by a two-tailed T-test are indicated by asterisks ($p < 0.01$).

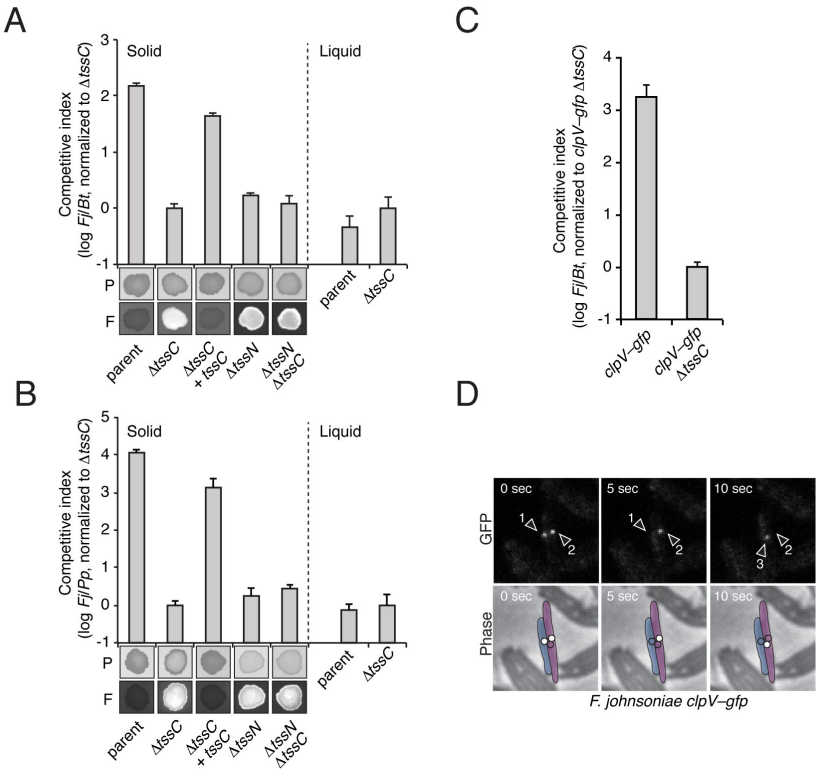

Figure 5.5: *F. johnsoniae* utilizes a dynamic T6SS^{iii} apparatus to target competitor organisms. (A-C) Growth experiments measuring fitness of the indicated *F. johnsoniae* (*Fj*) strains in co-culture for 20 hours with fluorescently-labeled competitors *B. thailandensis* (A and C, *Bt*) or *P. putida* (B, *Pp*). Competitive index is defined as the change in *F. johnsoniae* competitor colony forming units between initiation and harvest of the co-culture. Experiments were performed under contact-promoting (solid) and contact-inhibiting (liquid) conditions. Qualitative analysis of competition outcome by photographic (P) and fluorescence (F) imaging is shown for corresponding samples grown under contact-promoting conditions after 48 hours of co-culture. Error bars represent ± SD (n = 3). (D) Micrograph series depicting a 10s time course of wild-type *F. johnsoniae clpV–gfp*. Phase and GFP channels are presented separately. Three dynamic foci were observed over the duration of the experiment (arrowheads), and the presence or absence of each focus in each frame is schematized in the phase micrographs with white or unfilled circles, respectively.

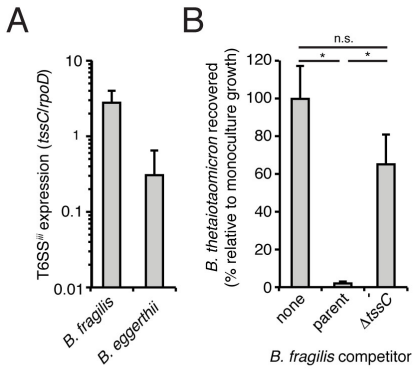

Figure 5.6: The T6SS^{iii} pathway is expressed and active in the genus Bacteroides. (A) Quantitative RT-PCR analysis of the *in vivo* expression of *tssC* for the indicated bacteria. Expression was measured in cecal samples from germfree mice colonized for one week with *B. fragilis*, *B. eggerthii*, and *E. coli* and normalized using species-specific primers for the housekeeping sigma factor, *rpoD*. Error bars represent ± standard error. (B) Growth competitions measuring viability of *B. thetaiotaomicron* after 24 h in the presence of the indicated *B. fragilis* strains on solid media. *B. thetaiotaomicron* growth was normalized to values obtained in the absence of *B. fragilis*. Viability was determined by colony forming units. Error bars represent ± SD (n = 3). Significance as indicated by asterisks was measured by a two-tailed T-test ($p<0.002$), n.s.; no statistical difference.

CHAPTER VI

Conclusions and future directions

Portions published as: Russell, A.B., Peterson, S.B., Mougous, J.D. 2014. *Nature Reviews Microbiology* 12, 137-148

A.B.R. contribution: Wrote the section excerpted in this chapter.

CONCLUSIONS

The type VI secretion system (T6SS) is a complex pathway mediating the delivery of antibacterial effector proteins between diverse Gram-negative organisms, and, rarely, virulence factors to eukaryotic cells. As the T6SS, unlike other mechanisms of competition such as contact-dependent growth inhibition (CDI) or bacteriocins, is relatively indiscriminate in targeting, its ecological consequences are potentially far-reaching (1, 61, 177). Increasing the impact of this pathway is its abundance throughout two significant Gram-negative phyla, the Proteobacteria and the Bacteroidetes – in which it can be found in at least one representative strain of approximately one fifth of all species (6, 228). Notably, this includes a number of environmental and human-associated organisms of interest such as the important commensal gut microbes and opportunistic pathogens *Escherichia coli* and *Bacteroides fragilis,* the ubiquitous oral commensal *Prevotella veroralis*, and a slew of opportunistic and professional pathogens such as *Pseudomonas aeruginosa*, *Vibrio cholerae*, and *Burkholderia pseudomallei*.

Initially in my thesis work, I characterized two effectors, type VI secretion exported 1 and 3 (Tse1 and 3), of the *P. aeruginosa* H1-T6SS. Through a collaborative effort, it was identified that Tse1 and Tse3 possess peptidoglycan amidase and glycosidase activity, respectively, attacking different bonds within the cell wall superstructure (105). Both of these effector proteins are delivered to the periplasmic compartment of recipient cells, and, due to this, their associated immunity proteins localize to that same compartment. These findings represented several important contributions to the field of interbacterial T6S: 1) That peptidoglycan, a bacterially-restricted molecule, can be the target of T6SS effectors, 2) that effector proteins can exert toxicity from the periplasmic compartment, and 3) that the effector–immunity paradigm first

established in the study of the H1-T6SS effector Tse2 and its immunity protein Tsi2 could be extended to additional substrates of the T6SS (14).

We also found that effectors possessing cell wall amidase activity are widespread in organisms possessing T6S. Using a heuristic approach derived from physical features of known interbacterial T6SS effectors we were able to identify four non-homologous families of T6S-delivered pepidoglycan amidases, named Tae1-4 (type VI amidase effector 1-4) (149). As peptidoglycan is unique to bacteria, the presence of a *tae* within a genome extended presumptive antibacterial activity to a number of before-uncharacterized T6SSs distributed throughout the Proteobacteria. Additionally, each Tae family was found to exhibit distinct substrate specificity, indicating that multiple bonds in the peptide crosslinks of peptidoglycan serve as sites of attack by interbacterial T6S. This potentially reflects adaptation to the modifications observed in Gram-negative peptidoglycan such as O-acetylation of glycans, modification of the free α-carboxylate of D-glutamate, and incorporation of non-canonical D-amino acids (129, 229, 230). Not only are distinct enzymatic activities displayed by each of the Tae families, but also immunity provided by cognate Tai (type VI amidase immunity) proteins exhibits allele specificity both within and between families. This indicates that there is not a common, conserved, interface by which an immunity protein interacts with its cognate effector, suggesting diversifying selection due to escalating arms races between bacteria with each striving to escape neutralization by a competitor's endogenous immunity.

Peptidoglycan is not the sole target of antibacterial effectors, and I was able to identify an additional superfamily of T6SS antibacterial effectors that possess phospholipase activity, the

Tle (type VI lipase effector) proteins (183). Like the Tae effectors and Tse3, Tle proteins are toxic when directed to the periplasm and are associated with cognate periplasmic immunity determinants, the Tli (type VI lipase immunity) proteins. Similar to the Tae superfamily, distinct families of Tle effectors exhibit different substrate specificities, with the characterized members of Tle1,2, and 5 families acting as phospholipase A2, A1, and D enzymes, respectively. Unlike peptidoglycan, the target of Tae proteins, phospholipids are conserved between eukaryotes and bacteria. Secreted and translocated phospholipases that target phospholipids that are either unique to eukarya, or that exhibit conditional activation upon delivery are commonly found in pathogens as potent mediators of virulence (145). Therefore early studies on Tle proteins focused only on their potential roles in pathogenesis. Indeed, several Tle proteins were found to contribute to virulence in animal and cell culture models of disease (47, 146, 197). However, our findings that bacterial-associated phospholipases could act in interbacterial antagonism has forced a reevaluation of assumptions concerning secreted phospholipases, and, for those instances where Tle proteins do appear to target both bacteria and eukaryotes, have suggested that interbacterial competition could be one factor enriching for the evolution of potent virulence factors.

Lastly, the presence of *tle1* homologs within the Bacteroidetes genus *Prevotella* led me to investigate the presence of the T6SS in this diverse phylum of Gram-negative bacteria (228). Initial analyses of the T6SS found the intact system limited to the Proteobacteria and a few Acidobacteria, Cyanobacteria, and Planctomycetes (6). Using paradigms of interbacterial effector–immunity pairs as a guide I was able to identify a large cluster of genes within Bacteroidetes containing clear homologs of the T6SS component *vgrG*, one or more likely

antibacterial proteins associated with putative immunity determinants, and eleven other conserved elements. Further analysis of all twelve (including *vgrG*) conserved genes revealed that they encode a putative secretion system containing distant homologs of nine of the thirteen components of the Proteobacterial T6SS and three unique proteins found only within Bacteroidetes. Subsequent study of this gene cluster in the organism *Flavobacterium johnsoniae* revealed that it encodes an active secretion apparatus which translocates antibacterial effectors to recipient bacteria in a contact-dependent fashion. These and other observations led us to the conclusion that Bacteroidetes possess a divergent T6SS comprised of a distinct assemblage of components. This explained the presence of T6SS effectors and associated domains in the Bacteroidetes, identified not only by our work, but also in larger informatic studies (184). Most importantly, the identification of T6S in the Bacteroidetes extended those findings procured in Proteobacteria to an even larger group of organisms, including those of human importance such as *B. fragilis*. Of particular relevance, our collaborators in Andrew Goodman's lab were able to demonstrate that the *B. fragilis* T6SS can be used to restrict the growth of another intestinal commensal of significant abundance, *Bacteroides thetaiotaomicron*, suggesting that further study is warranted concerning the impact of this system on the human microbiome.

The study of T6SS effectors has provided significant insight into the mechanisms and function of this secretion system. The work described in this dissertation is hardly the only research in this area, and it should be noted that significant strides have been made in identifying T6SS effectors by other, additional, studies (47, 51, 178, 231). Indeed, in addition to phospholipids and peptidoglycan, other targets of T6SS effectors, such as nucleic acids, have been identified (200, 232). However cataloging and characterizing effectors, while still useful, will likely no longer

provide the leaps in understanding provided by these initial studies. Rather, with the ability to examine distribution, regulation, and evolutionary history of effector proteins we may now generate more nuanced hypotheses as to the adaptive significance of the T6SS. This includes reconsidering whether the basal function of the T6SS is solely to serve as an antagonistic pathway, or whether there might be additional roles this system might play in interbacterial interactions. It is these possibilities, outlined below, that will be of great importance as the field of T6S moves forward.

FUTURE DIRECTIONS

The case for interbacterial antagonism mediated by the T6SS

Before considering alternate hypothesizes for the function of the T6SS, it is important to note the sum total of all evidence supporting the hypothesis that this system predominantly functions in interbacterial antagonism. This role for the T6S has received significant attention, and has been the basal hypothesis of this dissertation. Indeed reports describing systems in *Burkholderia thailandensis, P. aeruginosa*, *V. cholerae*, *V. parahaemolyticus, Serratia marcescens*, *Citrobacter rodentium*, *P. syringae*, *F. johnsoniae*, *B. fragilis*, *A. tumefaciens*, and *Acinetobacter baumanii* demonstrated that they provide increased fitness when these organisms are grown in competition with other bacteria in the laboratory (14, 58, 60, 107, 228, 232-236). It is important to note, however, that bacteria live in dynamic communities often consisting of many species in close-association with each other and with additional biotic and abiotic elements. As it is within these complex surroundings that T6S evolved, it is difficult based solely on laboratory competition experiments to define with confidence the adaptive significance of the pathway. Nevertheless, in combination with growth competition studies, the results of biochemical,

genomic, and regulatory analyses have – as outlined below – produced evidence to support the argument that many T6SSs do play a direct role in interbacterial competition. As mentioned, T6S effectors act on bacterial structures that are both essential and highly conserved. Therefore, these proteins seem to have evolved to exert deleterious effects on a broad array of competitors. The mechanisms by which these proteins attack and disrupt essential pathways further supports their role in antagonism. The structures of amidase-type T6S effectors have revealed open active sites, devoid of inhibitory regulatory domains present in similar housekeeping enzymes (45, 192-194, 237, 238). The measured activities of effectors support the predictions that these proteins lack stringent regulation, as many studied thus far display activity *in vitro* in the absence of co-activators (45, 105, 149, 239). Mirroring their *in vitro* activity, T6S-dependent intoxication of cells by amidase and phospholipase effector proteins results in rapid lysis due to cell wall and membrane damage, respectively (45, 151, 183). Overall, biochemical analyses of T6S effectors have provided evidence consistent with these proteins participating in antibacterial antagonism.

Genomic and evolutionary evidence further supports the involvement of T6S in interbacterial antagonism. First, immunity proteins are maintained in organisms lacking cognate effector proteins (149). While these orphan immunity proteins have no demonstrated functionality, their persistence suggests a selective pressure deriving from attack by other organisms. Second, active effector proteins are, without exception, found in the presence of immunity proteins. This underscores the fitness cost associated with effector intoxication in the absence of immunity. Lastly, the role of T6S in interbacterial antagonism is supported by the fact that bacteria-targeting T6S has not been demonstrated in organisms living in privileged sites protected from competition from other bacteria. Moreover, in one example, *Burkholderia mallei*, interbacterial

T6SS was lost concomitantly with its evolution from a free-living saprophyte to an obligate pathogen (58).

Observations regarding bacterial antagonism have led Cornforth and Foster to postulate that bacterially encoded antibacterial toxins could be preferentially produced in response to competition-specific stresses (240). Interestingly, it has been demonstrated both in intra- and inter-species interactions that the activation of the T6SS in one cell can stimulate the system in neighboring cells (151, 241). This recognition is sufficiently integral to the activity of the *P. aeruginosa* H1-T6SS that inactivation of the T6SS of a competitor organism grants resistance to intoxication. Therefore, the intercellular positive regulatory behavior of some T6SSs appears to conform to the predictions of an antagonistic pathway, although it should be noted that not all T6SSs appear to utilize this form of regulation (241).

The conditions that regulate the production of a pathway can provide valuable insights into its physiological function. Some T6SSs, such as the H1-T6SS of *P. aeruginosa* and the *V. cholerae* O1 T6SS, are repressed by quorum signaling (147, 242). This indicates that these systems are active when cells have not established a dense community, and therefore, if operating antagonistically, their function might be to aid in the colonization of surfaces via the displacement of competing bacteria. Conversely, other T6SSs, such as the H2-T6SS of *P. aeruginosa*, are induced under conditions of high cell density (147). These T6SSs could be involved in the defense of communities from invading organisms, or, alternatively, in the invasion of communities of organisms that produce compatible quorum signals. Additionally, some T6SSs are regulated by environmental cues, such as temperature, pH, or iron availability

(164, 243-246). With respect to interbacterial antagonism, these signals may indicate the passage of organisms to an environment in which competitor bacteria are present.

Potential roles for T6S beyond antagonism

While significant evidence exists for an antagonistic role for many T6SSs, there remains the possibility that some of these systems might serve purposes beyond competition. Similar to the original discovery that the T6SS could act between bacteria, these hypotheses could represent significant shifts in how the T6SS is studied. One of the most compelling pieces of evidence that indicates additional roles for the T6SS is that it is often activated under conditions of high cell density (109, 147, 242, 247). Since clonal expansion can lead to spatial segregation of cells as clusters of closely related groups, these T6S-activated cells are likely to be primarily contacting immediate progeny (248). Under such conditions, T6S could be utilized for defending the assemblage; however, the significant amount of kin-targeting that must also occur argues that additional hypotheses should be entertained. It is worth noting the diffusible antibiotics are also generally produced under high quorum (240). Nevertheless, unlike the T6SS these products can act on competitors located at a distance and thus are not restricted to acting on their likely isogenic neighbors.

An instructive frame of reference for generating hypotheses concerning isogenic intoxication is toxin-antitoxin (TA) systems (59, 249) and indeed, analogies have been made between TA systems and T6SS effectors (106). While TA systems are not generally thought to act *in trans* nor depend on additional machinery to exert their effects, when considering only isogenic

intoxication there exists the possibility of considerable functional overlap between TA systems and antibacterial T6SS E–I pairs. In this respect it is important to note that TA systems, once considered mainly in the context of plasmid addiction and selfish genetic elements, have recently received much attention for their roles in metabolic regulation, stress responses, biofilm formation, and phage defense (59, 250-255). It is in light of these, and other findings, that we below examine alternative roles for the T6SS, the testing of which will likely deepen our understanding of the T6SS.

T6S function in signaling

Many bacteria appear to only transiently exist as independent cells, and instead form complex multicellular communities punctuated by dispersal events (256). Communication is essential to the establishment and maintenance of these communities; however, previous studies have largely focused on this communication via soluble quorum signaling molecules, and not on contact-dependent mechanisms (257, 258). The latter has the advantage in tight quarters of also providing information concerning the number and the identities of immediately adjacent cells. Notably, in "true" multicellular organisms, direct cell-to-cell signaling is found alongside the production of soluble signaling molecules (259), underscoring the importance of both contact-dependent and contact-independent mechanisms.

It is possible that T6SS effector proteins might play a role in signaling between isogenic cells. This could be due to either residual activity of the effector or the E–I complex itself might act as a signaling molecule. The use of toxic effector proteins as signaling molecules is appealing in this respect, as intended recipient organisms successfully interpret the signal, whereas non-

intended recipients experience antagonistic effects. Also, the activities of cell wall remodeling effector proteins are consistent with known mechanisms of interbacterial signaling. For example, in *Mycobacterium tuberculosis* and *Micrococcus luteus* cell wall remodeling enzymes have been observed to trigger changes leading to recovery from the viable but non-culturable (VBNC) growth state (260-263). While Gram-positive organisms can be resuscitated by neighboring cells producing these enzymes, the Gram-negative outer membrane inhibits this mechanism. However, T6SS-dependent delivery of resuscitation enzymes to the periplasm could overcome this and allow active cells to "wake" their neighbors.

Enforcement of social behaviors

Cooperative activities are susceptible to the evolution of non-cooperating organisms, which take advantage of public goods without contributing to the metabolic cost of their production (264, 265). One mechanism that has been proposed to overcome this tendency is enforcement by imposing a cost to non-cooperation. Intoxication by T6SS effectors could be one means by which enforcement is accomplished. The known co-regulation of effectors and immunity proteins with social activities would prevent a target organism from failing to cooperate as it would also fail to produce immunity determinants. In *P. aeruginosa* and *P. protegens* it has been observed that E–I loci are within the Gac-Rsm regulon, which also includes a number of social behaviors such as the production of exopolysaccharides (14, 42, 119, 121, 231).

Community structure

Intoxication by effector proteins, while deleterious, might also contribute to the three-dimensional architecture of bacterial communities. Indeed, a gross defect in biofilm formation

has been observed for T6SS mutants in several organisms (10-12). In isogenic aggregates, cells undergo differentiation. Some of this differentiation, such as senescence or death with subsequent lysis, mirrors the results of attack by antagonistic molecules (266). The Tse2 effector of *P. aeruginosa* is bacteriostatic to other *P. aeruginosa* cells and could induce senescence (106). Interestingly, a role for Tse2 in interspecies competition has not been found, and, as it is present in all sequenced *P. aeruginosa* strains, Tse2 is unlikely to be a mediator of intrastrain competition (14). Another cell fate, lysis, which releases DNA, an important structural component of extracellular matrices, could likewise be induced by cell wall-degrading or phospholipase effector proteins (45, 105, 183, 267). Since all cells in an isogenic population would be expected to possess both immunity and effector genes, a mechanism for differential susceptibilities to exchanged effectors must be invoked. Heterogeneity in gene expression is frequently observed in cellular aggregates due to microenvironmental differences found within complex communities (268). In this manner positional cues might induce differential immunity expression, allowing T6SS-dependent intoxication.

Phage defense

It is known that TA systems can be used to induce suicide in phage-infected bacteria, which protects nearby cells from infection (254). The importance of this defense mechanism is underscored by the evolution of phage proteins that inhibit the pathway (269). T6S effector proteins could likewise be used to remove adjacent infected organisms. Analogous to TA-mediated phage defense, an infected organism whose cellular machinery has become hijacked to produce phage particles might then become susceptible to effector intoxication as its pre-existing immunity proteins become depleted. The use of T6S for this purpose may be particularly

advantageous, as T6S-assisted suicide does not depend on machinery within the infected cell. Thus, this strategy is possibly less susceptible to inhibition by the phage.

Research on the T6SS began with the assumption that it, like the T3SS and T4SS, would target potent effector proteins to eukaryotic cells. The finding that this system could mediate interbacterial interactions has granted significant insight into its function in the vast majority of bacteria. Moreover, these findings coincided with a renaissance in microbial ecology that has brought with it a greater appreciation for the dynamics of bacterial populations and the impact that microbial communities have on both human and environmental health. This work provides insight into the mechanisms by which bacteria influence each other via the T6SS, providing a solid basis for further ecological studies of the *in situ* roles that this system might fulfill.

REFERENCES

1. Russell, A. B., Peterson, S. B., and Mougous, J. D. (2014) Type VI secretion system effectors: poisons with a purpose. *Nat Rev Microbiol* **12**, 137-148
2. Coulthurst, S. J. (2013) The Type VI secretion system - a widespread and versatile cell targeting system. *Res Microbiol* **164**, 640-654
3. Benz, J., and Meinhart, A. (2014) Antibacterial effector/immunity systems: it's just the tip of the iceberg. *Curr Opin Microbiol* **17**, 1-10
4. Bladergroen, M. R., Badelt, K., and Spaink, H. P. (2003) Infection-blocking genes of a symbiotic *Rhizobium leguminosarum* strain that are involved in temperature-dependent protein secretion. *Mol Plant Microbe Interact* **16**, 53-64
5. Rao, P. S., Yamada, Y., Tan, Y. P., and Leung, K. Y. (2004) Use of proteomics to identify novel virulence determinants that are required for *Edwardsiella tarda* pathogenesis. *Mol Microbiol* **53**, 573-586
6. Boyer, F., Fichant, G., Berthod, J., Vandenbrouck, Y., and Attree, I. (2009) Dissecting the bacterial type VI secretion system by a genome wide in silico analysis: what can be learned from available microbial genomic resources? *BMC Genomics* **10**, 104
7. Das, S., and Chaudhuri, K. (2003) Identification of a unique IAHP (IcmF associated homologous proteins) cluster in *Vibrio cholerae* and other proteobacteria through in silico analysis. *In Silico Biol* **3**, 287-300
8. Suarez, G., Sierra, J. C., Sha, J., Wang, S., Erova, T. E., Fadl, A. A., Foltz, S. M., Horneman, A. J., and Chopra, A. K. (2008) Molecular characterization of a functional type VI secretion system from a clinical isolate of *Aeromonas hydrophila*. *Microb Pathog* **44**, 344-361
9. Pukatzki, S., Ma, A. T., Revel, A. T., Sturtevant, D., and Mekalanos, J. J. (2007) Type VI secretion system translocates a phage tail spike-like protein into target cells where it cross-links actin. *Proc Natl Acad Sci U S A* **104**, 15508-15513
10. Enos-Berlage, J. L., Guvener, Z. T., Keenan, C. E., and McCarter, L. L. (2005) Genetic determinants of biofilm development of opaque and translucent *Vibrio parahaemolyticus*. *Mol Microbiol* **55**, 1160-1182
11. Aschtgen, M. S., Bernard, C. S., De Bentzmann, S., Lloubes, R., and Cascales, E. (2008) SciN is an outer membrane lipoprotein required for Type VI secretion in enteroaggregative *Escherichia coli*. *J Bacteriol* **190**, 7523-7531
12. Sha, J., Rosenzweig, J. A., Kozlova, E. V., Wang, S., Erova, T. E., Kirtley, M. L., van Lier, C. J., and Chopra, A. K. (2013) Evaluation of the roles played by Hcp and VgrG type 6 secretion system effectors in *Aeromonas hydrophila* SSU pathogenesis. *Microbiology* **159**, 1120-1135
13. Suarez, G., Sierra, J. C., Erova, T. E., Sha, J., Horneman, A. J., and Chopra, A. K. (2010) A type VI secretion system effector protein, VgrG1, from *Aeromonas hydrophila* that induces host cell toxicity by ADP ribosylation of actin. *J Bacteriol* **192**, 155-168
14. Hood, R. D., Singh, P., Hsu, F., Guvener, T., Carl, M. A., Trinidad, R. R., Silverman, J. M., Ohlson, B. B., Hicks, K. G., Plemel, R. L., Li, M., Schwarz, S., Wang, W. Y., Merz, A. J., Goodlett, D. R., and Mougous, J. D. (2010) A type VI secretion system of *Pseudomonas aeruginosa* targets a toxin to bacteria. *Cell Host Microbe* **7**, 25-37

15. Silhavy, T. J., Kahne, D., and Walker, S. (2010) The bacterial cell envelope. *Cold Spring Harb Perspect Biol* **2**, a000414
16. Zhang, Y. M., and Rock, C. O. (2008) Membrane lipid homeostasis in bacteria. *Nat Rev Microbiol* **6**, 222-233
17. Cronan, J. E. (2003) Bacterial membrane lipids: where do we stand? *Annu Rev Microbiol* **57**, 203-224
18. Vollmer, W., Blanot, D., and de Pedro, M. A. (2008) Peptidoglycan structure and architecture. *FEMS Microbiol Rev* **32**, 149-167
19. Vollmer, W., Joris, B., Charlier, P., and Foster, S. (2008) Bacterial peptidoglycan (murein) hydrolases. *FEMS Microbiol Rev* **32**, 259-286
20. Cascales, E., Bernadac, A., Gavioli, M., Lazzaroni, J. C., and Lloubes, R. (2002) Pal lipoprotein of *Escherichia coli* plays a major role in outer membrane integrity. *J Bacteriol* **184**, 754-759
21. Matsuura, M. (2013) Structural Modifications of Bacterial Lipopolysaccharide that Facilitate Gram-Negative Bacteria Evasion of Host Innate Immunity. *Front Immunol* **4**, 109
22. Noinaj, N., Guillier, M., Barnard, T. J., and Buchanan, S. K. (2010) TonB-dependent transporters: regulation, structure, and function. *Annu Rev Microbiol* **64**, 43-60
23. Kanonenberg, K., Schwarz, C. K., and Schmitt, L. (2013) Type I secretion systems - a story of appendices. *Res Microbiol* **164**, 596-604
24. Korotkov, K. V., Sandkvist, M., and Hol, W. G. (2012) The type II secretion system: biogenesis, molecular architecture and mechanism. *Nat Rev Microbiol* **10**, 336-351
25. Galan, J. E., Lara-Tejero, M., Marlovits, T. C., and Wagner, S. (2014) Bacterial Type III Secretion Systems: Specialized Nanomachines for Protein Delivery into Target Cells. *Annu Rev Microbiol* **68**, 415–38
26. Christie, P. J., Whitaker, N., and Gonzalez-Rivera, C. (2014) Mechanism and structure of the bacterial type IV secretion systems. *Biochim Biophys Acta* **1843**, 1578-1591
27. Grijpstra, J., Arenas, J., Rutten, L., and Tommassen, J. (2013) Autotransporter secretion: varying on a theme. *Res Microbiol* **164**, 562-582
28. Silverman, J. M., Brunet, Y. R., Cascales, E., and Mougous, J. D. (2012) Structure and Regulation of the Type VI Secretion System. *Annu Rev Microbiol* **66**, 453-473
29. Desvaux, M., Hebraud, M., Talon, R., and Henderson, I. R. (2009) Secretion and subcellular localizations of bacterial proteins: a semantic awareness issue. *Trends Microbiol* **17**, 139-145
30. McBride, M. J., and Zhu, Y. (2013) Gliding motility and Por secretion system genes are widespread among members of the phylum Bacteroidetes. *J Bacteriol* **195**, 270-278
31. Galan, J. E. (2009) Common themes in the design and function of bacterial effectors. *Cell Host Microbe* **5**, 571-579
32. Aschtgen, M. S., Thomas, M. S., and Cascales, E. (2010) Anchoring the type VI secretion system to the peptidoglycan: TssL, TagL, TagP... what else? *Virulence* **1**, 535-540
33. Ma, L. S., Lin, J. S., and Lai, E. M. (2009) An IcmF family protein, ImpLM, is an integral inner membrane protein interacting with ImpKL, and its walker a motif is required for type VI secretion system-mediated Hcp secretion in *Agrobacterium tumefaciens*. *J Bacteriol* **191**, 4316-4329
34. Ma, L. S., Narberhaus, F., and Lai, E. M. (2012) IcmF Family Protein TssM Exhibits ATPase Activity and Energizes Type VI Secretion. *J Biol Chem* **287**, 15610-15621

35. Kanamaru, S. (2009) Structural similarity of tailed phages and pathogenic bacterial secretion systems. *Proc Natl Acad Sci U S A* **106**, 4067-4068
36. Leiman, P. G., Basler, M., Ramagopal, U. A., Bonanno, J. B., Sauder, J. M., Pukatzki, S., Burley, S. K., Almo, S. C., and Mekalanos, J. J. (2009) Type VI secretion apparatus and phage tail-associated protein complexes share a common evolutionary origin. *Proc Natl Acad Sci U S A* **106**, 4154-4159
37. Rakhuba, D. V., Kolomiets, E. I., Dey, E. S., and Novik, G. I. (2010) Bacteriophage receptors, mechanisms of phage adsorption and penetration into host cell. *Pol J Microbiol* **59**, 145-155
38. Basler, M., Pilhofer, M., Henderson, G. P., Jensen, G. J., and Mekalanos, J. J. (2012) Type VI secretion requires a dynamic contractile phage tail-like structure. *Nature* **483**, 182-186
39. Bonemann, G., Pietrosiuk, A., Diemand, A., Zentgraf, H., and Mogk, A. (2009) Remodelling of VipA/VipB tubules by ClpV-mediated threading is crucial for type VI protein secretion. *Embo J* **28**, 315-325
40. Schlieker, C., Zentgraf, H., Dersch, P., and Mogk, A. (2005) ClpV, a unique Hsp100/Clp member of pathogenic proteobacteria. *Biol Chem* **386**, 1115-1127
41. Kube, S., Kapitein, N., Zimniak, T., Herzog, F., Mogk, A., and Wendler, P. (2014) Structure of the VipA/B Type VI Secretion Complex Suggests a Contraction-State-Specific Recycling Mechanism. *Cell Rep* **8**, 20-30
42. Mougous, J. D., Cuff, M. E., Raunser, S., Shen, A., Zhou, M., Gifford, C. A., Goodman, A. L., Joachimiak, G., Ordonez, C. L., Lory, S., Walz, T., Joachimiak, A., and Mekalanos, J. J. (2006) A virulence locus of *Pseudomonas aeruginosa* encodes a protein secretion apparatus. *Science* **312**, 1526-1530
43. Brunet, Y. R., Henin, J., Celia, H., and Cascales, E. (2014) Type VI secretion and bacteriophage tail tubes share a common assembly pathway. *EMBO Rep* **15**, 315-321
44. Silverman, J. M., Agnello, D.M., Zheng, H., Andrews, B.T., Li, M., Catalano, C.E., Gonen, T., and Mougous, J.D. (2013) Haemolysin Co-regulated Protein is an Exported Receptor and Chaperone of Type VI Secretion Substrates. *Mol Cell* **51**, 584-593
45. Chou, S., Bui, N. K., Russell, A. B., Lexa, K. W., Gardiner, T. E., Leroux, M., Vollmer, W., and Mougous, J. D. (2012) Structure of a Peptidoglycan Amidase Effector Targeted to Gram-Negative Bacteria by the Type VI Secretion System. *Cell Rep* **1**, 656-664
46. Blondel, C. J., Jimenez, J. C., Contreras, I., and Santiviago, C. A. (2009) Comparative genomic analysis uncovers 3 novel loci encoding type six secretion systems differentially distributed in *Salmonella* serotypes. *BMC Genomics* **10**, 354
47. Dong, T. G., Ho, B. T., Yoder-Himes, D. R., and Mekalanos, J. J. (2013) Identification of T6SS-dependent effector and immunity proteins by Tn-seq in Vibrio cholerae. *Proc Natl Acad Sci U S A* **110**, 2623-2628
48. Shneider, M. M., Buth, S. A., Ho, B. T., Basler, M., Mekalanos, J. J., and Leiman, P. G. (2013) PAAR-repeat proteins sharpen and diversify the type VI secretion system spike. *Nature* **500**, 350-353
49. Miyata, S. T., Unterweger, D., Rudko, S. P., and Pukatzki, S. (2013) Dual expression profile of type VI secretion system immunity genes protects pandemic *Vibrio cholerae*. *PLoS Pathog* **9**, e1003752

50. Barret, M., Egan, F., Fargier, E., Morrissey, J. P., and O'Gara, F. (2011) Genomic analysis of the type VI secretion systems in *Pseudomonas* spp.: novel clusters and putative effectors uncovered. *Microbiology* **157**, 1726-1739
51. Whitney, J. C., Beck, C. M., Goo, Y. A., Russell, A. B., Harding, B. N., De Leon, J. A., Cunningham, D. A., Tran, B. Q., Low, D. A., Goodlett, D. R., Hayes, C. S., and Mougous, J. D. (2014) Genetically distinct pathways guide effector export through the type VI secretion system. *Mol Microbiol* **92**, 529-542
52. Zoued, A., Durand, E., Bebeacua, C., Brunet, Y. R., Douzi, B., Cambillau, C., Cascales, E., and Journet, L. (2013) TssK is a trimeric cytoplasmic protein interacting with components of both phage-like and membrane anchoring complexes of the type VI secretion system. *J Biol Chem* **288**, 27031-27041
53. English, G., Byron, O., Cianfanelli, F. R., Prescott, A. R., and Coulthurst, S. J. (2014) Biochemical analysis of TssK, a core component of the bacterial Type VI secretion system, reveals distinct oligomeric states of TssK and identifies a TssK-TssFG subcomplex. *Biochem J* **461**, 291-304
54. Pukatzki, S., Ma, A. T., Sturtevant, D., Krastins, B., Sarracino, D., Nelson, W. C., Heidelberg, J. F., and Mekalanos, J. J. (2006) Identification of a conserved bacterial protein secretion system in *Vibrio cholerae* using the *Dictyostelium* host model system. *Proc Natl Acad Sci U S A* **103**, 1528-1533
55. Ma, A. T., McAuley, S., Pukatzki, S., and Mekalanos, J. J. (2009) Translocation of a *Vibrio cholerae* type VI secretion effector requires bacterial endocytosis by host cells. *Cell Host Microbe* **5**, 234-243
56. Glaser, P., Sakamoto, H., Bellalou, J., Ullmann, A., and Danchin, A. (1988) Secretion of cyclolysin, the calmodulin-sensitive adenylate cyclase-haemolysin bifunctional protein of Bordetella pertussis. *Embo J* **7**, 3997-4004
57. Schwarz, S., Hood, R. D., and Mougous, J. D. (2010) What is type VI secretion doing in all those bugs? *Trends Microbiol* **18**, 531-537
58. Schwarz, S., West, T. E., Boyer, F., Chiang, W. C., Carl, M. A., Hood, R. D., Rohmer, L., Tolker-Nielsen, T., Skerrett, S. J., and Mougous, J. D. (2010) *Burkholderia* type VI secretion systems have distinct roles in eukaryotic and bacterial cell interactions. *PLoS Pathog* **6**
59. Yamaguchi, Y., Park, J. H., and Inouye, M. (2011) Toxin-antitoxin systems in bacteria and archaea. *Annual review of genetics* **45**, 61-79
60. MacIntyre, D. L., Miyata, S. T., Kitaoka, M., and Pukatzki, S. (2010) The *Vibrio cholerae* type VI secretion system displays antimicrobial properties. *Proc Natl Acad Sci U S A* **107**, 19520-19524
61. Riley, M. A., and Wertz, J. E. (2002) Bacteriocins: evolution, ecology, and application. *Annu Rev Microbiol* **56**, 117-137
62. Hayes, C. S., Aoki, S. K., and Low, D. A. (2010) Bacterial contact-dependent delivery systems. *Annu Rev Genet* **44**, 71-90
63. Hibbing, M. E., Fuqua, C., Parsek, M. R., and Peterson, S. B. (2010) Bacterial competition: surviving and thriving in the microbial jungle. *Nat Rev Microbiol* **8**, 15-25
64. Grundling, A., and Schneewind, O. (2006) Cross-linked peptidoglycan mediates lysostaphin binding to the cell wall envelope of *Staphylococcus aureus*. *J Bacteriol* **188**, 2463-2472

65. Vollmer, W., Pilsl, H., Hantke, K., Holtje, J. V., and Braun, V. (1997) Pesticin displays muramidase activity. *J Bacteriol* **179**, 1580-1583
66. Brotz, H., Bierbaum, G., Markus, A., Molitor, E., and Sahl, H. G. (1995) Mode of action of the lantibiotic mersacidin: inhibition of peptidoglycan biosynthesis via a novel mechanism? *Antimicrob Agents Chemother* **39**, 714-719
67. Cascales, E. (2008) The type VI secretion toolkit. *EMBO Rep* **9**, 735-741
68. Ballister, E. R., Lai, A. H., Zuckermann, R. N., Cheng, Y., and Mougous, J. D. (2008) In Vitro Self-Assembly of Tailorable Nanotubes from a Simple Protein Building Block. *Proc. Natl. Acad. Sci. U.S.A.* **105**, 3733-3738
69. Christie, P. J., Atmakuri, K., Krishnamoorthy, V., Jakubowski, S., and Cascales, E. (2005) Biogenesis, architecture, and function of bacterial type iv secretion systems. *Annu Rev Microbiol* **59**, 451-485
70. Kelley, L. A., and Sternberg, M. J. (2009) Protein structure prediction on the Web: a case study using the Phyre server. *Nat Protoc* **4**, 363-371
71. Anantharaman, V., and Aravind, L. (2003) Evolutionary history, structural features and biochemical diversity of the NlpC/P60 superfamily of enzymes. *Genome Biol* **4**, R11
72. Scheurwater, E., Reid, C. W., and Clarke, A. J. (2008) Lytic transglycosylases: bacterial space-making autolysins. *Int J Biochem Cell Biol* **40**, 586-591
73. Gerdes, K., Christensen, S. K., and Lobner-Olesen, A. (2005) Prokaryotic toxin-antitoxin stress response loci. *Nat Rev Microbiol* **3**, 371-382
74. Hall-Stoodley, L., Costerton, J. W., and Stoodley, P. (2004) Bacterial biofilms: from the natural environment to infectious diseases. *Nat Rev Microbiol* **2**, 95-108
75. Mortensen, J. E., Fisher, M. C., and LiPuma, J. J. (1995) Recovery of *Pseudomonas cepacia* and other *Pseudomonas* species from the environment. *Infect Control Hosp Epidemiol* **16**, 30-32
76. Nelson, K. E., Weinel, C., Paulsen, I. T., Dodson, R. J., Hilbert, H., Martins dos Santos, V. A., Fouts, D. E., Gill, S. R., Pop, M., Holmes, M., Brinkac, L., Beanan, M., DeBoy, R. T., Daugherty, S., Kolonay, J., Madupu, R., Nelson, W., White, O., Peterson, J., Khouri, H., Hance, I., Chris Lee, P., Holtzapple, E., Scanlan, D., Tran, K., Moazzez, A., Utterback, T., Rizzo, M., Lee, K., Kosack, D., Moestl, D., Wedler, H., Lauber, J., Stjepandic, D., Hoheisel, J., Straetz, M., Heim, S., Kiewitz, C., Eisen, J. A., Timmis, K. N., Dusterhoft, A., Tummler, B., and Fraser, C. M. (2002) Complete genome sequence and comparative analysis of the metabolically versatile *Pseudomonas putida* KT2440. *Environ Microbiol* **4**, 799-808
77. Nelson, K. E., Weinstock, G. M., Highlander, S. K., Worley, K. C., Creasy, H. H., Wortman, J. R., Rusch, D. B., Mitreva, M., Sodergren, E., Chinwalla, A. T., Feldgarden, M., Gevers, D., Haas, B. J., Madupu, R., Ward, D. V., Birren, B. W., Gibbs, R. A., Methe, B., Petrosino, J. F., Strausberg, R. L., Sutton, G. G., White, O. R., Wilson, R. K., Durkin, S., Giglio, M. G., Gujja, S., Howarth, C., Kodira, C. D., Kyrpides, N., Mehta, T., Muzny, D. M., Pearson, M., Pepin, K., Pati, A., Qin, X., Yandava, C., Zeng, Q., Zhang, L., Berlin, A. M., Chen, L., Hepburn, T. A., Johnson, J., McCorrison, J., Miller, J., Minx, P., Nusbaum, C., Russ, C., Sykes, S. M., Tomlinson, C. M., Young, S., Warren, W. C., Badger, J., Crabtree, J., Markowitz, V. M., Orvis, J., Cree, A., Ferriera, S., Fulton, L. L., Fulton, R. S., Gillis, M., Hemphill, L. D., Joshi, V., Kovar, C., Torralba, M., Wetterstrand, K. A., Abouellleil, A., Wollam, A. M., Buhay, C. J., Ding, Y., Dugan, S., FitzGerald, M. G., Holder, M., Hostetler, J., Clifton, S. W., Allen-Vercoe, E., Earl, A.

M., Farmer, C. N., Liolios, K., Surette, M. G., Xu, Q., Pohl, C., Wilczek-Boney, K., and Zhu, D. (2010) A catalog of reference genomes from the human microbiome. *Science* **328**, 994-999

78. Qin, J., Li, R., Raes, J., Arumugam, M., Burgdorf, K. S., Manichanh, C., Nielsen, T., Pons, N., Levenez, F., Yamada, T., Mende, D. R., Li, J., Xu, J., Li, S., Li, D., Cao, J., Wang, B., Liang, H., Zheng, H., Xie, Y., Tap, J., Lepage, P., Bertalan, M., Batto, J. M., Hansen, T., Le Paslier, D., Linneberg, A., Nielsen, H. B., Pelletier, E., Renault, P., Sicheritz-Ponten, T., Turner, K., Zhu, H., Yu, C., Jian, M., Zhou, Y., Li, Y., Zhang, X., Qin, N., Yang, H., Wang, J., Brunak, S., Dore, J., Guarner, F., Kristiansen, K., Pedersen, O., Parkhill, J., Weissenbach, J., Bork, P., and Ehrlich, S. D. (2010) A human gut microbial gene catalogue established by metagenomic sequencing. *Nature* **464**, 59-65
79. Brook, I. (1999) Bacterial interference. *Critical reviews in microbiology* **25**, 155-172
80. Iwase, T., Uehara, Y., Shinji, H., Tajima, A., Seo, H., Takada, K., Agata, T., and Mizunoe, Y. (2010) *Staphylococcus epidermidis* Esp inhibits *Staphylococcus aureus* biofilm formation and nasal colonization. *Nature* **465**, 346-349
81. Reid, G., Howard, J., and Gan, B. S. (2001) Can bacterial interference prevent infection? *Trends Microbiol* **9**, 424-428
82. Gjodsbol, K., Christensen, J. J., Karlsmark, T., Jorgensen, B., Klein, B. M., and Krogfelt, K. A. (2006) Multiple bacterial species reside in chronic wounds: a longitudinal study. *Int Wound J* **3**, 225-231
83. Stover, C. K., Pham, X. Q., Erwin, A. L., Mizoguchi, S. D., Warrener, P., Hickey, M. J., Brinkman, F. S., Hufnagle, W. O., Kowalik, D. J., Lagrou, M., Garber, R. L., Goltry, L., Tolentino, E., Westbrock-Wadman, S., Yuan, Y., Brody, L. L., Coulter, S. N., Folger, K. R., Kas, A., Larbig, K., Lim, R., Smith, K., Spencer, D., Wong, G. K., Wu, Z., Paulsen, I. T., Reizer, J., Saier, M. H., Hancock, R. E., Lory, S., and Olson, M. V. (2000) Complete genome sequence of *Pseudomonas aeruginosa* PA01, an opportunistic pathogen. *Nature* **406**, 959-964
84. Cardona, S. T., and Valvano, M. A. (2005) An expression vector containing a rhamnose-inducible promoter provides tightly regulated gene expression in *Burkholderia cenocepacia*. *Plasmid* **54**, 219-228
85. Hsu, F., Schwarz, S., and Mougous, J. D. (2009) TagR promotes PpkA-catalysed type VI secretion activation in *Pseudomonas aeruginosa*. *Mol Microbiol* **72**, 1111-1125
86. Rietsch, A., Vallet-Gely, I., Dove, S. L., and Mekalanos, J. J. (2005) ExsE, a secreted regulator of type III secretion genes in *Pseudomonas aeruginosa*. *Proc Natl Acad Sci U S A* **102**, 8006-8011
87. Horton, R. M., Ho, S. N., Pullen, J. K., Hunt, H. D., Cai, Z., and Pease, L. R. (1993) Gene splicing by overlap extension. *Methods Enzymol* **217**, 270-279
88. Imperi, F., Ciccosanti, F., Perdomo, A. B., Tiburzi, F., Mancone, C., Alonzi, T., Ascenzi, P., Piacentini, M., Visca, P., and Fimia, G. M. (2009) Analysis of the periplasmic proteome of *Pseudomonas aeruginosa*, a metabolically versatile opportunistic pathogen. *Proteomics* **9**, 1901-1915
89. Wood, P. M. (1978) Periplasmic location of the terminal reductase in nitrite respiration. *FEBS Lett* **92**, 214-218
90. Liu, J., and Walsh, C. T. (1990) Peptidyl-prolyl cis-trans-isomerase from *Escherichia coli*: a periplasmic homolog of cyclophilin that is not inhibited by cyclosporin A. *Proc Natl Acad Sci U S A* **87**, 4028-4032

91. Mougous, J. D., Petzold, C. J., Senaratne, R. H., Lee, D. H., Akey, D. L., Lin, F. L., Munchel, S. E., Pratt, M. R., Riley, L. W., Leary, J. A., Berger, J. M., and Bertozzi, C. R. (2004) Identification, function and structure of the mycobacterial sulfotransferase that initiates sulfolipid-1 biosynthesis. *Nat Struct Mol Biol* **11**, 721-729
92. Armougom, F., Moretti, S., Poirot, O., Audic, S., Dumas, P., Schaeli, B., Keduas, V., and Notredame, C. (2006) Expresso: automatic incorporation of structural information in multiple sequence alignments using 3D-Coffee. *Nucleic Acids Res* **34**, W604-608
93. Finn, R. D., Mistry, J., Tate, J., Coggill, P., Heger, A., Pollington, J. E., Gavin, O. L., Gunasekaran, P., Ceric, G., Forslund, K., Holm, L., Sonnhammer, E. L., Eddy, S. R., and Bateman, A. (2010) The Pfam protein families database. *Nucleic Acids Res* **38**, D211-222
94. Glauner, B. (1988) Separation and quantification of muropeptides with high-performance liquid chromatography. *Anal Biochem* **172**, 451-464
95. Bui, N. K., Gray, J., Schwarz, H., Schumann, P., Blanot, D., and Vollmer, W. (2009) The peptidoglycan sacculus of *Myxococcus xanthu*s has unusual structural features and is degraded during glycerol-induced myxospore development. *J Bacteriol* **191**, 494-505
96. Watt, S. R., and Clarke, A. J. (1994) Role of autolysins in the EDTA-induced lysis of Pseudomonas aeruginosa. *FEMS Microbiol Lett* **124**, 113-119
97. Lei, S. P., Lin, H. C., Wang, S. S., Callaway, J., and Wilcox, G. (1987) Characterization of the *Erwinia carotovora pelB* gene and its product pectate lyase. *J Bacteriol* **169**, 4379-4383
98. Goodman, A. L., Kulasekara, B., Rietsch, A., Boyd, D., Smith, R. S., and Lory, S. (2004) A signaling network reciprocally regulates genes associated with acute infection and chronic persistence in *Pseudomonas aeruginosa*. *Dev Cell* **7**, 745-754
99. Konovalova, A., and Sogaard-Andersen, L. (2011) Close encounters: contact-dependent interactions in bacteria. *Mol Microbiol* **81**, 297-301
100. Rendueles, O., and Ghigo, J. M. (2012) Multi-species biofilms: How to avoid unfriendly neighbors. *FEMS Microbiol Rev* **36**, 972-989
101. El Ghachi, M., Bouhss, A., Barreteau, H., Touze, T., Auger, G., Blanot, D., and Mengin-Lecreulx, D. (2006) Colicin M exerts its bacteriolytic effect via enzymatic degradation of undecaprenyl phosphate-linked peptidoglycan precursors. *J Biol Chem* **281**, 22761-22772
102. Jani, A. J., and Cotter, P. A. (2010) Type VI secretion: not just for pathogenesis anymore. *Cell Host Microbe* **8**, 2-6
103. Records, A. R. (2011) The type VI secretion system: a multipurpose delivery system with a phage-like machinery. *Mol Plant Microbe Interact* **24**, 751-757
104. Veesler, D., and Cambillau, C. (2011) A common evolutionary origin for tailed-bacteriophage functional modules and bacterial machineries. *Microbiol Mol Biol Rev* **75**, 423-433
105. Russell, A. B., Hood, R. D., Bui, N. K., LeRoux, M., Vollmer, W., and Mougous, J. D. (2011) Type VI secretion delivers bacteriolytic effectors to target cells. *Nature* **475**, 343-347
106. Li, M., Le Trong, I., Carl, M. A., Larson, E. T., Chou, S., De Leon, J. A., Dove, S. L., Stenkamp, R. E., and Mougous, J. D. (2012) Structural basis for type VI secretion effector recognition by a cognate immunity protein. *PLoS Pathog* **8**, e1002613
107. Murdoch, S. L., Trunk, K., English, G., Fritsch, M. J., Pourkarimi, E., and Coulthurst, S. J. (2011) The opportunistic pathogen *Serratia marcescens* utilises Type VI Secretion to target bacterial competitors. *J Bacteriol* **193**, 6057-6069

108. Silverman, J. M., Austin, L. S., Hsu, F., Hicks, K. G., Hood, R. D., and Mougous, J. D. (2011) Separate inputs modulate phosphorylation-dependent and -independent type VI secretion activation. *Mol Microbiol* **82**, 1277-1290
109. Bernard, C. S., Brunet, Y. R., Gueguen, E., and Cascales, E. (2010) Nooks and Crannies in type VI secretion regulation. *J Bacteriol* **192**, 3850-3860
110. Pilatz, S., Breitbach, K., Hein, N., Fehlhaber, B., Schulze, J., Brenneke, B., Eberl, L., and Steinmetz, I. (2006) Identification of *Burkholderia pseudomallei* genes required for the intracellular life cycle and in vivo virulence. *Infect Immun* **74**, 3576-3586
111. Schell, M. A., Ulrich, R. L., Ribot, W. J., Brueggemann, E. E., Hines, H. B., Chen, D., Lipscomb, L., Kim, H. S., Mrazek, J., Nierman, W. C., and Deshazer, D. (2007) Type VI secretion is a major virulence determinant in *Burkholderia mallei*. *Mol Microbiol* **64**, 1466-1485
112. Cascales, E., Buchanan, S. K., Duche, D., Kleanthous, C., Lloubes, R., Postle, K., Riley, M., Slatin, S., and Cavard, D. (2007) Colicin biology. *Microbiol Mol Biol Rev* **71**, 158-229
113. Parret, A. H., Schoofs, G., Proost, P., and De Mot, R. (2003) Plant lectin-like bacteriocin from a rhizosphere-colonizing *Pseudomonas* isolate. *J Bacteriol* **185**, 897-908
114. Firczuk, M., and Bochtler, M. (2007) Folds and activities of peptidoglycan amidases. *FEMS Microbiol Rev* **31**, 676-691
115. Bateman, A., and Rawlings, N. D. (2003) The CHAP domain: a large family of amidases including GSP amidase and peptidoglycan hydrolases. *Trends Biochem Sci* **28**, 234-237
116. Rigden, D. J., Jedrzejas, M. J., and Galperin, M. Y. (2003) Amidase domains from bacterial and phage autolysins define a family of gamma-D,L-glutamate-specific amidohydrolases. *Trends Biochem Sci* **28**, 230-234
117. Collmer, A., Lindeberg, M., Petnicki-Ocwieja, T., Schneider, D. J., and Alfano, J. R. (2002) Genomic mining type III secretion system effectors in *Pseudomonas syringae* yields new picks for all TTSS prospectors. *Trends Microbiol* **10**, 462-469
118. Petnicki-Ocwieja, T., Schneider, D. J., Tam, V. C., Chancey, S. T., Shan, L., Jamir, Y., Schechter, L. M., Janes, M. D., Buell, C. R., Tang, X., Collmer, A., and Alfano, J. R. (2002) Genomewide identification of proteins secreted by the Hrp type III protein secretion system of *Pseudomonas syringae* pv. tomato DC3000. *Proc Natl Acad Sci U S A* **99**, 7652-7657
119. Lapouge, K., Schubert, M., Allain, F. H., and Haas, D. (2008) Gac/Rsm signal transduction pathway of gamma-proteobacteria: from RNA recognition to regulation of social behaviour. *Mol Microbiol* **67**, 241-253
120. Brencic, A., and Lory, S. (2009) Determination of the regulon and identification of novel mRNA targets of Pseudomonas aeruginosa RsmA. *Mol Microbiol* **72**, 612-632
121. Hassan, K. A., Johnson, A., Shaffer, B. T., Ren, Q., Kidarsa, T. A., Elbourne, L. D., Hartney, S., Duboy, R., Goebel, N. C., Zabriskie, T. M., Paulsen, I. T., and Loper, J. E. (2010) Inactivation of the GacA response regulator in *Pseudomonas fluorescens* Pf-5 has far-reaching transcriptomic consequences. *Environ Microbiol* **12**, 899-915
122. Workentine, M. L., Chang, L., Ceri, H., and Turner, R. J. (2009) The GacS-GacA two-component regulatory system of *Pseudomonas fluorescens*: a bacterial two-hybrid analysis. *FEMS Microbiol Lett* **292**, 50-56
123. Aoki, S. K., Diner, E. J., de Roodenbeke, C. T., Burgess, B. R., Poole, S. J., Braaten, B. A., Jones, A. M., Webb, J. S., Hayes, C. S., Cotter, P. A., and Low, D. A. (2010) A

widespread family of polymorphic contact-dependent toxin delivery systems in bacteria. *Nature* **468**, 439-442
124. Papadakos, G., Wojdyla, J. A., and Kleanthous, C. (2011) Nuclease colicins and their immunity proteins. *Q Rev Biophys*, 1-47
125. Zheng, J., and Leung, K. Y. (2007) Dissection of a type VI secretion system in Edwardsiella tarda. *Mol Microbiol* **66**, 1192-1206
126. Vollmer, W. (2008) Structural variation in the glycan strands of bacterial peptidoglycan. *FEMS Microbiol Rev* **32**, 287-306
127. Davis, K. M., and Weiser, J. N. (2011) Modifications to the peptidoglycan backbone help bacteria to establish infection. *Infect Immun* **79**, 562-570
128. Lam, H., Oh, D. C., Cava, F., Takacs, C. N., Clardy, J., de Pedro, M. A., and Waldor, M. K. (2009) D-amino acids govern stationary phase cell wall remodeling in bacteria. *Science* **325**, 1552-1555
129. Cava, F., de Pedro, M. A., Lam, H., Davis, B. M., and Waldor, M. K. (2011) Distinct pathways for modification of the bacterial cell wall by non-canonical D-amino acids. *Embo J* **30**, 3442-3453
130. Magnet, S., Dubost, L., Marie, A., Arthur, M., and Gutmann, L. (2008) Identification of the L,D-transpeptidases for peptidoglycan cross-linking in Escherichia coli. *J Bacteriol* **190**, 4782-4785
131. Roesch, L. F., Fulthorpe, R. R., Riva, A., Casella, G., Hadwin, A. K., Kent, A. D., Daroub, S. H., Camargo, F. A., Farmerie, W. G., and Triplett, E. W. (2007) Pyrosequencing enumerates and contrasts soil microbial diversity. *ISME J* **1**, 283-290
132. Walter, J., and Ley, R. (2011) The human gut microbiome: ecology and recent evolutionary changes. *Annu Rev Microbiol* **65**, 411-429
133. Cohan, F. M. (2002) Sexual isolation and speciation in bacteria. *Genetica* **116**, 359-370
134. Majewski, J. (2001) Sexual isolation in bacteria. *FEMS Microbiol Lett* **199**, 161-169
135. Strassmann, J. E., Gilbert, O. M., and Queller, D. C. (2011) Kin discrimination and cooperation in microbes. *Annu Rev Microbiol* **65**, 349-367
136. Kim, H. S., Schell, M. A., Yu, Y., Ulrich, R. L., Sarria, S. H., Nierman, W. C., and DeShazer, D. (2005) Bacterial genome adaptation to niches: divergence of the potential virulence genes in three *Burkholderia* species of different survival strategies. *BMC Genomics* **6**, 174
137. Chandler, J. R., Duerkop, B. A., Hinz, A., West, T. E., Herman, J. P., Churchill, M. E., Skerrett, S. J., and Greenberg, E. P. (2009) Mutational analysis of *Burkholderia thailandensis* quorum sensing and self-aggregation. *J Bacteriol* **191**, 5901-5909
138. Paulsen, I. T., Press, C. M., Ravel, J., Kobayashi, D. Y., Myers, G. S., Mavrodi, D. V., DeBoy, R. T., Seshadri, R., Ren, Q., Madupu, R., Dodson, R. J., Durkin, A. S., Brinkac, L. M., Daugherty, S. C., Sullivan, S. A., Rosovitz, M. J., Gwinn, M. L., Zhou, L., Schneider, D. J., Cartinhour, S. W., Nelson, W. C., Weidman, J., Watkins, K., Tran, K., Khouri, H., Pierson, E. A., Pierson, L. S., 3rd, Thomashow, L. S., and Loper, J. E. (2005) Complete genome sequence of the plant commensal *Pseudomonas fluorescens* Pf-5. *Nat Biotechnol* **23**, 873-878
139. Bendtsen, J. D., Nielsen, H., von Heijne, G., and Brunak, S. (2004) Improved prediction of signal peptides: SignalP 3.0. *J Mol Biol* **340**, 783-795
140. Soding, J., Biegert, A., and Lupas, A. N. (2005) The HHpred interactive server for protein homology detection and structure prediction. *Nucleic Acids Res* **33**, W244-248

141. Eng, J. K., McCormack, A. L., and Yates, J. R. (1994) An approach to correlate tandem mass-spectral data of peptides with amino-acid sequences in a protein database. *J. Am. Soc. Mass Spectrom.* **5**, 976-989
142. Liu, H., Sadygov, R. G., and Yates, J. R., 3rd (2004) A model for random sampling and estimation of relative protein abundance in shotgun proteomics. *Anal Chem* **76**, 4193-4201
143. Meberg, B. M., Sailer, F. C., Nelson, D. E., and Young, K. D. (2001) Reconstruction of *Escherichia coli mrcA* (PBP1a) mutants lacking multiple combinations of penicillin binding proteins. *J Bacteriol* **183**, 6148-6149
144. Aloulou, A., Ali, Y. B., Bezzine, S., Gargouri, Y., and Gelb, M. H. (2012) Phospholipases: an overview. *Methods in Molecular Biology* **861**, 63-85
145. Schmiel, D. H., and Miller, V. L. (1999) Bacterial phospholipases and pathogenesis. *Microbes Infect* **1**, 1103-1112
146. Wilderman, P. J., Vasil, A. I., Johnson, Z., and Vasil, M. L. (2001) Genetic and biochemical analyses of a eukaryotic-like phospholipase D of *Pseudomonas aeruginosa* suggest horizontal acquisition and a role for persistence in a chronic pulmonary infection model. *Mol Microbiol* **39**, 291-303
147. Lesic, B., Starkey, M., He, J., Hazan, R., and Rahme, L. G. (2009) Quorum sensing differentially regulates *Pseudomonas aeruginosa* type VI secretion locus I and homologous loci II and III, which are required for pathogenesis. *Microbiology* **155**, 2845-2855
148. Sana, T. G., Hachani, A., Bucior, I., Soscia, C., Garvis, S., Termine, E., Engel, J., Filloux, A., and Bleves, S. (2012) The second type VI secretion system of *Pseudomonas aeruginosa* strain PAO1 is regulated by quorum sensing and Fur and modulates internalization in epithelial cells. *J Biol Chem* **287**, 27095-27105
149. Russell, A. B., Singh, P., Brittnacher, M., Bui, N. K., Hood, R. D., Carl, M. A., Agnello, D. M., Schwarz, S., Goodlett, D. R., Vollmer, W., and Mougous, J. D. (2012) A widespread bacterial type VI secretion effector superfamily identified using a heuristic approach. *Cell Host Microbe* **11**, 538-549
150. Ishikawa, T., Sabharwal, D., Broms, J., Milton, D. L., Sjostedt, A., Uhlin, B. E., and Wai, S. N. (2012) Pathoadaptive conditional regulation of the type VI secretion system in *Vibrio cholerae* O1 strains. *Infect. Immun.* **80,** 575–584
151. Leroux, M., De Leon, J. A., Kuwada, N. J., Russell, A. B., Pinto-Santini, D., Hood, R. D., Agnello, D. M., Robertson, S. M., Wiggins, P. A., and Mougous, J. D. (2012) Quantitative single-cell characterization of bacterial interactions reveals type VI secretion is a double-edged sword. *Proc Natl Acad Sci U S A* **109**, 19804-19809
152. Stace, C. L., and Ktistakis, N. T. (2006) Phosphatidic acid- and phosphatidylserine-binding proteins. *Biochim Biophys Acta* **1761**, 913-926
153. Yildiz, F. H., and Schoolnik, G. K. (1998) Role of *rpoS* in stress survival and virulence of *Vibrio cholerae*. *J Bacteriol* **180**, 773-784
154. Vaitkevicius, K., Lindmark, B., Ou, G., Song, T., Toma, C., Iwanaga, M., Zhu, J., Andersson, A., Hammarstrom, M. L., Tuck, S., and Wai, S. N. (2006) A *Vibrio cholerae* protease needed for killing of *Caenorhabditis elegans* has a role in protection from natural predator grazing. *Proc Natl Acad Sci U S A* **103**, 9280-9285

155. Valeru, S. P., Rompikuntal, P. K., Ishikawa, T., Vaitkevicius, K., Sjoling, A., Dolganov, N., Zhu, J., Schoolnik, G., and Wai, S. N. (2009) Role of melanin pigment in expression of Vibrio cholerae virulence factors. *Infect Immun* **77**, 935-942
156. Palmer, K. L., Aye, L. M., and Whiteley, M. (2007) Nutritional cues control *Pseudomonas aeruginosa* multicellular behavior in cystic fibrosis sputum. *J Bacteriol* **189**, 8079-8087
157. Korotkov, K. V., and Hol, W. G. (2013) Crystal structure of the pilotin from the enterohemorrhagic *Escherichia coli* type II secretion system. *Journal of structural biology* **182**, 186-191
158. Guzman, L. M., Belin, D., Carson, M. J., and Beckwith, J. (1995) Tight regulation, modulation, and high-level expression by vectors containing the arabinose PBAD promoter. *J Bacteriol* **177**, 4121-4130
159. Donnenberg, M. S., and Kaper, J. B. (1991) Construction of an eae deletion mutant of enteropathogenic *Escherichia coli* by using a positive-selection suicide vector. *Infect Immun* **59**, 4310-4317
160. Edgar, R. C. (2004) MUSCLE: multiple sequence alignment with high accuracy and high throughput. *Nucleic Acids Res* **32**, 1792-1797
161. Guindon, S., Dufayard, J. F., Lefort, V., Anisimova, M., Hordijk, W., and Gascuel, O. (2010) New algorithms and methods to estimate maximum-likelihood phylogenies: assessing the performance of PhyML 3.0. *Syst Biol* **59**, 307-321
162. Emanuelsson, O., Brunak, S., von Heijne, G., and Nielsen, H. (2007) Locating proteins in the cell using TargetP, SignalP and related tools. *Nat Protoc* **2**, 953-971
163. Balsalobre, C., Silvan, J. M., Berglund, S., Mizunoe, Y., Uhlin, B. E., and Wai, S. N. (2006) Release of the type I secreted alpha-haemolysin via outer membrane vesicles from Escherichia coli. *Mol Microbiol* **59**, 99-112
164. Termine, E., and Michel, G. P. (2009) Transcriptome and secretome analyses of the adaptive response of *Pseudomonas aeruginosa* to suboptimal growth temperature. *Int Microbiol* **12**, 7-12
165. Vance, R. E., Rietsch, A., and Mekalanos, J. J. (2005) Role of the type III secreted exoenzymes S, T, and Y in systemic spread of *Pseudomonas aeruginosa* PAO1 in vivo. *Infect Immun* **73**, 1706-1713
166. Bligh, E. G., and Dyer, W. J. (1959) A rapid method of total lipid extraction and purification. *Can J Biochem Physiol* **37**, 911-917
167. Brugger, B., Erben, G., Sandhoff, R., Wieland, F. T., and Lehmann, W. D. (1997) Quantitative analysis of biological membrane lipids at the low picomole level by nano-electrospray ionization tandem mass spectrometry. *Proc Natl Acad Sci U S A* **94**, 2339-2344
168. Devaiah, S. P., Roth, M. R., Baughman, E., Li, M., Tamura, P., Jeannotte, R., Welti, R., and Wang, X. (2006) Quantitative profiling of polar glycerolipid species from organs of wild-type *Arabidopsis* and a phospholipase Dalpha1 knockout mutant. *Phytochemistry* **67**, 1907-1924
169. Welti, R., Li, W., Li, M., Sang, Y., Biesiada, H., Zhou, H. E., Rajashekar, C. B., Williams, T. D., and Wang, X. (2002) Profiling membrane lipids in plant stress responses. Role of phospholipase D alpha in freezing-induced lipid changes in *Arabidopsis*. *J Biol Chem* **277**, 31994-32002

170. Thomas, F., Hehemann, J. H., Rebuffet, E., Czjzek, M., and Michel, G. (2011) Environmental and gut bacteroidetes: the food connection. *Front Microbiol* **2**, 93
171. Lozupone, C. A., Stombaugh, J. I., Gordon, J. I., Jansson, J. K., and Knight, R. (2012) Diversity, stability and resilience of the human gut microbiota. *Nature* **489**, 220-230
172. Smith, J. C., Rocha, E. R., and J., P. B. (2006) *The Medically Important Bacteroides spp. in Health and Disease* Vol. 7
173. Human Microbiome Project Consortium, T. (2012) Structure, function and diversity of the healthy human microbiome. *Nature* **486**, 207-214
174. Round, J. L., and Mazmanian, S. K. (2009) The gut microbiota shapes intestinal immune responses during health and disease. *Nat Rev Immunol* **9**, 313-323
175. Fischbach, M. A., and Sonnenburg, J. L. (2011) Eating for two: how metabolism establishes interspecies interactions in the gut. *Cell Host Microbe* **10**, 336-347
176. Rey, F. E., Faith, J. J., Bain, J., Muehlbauer, M. J., Stevens, R. D., Newgard, C. B., and Gordon, J. I. (2010) Dissecting the in vivo metabolic potential of two human gut acetogens. *J Biol Chem* **285**, 22082-22090
177. Hayes, C. S., Koskiniemi, S., Ruhe, Z. C., Poole, S. J., and Low, D. A. (2014) Mechanisms and biological roles of contact-dependent growth inhibition systems. *Cold Spring Harb Perspect Med* **4**
178. English, G., Trunk, K., Rao, V. A., Srikannathasan, V., Hunter, W. N., and Coulthurst, S. J. (2012) New secreted toxins and immunity proteins encoded within the Type VI secretion system gene cluster of *Serratia marcescens*. *Mol Microbiol* **86**, 921-936
179. Cascales, E., and Cambillau, C. (2012) Structural biology of type VI secretion systems. *Philos Trans R Soc Lond B Biol Sci* **367**, 1102-1111
180. Felisberto-Rodrigues, C., Durand, E., Aschtgen, M. S., Blangy, S., Ortiz-Lombardia, M., Douzi, B., Cambillau, C., and Cascales, E. (2011) Towards a structural comprehension of bacterial type VI secretion systems: characterization of the TssJ-TssM complex of an *Escherichia coli* pathovar. *PLoS Pathog* **7**, e1002386
181. Aschtgen, M. S., Gavioli, M., Dessen, A., Lloubes, R., and Cascales, E. (2010) The SciZ protein anchors the enteroaggregative *Escherichia coli* Type VI secretion system to the cell wall. *Mol Microbiol* **75**, 886-899
182. Falagas, M. E., and Siakavellas, E. (2000) *Bacteroides*, *Prevotella*, and *Porphyromonas* species: a review of antibiotic resistance and therapeutic options. *Int J Antimicrob Agents* **15**, 1-9
183. Russell, A. B., LeRoux, M., Hathazi, K., Agnello, D. M., Ishikawa, T., Wiggins, P. A., Wai, S. N., and Mougous, J. D. (2013) Diverse type VI secretion phospholipases are functionally plastic antibacterial effectors. *Nature* **496**, 508-512
184. Zhang, D., de Souza, R. F., Anantharaman, V., Iyer, L. M., and Aravind, L. (2012) Polymorphic toxin systems: Comprehensive characterization of trafficking modes, processing, mechanisms of action, immunity and ecology using comparative genomics. *Biol Direct* **7**, 18
185. Altschul, S. F., Madden, T. L., Schaffer, A. A., Zhang, J., Zhang, Z., Miller, W., and Lipman, D. J. (1997) Gapped BLAST and PSI-BLAST: a new generation of protein database search programs. *Nucleic Acids Res* **25**, 3389-3402
186. Johnson, L. S., Eddy, S. R., and Portugaly, E. (2010) Hidden Markov model speed heuristic and iterative HMM search procedure. *BMC Bioinformatics* **11**, 431

187. McBride, M. J., Xie, G., Martens, E. C., Lapidus, A., Henrissat, B., Rhodes, R. G., Goltsman, E., Wang, W., Xu, J., Hunnicutt, D. W., Staroscik, A. M., Hoover, T. R., Cheng, Y. Q., and Stein, J. L. (2009) Novel features of the polysaccharide-digesting gliding bacterium *Flavobacterium johnsoniae* as revealed by genome sequence analysis. *Appl Environ Microbiol* **75**, 6864-6875
188. Broms, J. E., Sjostedt, A., and Lavander, M. (2010) The Role of the *Francisella Tularensis* Pathogenicity Island in Type VI Secretion, Intracellular Survival, and Modulation of Host Cell Signaling. *Front Microbiol* **1**, 136
189. Coyne, M. J., Zitomersky, N. L., McGuire, A. M., Earl, A. M., and Comstock, L. E. (2014) Evidence of Extensive DNA Transfer between Bacteroidales Species within the Human Gut. *MBio* **5**
190. Rhodes, R. G., Pucker, H. G., and McBride, M. J. (2011) Development and use of a gene deletion strategy for *Flavobacterium johnsoniae* to identify the redundant gliding motility genes *remF, remG, remH*, and *remI*. *J Bacteriol* **193**, 2418-2428
191. Fritsch, M. J., Trunk, K., Alcoforado Diniz, J., Guo, M., Trost, M., and Coulthurst, S. J. (2013) Proteomic identification of novel secreted anti-bacterial toxins of the *Serratia marcescens* Type VI secretion system. *Mol Cell Proteomics* **12**, 2735-2749
192. Dong, C., Zhang, H., Gao, Z. Q., Wang, W. J., She, Z., Liu, G. F., Shen, Y. Q., Su, X. D., and Dong, Y. H. (2013) Structural insights into the inhibition of type VI effector Tae3 by its immunity protein Tai3. *Biochem J*
193. Zhang, H., Gao, Z. Q., Wang, W. J., Liu, G. F., Xu, J. H., Su, X. D., and Dong, Y. H. (2013) Structure of the type VI effector-immunity complex (Tae4-Tai4) provides novel insights into the inhibition mechanism of the effector by its immunity protein. *J Biol Chem* **288**, 5928-5939
194. Benz, J., Sendlmeier, C., Barends, T. R., and Meinhart, A. (2012) Structural insights into the effector-immunity system Tse1/Tsi1 from Pseudomonas aeruginosa. *PLoS One* **7**, e40453
195. Schwarz, S., Singh, P., Robertson, J. D., LeRoux, M., Skerrett, S. J., Goodlett, D. R., West, T. E., and Mougous, J. D. (2014) VgrG-5 is a *Burkholderia* type VI secretion system-exported protein required for multinucleated giant cell formation and virulence. *Infect Immun* **82**, 1445-1452
196. Toesca, I. J., French, C. T., and Miller, J. F. (2014) The Type VI secretion system spike protein VgrG5 mediates membrane fusion during intercellular spread by *pseudomallei* group *Burkholderia* species. *Infect Immun* **82**, 1436-1444
197. Jiang, F., Waterfield, N. R., Yang, J., Yang, G., and Jin, Q. (2014) A *Pseudomonas aeruginosa* Type VI Secretion Phospholipase D Effector Targets Both Prokaryotic and Eukaryotic Cells. *Cell Host Microbe* **15**, 600-610
198. Aschtgen, M. S., Zoued, A., Lloubes, R., Journet, L., and Cascales, E. (2012) The C-tail anchored TssL subunit, an essential protein of the enteroaggregative *Escherichia coli* Sci-1 Type VI secretion system, is inserted by YidC. *Microbiologyopen* **1**, 71-82
199. Poole, S. J., Diner, E. J., Aoki, S. K., Braaten, B. A., t'Kint de Roodenbeke, C., Low, D. A., and Hayes, C. S. (2011) Identification of functional toxin/immunity genes linked to contact-dependent growth inhibition (CDI) and rearrangement hotspot (Rhs) systems. *PLoS Genet* **7**, e1002217

200. Koskiniemi, S., Lamoureux, J. G., Nikolakakis, K. C., t'Kint de Roodenbeke, C., Kaplan, M. D., Low, D. A., and Hayes, C. S. (2013) Rhs proteins from diverse bacteria mediate intercellular competition. *Proc Natl Acad Sci U S A* **110**, 7032-7037
201. Stecher, B., and Hardt, W. D. (2011) Mechanisms controlling pathogen colonization of the gut. *Curr Opin Microbiol* **14**, 82-91
202. Lawley, T. D., and Walker, A. W. (2013) Intestinal colonization resistance. *Immunology* **138**, 1-11
203. Faith, J. J., Guruge, J. L., Charbonneau, M., Subramanian, S., Seedorf, H., Goodman, A. L., Clemente, J. C., Knight, R., Heath, A. C., Leibel, R. L., Rosenbaum, M., and Gordon, J. I. (2013) The long-term stability of the human gut microbiota. *Science* **341**, 1237439
204. Turnbaugh, P. J., Hamady, M., Yatsunenko, T., Cantarel, B. L., Duncan, A., Ley, R. E., Sogin, M. L., Jones, W. J., Roe, B. A., Affourtit, J. P., Egholm, M., Henrissat, B., Heath, A. C., Knight, R., and Gordon, J. I. (2009) A core gut microbiome in obese and lean twins. *Nature* **457**, 480-484
205. Lee, S. M., Donaldson, G. P., Mikulski, Z., Boyajian, S., Ley, K., and Mazmanian, S. K. (2013) Bacterial colonization factors control specificity and stability of the gut microbiota. *Nature* **501**, 426-429
206. Pujol, A., Crost, E. H., Simon, G., Barbe, V., Vallenet, D., Gomez, A., and Fons, M. (2011) Characterization and distribution of the gene cluster encoding RumC, an anti-*Clostridium perfringens* bacteriocin produced in the gut. *FEMS Microbiol Ecol* **78**, 405-415
207. Maurice, C. F., Haiser, H. J., and Turnbaugh, P. J. (2013) Xenobiotics shape the physiology and gene expression of the active human gut microbiome. *Cell* **152**, 39-50
208. Fu, Y., Waldor, M. K., and Mekalanos, J. J. (2013) Tn-Seq analysis of *Vibrio cholerae* intestinal colonization reveals a role for T6SS-mediated antibacterial activity in the host. *Cell Host Microbe* **14**, 652-663
209. Xu, J., Bjursell, M. K., Himrod, J., Deng, S., Carmichael, L. K., Chiang, H. C., Hooper, L. V., and Gordon, J. I. (2003) A genomic view of the human-*Bacteroides thetaiotaomicron* symbiosis. *Science* **299**, 2074-2076
210. McBride, M. J., and Kempf, M. J. (1996) Development of techniques for the genetic manipulation of the gliding bacterium *Cytophaga johnsonae*. *J Bacteriol* **178**, 583-590
211. Agarwal, S., Hunnicutt, D. W., and McBride, M. J. (1997) Cloning and characterization of the *Flavobacterium johnsoniae* (*Cytophaga johnsonae*) gliding motility gene, *gldA*. *Proc Natl Acad Sci U S A* **94**, 12139-12144
212. Holdeman, L. V., Cato, E. D., and Moore, W. E. C. (1977) *Anaerobe Laboratory Manual*, Virginia Polytechnic Institute and State University Anaerobe Laboratory, Blacksburg, VA
213. Choi, K. H., Gaynor, J. B., White, K. G., Lopez, C., Bosio, C. M., Karkhoff-Schweizer, R. R., and Schweizer, H. P. (2005) A Tn7-based broad-range bacterial cloning and expression system. *Nat Methods* **2**, 443-448
214. Martens, E. C., Chiang, H. C., and Gordon, J. I. (2008) Mucosal glycan foraging enhances fitness and transmission of a saccharolytic human gut bacterial symbiont. *Cell Host Microbe* **4**, 447-457
215. Stevens, A. M., Shoemaker, N. B., and Salyers, A. A. (1990) The region of a *Bacteroides* conjugal chromosomal tetracycline resistance element which is responsible for

production of plasmidlike forms from unlinked chromosomal DNA might also be involved in transfer of the element. *J Bacteriol* **172**, 4271-4279
216. Alvarez, B., Secades, P., McBride, M. J., and Guijarro, J. A. (2004) Development of genetic techniques for the psychrotrophic fish pathogen *Flavobacterium psychrophilum*. *Appl Environ Microbiol* **70**, 581-587
217. Warrens, A. N., Jones, M. D., and Lechler, R. I. (1997) Splicing by overlap extension by PCR using asymmetric amplification: an improved technique for the generation of hybrid proteins of immunological interest. *Gene* **186**, 29-35
218. Altschul, S. F., Gish, W., Miller, W., Myers, E. W., and Lipman, D. J. (1990) Basic local alignment search tool. *J Mol Biol* **215**, 403-410
219. Finn, R. D., Clements, J., and Eddy, S. R. (2011) HMMER web server: interactive sequence similarity searching. *Nucleic Acids Res* **39**, W29-37
220. Katoh, K., and Standley, D. M. (2013) MAFFT multiple sequence alignment software version 7: improvements in performance and usability. *Mol Biol Evol* **30**, 772-780
221. Capella-Gutierrez, S., Silla-Martinez, J. M., and Gabaldon, T. (2009) trimAl: a tool for automated alignment trimming in large-scale phylogenetic analyses. *Bioinformatics* **25**, 1972-1973
222. Anisimova, M., Gil, M., Dufayard, J. F., Dessimoz, C., and Gascuel, O. (2011) Survey of branch support methods demonstrates accuracy, power, and robustness of fast likelihood-based approximation schemes. *Syst Biol* **60**, 685-699
223. Petersen, T. N., Brunak, S., von Heijne, G., and Nielsen, H. (2011) SignalP 4.0: discriminating signal peptides from transmembrane regions. *Nat Methods* **8**, 785-786
224. Krogh, A., Larsson, B., von Heijne, G., and Sonnhammer, E. L. (2001) Predicting transmembrane protein topology with a hidden Markov model: application to complete genomes. *J Mol Biol* **305**, 567-580
225. Cox, J., and Mann, M. (2008) MaxQuant enables high peptide identification rates, individualized p.p.b.-range mass accuracies and proteome-wide protein quantification. *Nat Biotechnol* **26**, 1367-1372
226. Ohi, M., Li, Y., Cheng, Y., and Walz, T. (2004) Negative Staining and Image Classification - Powerful Tools in Modern Electron Microscopy. *Biol Proced Online* **6**, 23-34
227. Degnan, P. H., Barry, N. A., Mok, K. C., Taga, M. E., and Goodman, A. L. (2014) Human gut microbes use multiple transporters to distinguish vitamin B^{12} analogs and compete in the gut. *Cell Host Microbe* **15**, 47-57
228. Russell, A. B., Wexler, A. G., Harding, B. N., Whitney, J. C., Bohn, A. J., Goo, Y. A., Tran, B. Q., Barry, N. A., Zheng, H., Peterson, S. B., Chou, S., Gonen, T., Goodlett, D. R., Goodman, A. L., and Mougous, J. D. (2014) A Type VI Secretion-Related Pathway in *Bacteroidetes* Mediates Interbacterial Antagonism. *Cell Host Microbe* **16**, 227-236
229. Moynihan, P. J., and Clarke, A. J. (2010) O-acetylation of peptidoglycan in gram-negative bacteria: identification and characterization of peptidoglycan O-acetyltransferase in Neisseria gonorrhoeae. *J Biol Chem* **285**, 13264-13273
230. Kamio, Y., Itoh, Y., Terawaki, Y., and Kusano, T. (1981) Cadaverine is covalently linked to peptidoglycan in Selenomonas ruminantium. *J Bacteriol* **145**, 122-128
231. Whitney, J. C., Chou, S., Russell, A. B., Biboy, J., Gardiner, T. E., Ferrin, M. A., Brittnacher, M., Vollmer, W., and Mougous, J. D. (2013) Identification, Structure, and

Function of a Novel Type VI Secretion Peptidoglycan Glycoside Hydrolase Effector-Immunity Pair. *J Biol Chem* **288**, 26616-26624
232. Ma, L. S., Hachani, A., Lin, J. S., Filloux, A., and Lai, E. M. (2014) *Agrobacterium tumefaciens* Deploys a Superfamily of Type VI Secretion DNase Effectors as Weapons for Interbacterial Competition In Planta. *Cell Host Microbe* **16**, 94-104
233. Salomon, D., Gonzalez, H., Updegraff, B. L., and Orth, K. (2013) *Vibrio parahaemolyticus* type VI secretion system 1 is activated in marine conditions to target bacteria, and is differentially regulated from system 2. *PloS one* **8**, e61086
234. Gueguen, E., and Cascales, E. (2013) Promoter swapping unveils the role of the *Citrobacter rodentium* CTS1 type VI secretion system in interbacterial competition. *Appl Environ Microbiol* **79**, 32-38
235. Haapalainen, M., Mosorin, H., Dorati, F., Wu, R. F., Roine, E., Taira, S., Nissinen, R., Mattinen, L., Jackson, R., Pirhonen, M., and Lin, N. C. (2012) Hcp2, a secreted protein of the phytopathogen *Pseudomonas syringae* pv. tomato DC3000, is required for fitness for competition against bacteria and yeasts. *J Bacteriol* **194**, 4810-4822
236. Carruthers, M. D., Nicholson, P. A., Tracy, E. N., and Munson, R. S., Jr. (2013) *Acinetobacter baumannii* utilizes a type VI secretion system for bacterial competition. *PLoS One* **8**, e59388
237. Ding, J., Wang, W., Feng, H., Zhang, Y., and Wang, D. C. (2012) Structural insights into the *Pseudomonas aeruginosa* type VI virulence effector Tse1 bacteriolysis and self-protection mechanisms. *The Journal of biological chemistry* **287**, 26911-26920
238. Zhang, H., Gao, Z.-Q., Su, X.-D., and Dong, Y.-H. (2012) Crystal structure of type VI effector Tse1 from *Pseudomonas aeruginosa*. *FEBS Letters* **586**, 3193-3199
239. Brooks, T. M., Unterweger, D., Bachmann, V., Kostiuk, B., and Pukatzki, S. (2013) Lytic Activity of the *Vibrio cholerae* Type VI Secretion Toxin VgrG-3 is Inhibited by the Antitoxin TsaB. *J Biol Chem*
240. Cornforth, D. M., and Foster, K. R. (2013) Competition sensing: the social side of bacterial stress responses. *Nat Rev Microbiol* **11**, 285-293
241. Basler, M., and Mekalanos, J. J. (2012) Type 6 Secretion Dynamics Within and Between Bacterial Cells. *Science* **337**, 815
242. Ishikawa, T., Rompikuntal, P. K., Lindmark, B., Milton, D. L., and Wai, S. N. (2009) Quorum sensing regulation of the two hcp alleles in Vibrio cholerae O1 strains. *PLoS One* **4**, e6734
243. Wu, C. F., Lin, J. S., Shaw, G. C., and Lai, E. M. (2012) Acid-induced type VI secretion system is regulated by ExoR-ChvG/ChvI signaling cascade in Agrobacterium tumefaciens. *PLoS Pathog* **8**, e1002938
244. Robinson, J. B., Telepnev, M. V., Zudina, I. V., Bouyer, D., Montenieri, J. A., Bearden, S. W., Gage, K. L., Agar, S. L., Foltz, S. M., Chauhan, S., Chopra, A. K., and Motin, V. L. (2009) Evaluation of a Yersinia pestis mutant impaired in a thermoregulated type VI-like secretion system in flea, macrophage and murine models. *Microb Pathog* **47**, 243-251
245. Brunet, Y. R., Bernard, C. S., Gavioli, M., Lloubes, R., and Cascales, E. (2011) An epigenetic switch involving overlapping fur and DNA methylation optimizes expression of a type VI secretion gene cluster. *PLoS Genet* **7**, e1002205

246. Ishikawa, T., Sabharwal, D., Broms, J., Milton, D. L., Sjostedt, A., Uhlin, B. E., and Wai, S. N. (2012) Pathoadaptive conditional regulation of the type VI secretion system in *Vibrio cholerae* O1 strains. *Infect Immun* **80**, 575-584
247. Zhang, W., Xu, S., Li, J., Shen, X., Wang, Y., and Yuan, Z. (2011) Modulation of a thermoregulated type VI secretion system by AHL-dependent quorum sensing in *Yersinia pseudotuberculosis*. *Arch Microbiol* **193**, 351-363
248. Nadell, C. D., Foster, K. R., and Xavier, J. B. (2010) Emergence of spatial structure in cell groups and the evolution of cooperation. *PLoS Comput Biol* **6**, e1000716
249. Engelberg-Kulka, H., and Glaser, G. (1999) Addiction modules and programmed cell death and antideath in bacterial cultures. *Annual review of microbiology* **53**, 43-70
250. Van Melderen, L., and Saavedra De Bast, M. (2009) Bacterial toxin-antitoxin systems: more than selfish entities? *PLoS genetics* **5**, e1000437
251. Yamaguchi, Y., and Inouye, M. (2011) Regulation of growth and death in *Escherichia coli* by toxin-antitoxin systems. *Nat Rev Microbiol* **9**, 779-790
252. Wang, X., and Wood, T. K. (2011) Toxin-antitoxin systems influence biofilm and persister cell formation and the general stress response. *Applied and environmental microbiology* **77**, 5577-5583
253. Frampton, R., Aggio, R. B., Villas-Boas, S. G., Arcus, V. L., and Cook, G. M. (2012) Toxin-antitoxin systems of *Mycobacterium smegmatis* are essential for cell survival. *The Journal of biological chemistry* **287**, 5340-5356
254. Hazan, R., and Engelberg-Kulka, H. (2004) *Escherichia coli mazEF*-mediated cell death as a defense mechanism that inhibits the spread of phage P1. *Mol Genet Genomics* **272**, 227-234
255. Gerdes, K., and Maisonneuve, E. (2012) Bacterial persistence and toxin-antitoxin loci. *Annual review of microbiology* **66**, 103-123
256. Stoodley, P., Sauer, K., Davies, D. G., and Costerton, J. W. (2002) Biofilms as complex differentiated communities. *Annual review of microbiology* **56**, 187-209
257. Parsek, M. R., and Greenberg, E. P. (2005) Sociomicrobiology: the connections between quorum sensing and biofilms. *Trends Microbiol* **13**, 27-33
258. Blango, M. G., and Mulvey, M. A. (2009) Bacterial landlines: contact-dependent signaling in bacterial populations. *Curr Opin Microbiol* **12**, 177-181
259. Fagotto, F., and Gumbiner, B. M. (1996) Cell contact-dependent signaling. *Dev Biol* **180**, 445-454
260. Downing, K. J., Mischenko, V. V., Shleeva, M. O., Young, D. I., Young, M., Kaprelyants, A. S., Apt, A. S., and Mizrahi, V. (2005) Mutants of *Mycobacterium tuberculosis* lacking three of the five *rpf*-like genes are defective for growth in vivo and for resuscitation in vitro. *Infection and immunity* **73**, 3038-3043
261. Mukamolova, G. V., Murzin, A. G., Salina, E. G., Demina, G. R., Kell, D. B., Kaprelyants, A. S., and Young, M. (2006) Muralytic activity of *Micrococcus luteus* Rpf and its relationship to physiological activity in promoting bacterial growth and resuscitation. *Mol Microbiol* **59**, 84-98
262. Mukamolova, G. V., Turapov, O. A., Kazarian, K., Telkov, M., Kaprelyants, A. S., Kell, D. B., and Young, M. (2002) The *rpf* gene of *Micrococcus luteus* encodes an essential secreted growth factor. *Mol Microbiol* **46**, 611-621

263. Ravagnani, A., Finan, C. L., and Young, M. (2005) A novel firmicute protein family related to the actinobacterial resuscitation-promoting factors by non-orthologous domain displacement. *BMC Genomics* **6**, 39
264. West, S. A., Griffin, A. S., and Gardner, A. (2007) Evolutionary explanations for cooperation. *Curr Biol* **17**, R661-672
265. Diggle, S. P., Griffin, A. S., Campbell, G. S., and West, S. A. (2007) Cooperation and conflict in quorum-sensing bacterial populations. *Nature* **450**, 411-414
266. Webb, J. S., Givskov, M., and Kjelleberg, S. (2003) Bacterial biofilms: prokaryotic adventures in multicellularity. *Current opinion in microbiology* **6**, 578-585
267. Whitchurch, C. B., Tolker-Nielsen, T., Ragas, P. C., and Mattick, J. S. (2002) Extracellular DNA required for bacterial biofilm formation. *Science* **295**, 1487
268. Stewart, P. S., and Franklin, M. J. (2008) Physiological heterogeneity in biofilms. *Nat Rev Microbiol* **6**, 199-210
269. Otsuka, Y., and Yonesaki, T. (2012) Dmd of bacteriophage T4 functions as an antitoxin against *Escherichia coli* LsoA and RnlA toxins. *Mol Microbiol* **83**, 669-681

VITA

Alistair Brian Russell was born in Tuebingen, Germany on October 11, 1986 to Maureen and David Russell. He graduated from Ithaca High School in 2005, and obtained a B.A. from Cornell University in 2009 in Biology with a concentration in Microbiology. During his time at Cornell University Alistair worked in the laboratory of Alan R. Collmer on the plant-pathogenic bacterium *Pseudomonas syringae* under the direct mentorship of Brian Kvitko. In 2014 Dr. Russell received a Doctor of Philosophy degree from the University of Washington, Department of Microbiology, for his work on antibacterial effectors of the type VI secretion system under the mentorship of Dr. Joseph D. Mougous.